THE ROLE OF SELENIUM IN DOPAMINE TRANSMISSION AND MODULATION BY METHAMPHETAMINE

A DISSERTATION SUBMITTED TO THE GRADUATE DIVISION OF THE UNIVERSITY OF HAWAIʻI AT MĀNOA IN PARTIAL FULFILLMENT OF THE REQUIREMENTS FOR THE DEGREE OF

DOCTOR OF PHILOSOPHY

IN

CELL AND MOLECULAR BIOLOGY (NEUROSCIENCES)

JULY 2017

By

Daniel J. Torres

Dissertation Committee:

Frederick Bellinger, Chairperson
Robert Nichols
Matthew Pitts
Jun Panee
Andrew Stenger

Keywords: Selenium, Selenoprotein, Dopamine, Methamphetamine, Fast-scan cyclic voltammetry

TABLE OF CONTENTS

ACKNOWLEDGMENTS

There are many people without whom this work would not have been possible.

I would like to thank my committee members for their valuable feedback with my project. In particular, I would like to thank my advisor Rick Bellinger for all his expert guidance over the past four years and for introducing me to the world of electrophysiology.

I would also like to thank our collaborators. In particular, Scott Steffensen for introducing us to fast-scan cyclic voltammetry and Jordan Yorgason for writing the voltammetry software. Marilou Andres and Suguru Kurokawa were also important collaborators.

There are also many Bellinger lab members past and present that have contributed to this project: Stephanie Barayuga, Rachel Rueli, Arlene Kiyohara, Jane Uyehara-Lock, Catherine Chao, Ayaka Hagiwara, Jenna Pak, and Courtney Zavaleta. Berry lab manager Ann Hashimoto also provided invaluable technical support.

Finally, I would like to thank my parents for their great example and encouragement. Without their support, I never would have made it this far. Finally, I must also acknowledge my wife Miyoung for all of her love and support.

ABSTRACT

Selenium (Se) is an antioxidant trace element that is important for normal brain function. Se is incorporated into selenoproteins, a family of proteins with multiple functions that include protection from oxidative stress. Methamphetamine (METH) increases dopamine (DA) signaling by causing efflux of DA out of nerve terminals, resulting in increased oxidative stress from oxidized DA, and eventual degeneration of dopaminergic terminals. Se protects against METH-induced neurotoxicity while Se deficiency potentiates toxicity. Se may also be involved in DA transmision as Se deficiency increases DA turnover in rodents. We explored the possibility that Se may affect the physiological response to METH by using fast-scan cyclic voltammetry (FSCV) to record DA release and uptake kinetics in mouse brain slices. Action potential-dependent phasic DA release was simulated in the present study by electrically evoking release in brain slices. METH was applied to brain slices and phasic release recorded, as well as DA efflux, which was monitored in the absence of stimulation. Dietary Se restriction lasting 2 weeks reduced METH-induced DA efflux. Inhibition of the selenoprotein glutathione peroxidase (GPx) also reduced DA efflux through mechanisms involving ATP-sensitive K^+ channels (K_{ATP} channels) and cannabinoid receptor 1 (CB1R). Chronic Se-deficient mice had reduced basal DA uptake rates, but no change in basal release. In response to METH chronic Se deficiency caused reduced DA efflux compared to Se-sufficient mice. METH also caused and increase in phasic DA release in chronic Se-deficient mice that can be attributed to increased DA vesicular release. Selenoprotein P (Sepp1)-KO mice had reduced baseline phasic DA release and uptake rates. In response to METH, phasic release was significantly potentiated due to increased DA vesicular release. METH-induced vesicular DA release

in wild-type mice was found to be masked by D2R auto-inhibition, which may be dysfunctional in Sepp1-KO mice. METH-induced vesicular DA release was prevented in Sepp1-KO mice by purified Sepp1 protein acting on ApoER2 to promote D2R function. These results indicate that Se is directly involved in DA neurotransmission and modulates the DA response to METH. Furthermore, specific selenproteins play differential roles in regulating DA physiology.

LIST OF FIGURES

CHAPTER 1: INTRODUCTION

This research project seeks to uncover the role of selenium (Se) in mesolimbic dopamine (DA) transmission and in mediating dopaminergic responses to methamphetamine (METH). The first aim explores the short-term influence of dietary Se levels and the selenoprotein glutathione peroxidase (GPx) in mediating extracellular DA concentrations and METH-induced DA elevations. The second aim describes the consequences of chronic Se deficiency on dopaminergic activity. Finally, the third aim investigates the specific role of Selenoprotein P (Sepp1) in DA release regulation. Overall, this study highlights the importance of Se in the DA system while providing new insight on redox and non-redox selenoprotein activity. The findings reported here also have some implications for the mechanism of action of METH.

Neurotransmission

Excitation and inhibition:

Although the present study is restricted to dopaminergic transmission, there are implications for the involvement of other neurotransmitter systems. Glutamate is the most abundant neurotransmitter in the brain and responsible for excitatory transmission. Released pre-synaptically, glutamate activates four different classes of receptors: α-amino-3-hydroxy-5-methyl-4-isoxazolepropionic acid receptors (AMPARs), N-methyl-D-aspartate receptors (NMDARs), metabotropic glutamate receptors (mGLURs) and kainate receptors (Meldrum, 2000). Activation of AMPARs opens ion channels to promote membrane depolarization. NMDAR require partial membrane depolarization, in addition to glutamate binding, to activate. Both receptor types differ in their kinetics, composition, and ion specificity (Laube et al., 1998). AMPARs are fast-acting and mainly responsible for Na^{2+} influx with precise ion permeabilities depending on protein subunit composition (Chater and Goda, 2014). NMDARs are slower, have a high ratio of Ca^{2+} to Na^{+} permeability, and require depolarization for activation (Iacobucci and Popescu, 2017). The mGLURs are G-protein-coupled receptors (GPCRs) that activate intracellular signaling pathways primarily to modulate neurotransmission and membrane excitability (Niswender and Conn, 2010).

The main inhibitory neurotransmitter is γ-aminobutyric acid (GABA), which reduces neuronal excitability. GABA works on two classes of receptors: $GABA_A$ receptors, which are ion channels that induce hyperpolarization via Cl^- conductance, and $GABA_B$ receptors, which are

GPCRs that can activate K^+ channels as well as intracellular signaling pathways (Chebib and Johnston, 1999).

Dopamine metabolism and recycling:

DA is a monoamine synthesized from the amino acid precursor L-DOPA by the enzyme DOPA decarboxylase (Meiser et al., 2013). L-DOPA itself is generated by the removal of a hydroxyl group (OH) from L-Tyrosine by the enzyme tyrosine hydroxylase (TH) (Daubner et al., 2011). This is a rate-limiting step and, thus, TH expression and activity are used as indicators of DA synthesis and activity.

Following synthesis, cytosolic DA is packaged into synaptic vesicles by the vesicular monoamine transporter-2 (VMAT-2). Synaptic vesicles have an internal acidity that is maintained by the vacuolar-type H^+-ATPase (V-ATPase) which pumps protons into the vesicle in an ATP-dependent manner (Cidon et al., 1983; Cidon and Nelson, 1983). The resulting pH gradient is used by VMAT-2 to pump DA into the vesicle by exchanging 2 protons for one DA molecule (Zhang et al., 2012).

Vesicular DA is released into the synapse following sufficient neural activity. Vesicular DA release is proposed to occur through a process called 'kiss-and-run'. This model of vesicular release is unique in that it purports that the vesicle fuses with the plasma membrane just enough to open a pore, release DA, and then close the pore to be recycled back into the synaptic vesicle pool (Wightman and Haynes, 2004; Trouillon and Ewing, 2014). The vesicle is conserved for use rather than undergoing full collapse fusion and being recycled through the plasma membrane. While it remains a topic of debate 'kiss-and-run' is thought to be resource efficient and increase the capacity of pre-synaptic terminals to respond to high frequency inputs (Harata et al., 2006).

Synaptic DA can also be taken back up into the pre-synaptic terminal via the plasma membrane dopamine active transporter (DAT) and subsequently re-packaged into vesicles by (VMAT-2) (Torres et al., 2003; Wimalasena, 2011). DAT uses similar principles as VMAT-2 to transport DA across the membrane. DAT uses an electrochemical gradient to co-transport 2 Na^+ ions and one Cl^- ion along with DA from the extracellular space into the cell (Krueger, 1990). Na^+/K^+-ATPase maintains this gradient that powers DAT activity by pumping Na^+ out of the neuron and K^+ in, an action that primarily serves to maintain the resting membrane potential (Torres et al., 2003).

Alternatively, synaptic DA can be broken down by the enzymes monoamine oxidase (MAO), catechol-O-methyl transferase (COMT), and aldehyde dehydrogenase (ALDH). The metabolic products, which include homovanillic acid (HVA) and 3,4-Dihydroxyphenylacetic acid (DOPAC), can be measured to evaluate DA turnover rates (Elsworth and Roth, 1997).

Dopamine receptors:

DA signaling plays a neuromodulatory role in the brain. DA receptors are GPCRs that fall into two families of opposing influences. The D1-like family, which includes D1R and D5R, activates adenylyl cyclase (AC) to up-regulate the cyclic adenosine monophosphate (cAMP) pathway, potentially having numerous effects including increasing intracellular Ca^{2+}. The D2-like family, which includes D2R, D3R, and D4R, and inhibits AC to down-regulate the cAMP pathway (Beaulieu and Gainetdinov, 2011). While D1R and D2R are both localized post-synaptically, D2Rs are also present as a shorter isoform on pre-synaptic terminals where they carry out auto-inhibitory action. Activation of pre-synaptic D2Rs can suppress DA release by decreasing release probability via K^+ channel activation, down-regulating DA synthesis by inhibiting TH, and up-regulating DA uptake from the synapse by increasing DAT surface expression (Ford, 2014). Additionally, D2Rs can inhibit VGCCs via G-protein coupled signaling. The present study investigates the D2R auto-inhibitory component of the dopaminergic response to METH.

Other neurotransmitters:

There are several other neurotransmitter systems with neuromodulatory properties within the brain that, while not directly investigated, can affect dopaminergic transmission. Acetylcholine (ACh) modulates synaptic transmission and excitability by binding two classes of receptors: muscarinic receptors (mAChRs) (Wess, 2003), which are GPCRs that can activate multiple pathways through phospholipase C and AC signaling, and nicotinic receptors (nAChRs), which are non-selective ion channels distributed across the neuronal surface (Picciotto et al., 2012). Serotonin (SER) and norepinephrine (NE), two other monoamines, act on a diverse range of GPCRs as well as Na^+/K^+ channels in the case of SER (Mohammad-Zadeh et al., 2008; Xing et al., 2016).

The endocannabinoid system:

Part of this study addresses the role of the retrograde signaling endocannabinoid system. Endocannabinoids are lipid-based molecules that incorporate the phospholipid membrane-resident fatty acid arachidonic acid (ARA) (Mechoulam and Parker, 2013). The major endocannabinoids are anandamide (AEA) and 2-arachidonoylglycerol (2-AG), which are derived from the phospholipids phosphatidylethanolamine and phosphatidylinositol, respectively (Murataeva et al., 2014; Maccarrone, 2017). The metabolic processes involved are complex and involve multiple hydrolytic pathways carried out by enzymes such as phospholipase D and diacylglycerol lipase. AEA and 2-AG are primarily broken down by fatty acid amide hydrolase (FAAH), yielding ARA and other metabolites (Mechoulam and Parker, 2013).

Endocannabinoids act on two types of pre-synaptic receptors: cannabinoid receptor 1 (CB1R) and cannabinoid receptor 2 (CB2R). Both receptors are GPCRs that down-regulate AC activity to inhibit neurotransmitter release (Pertwee, 2006). Interestingly, CB1R has been implicated in the ability of AMPH to elevate striatal DA levels (Covey et al., 2016). CB1R receptor activity may also be involved in H_2O_2-K_{ATP} channel suppression of evoked DA release (Sidlo et al., 2008). Additionally, CB2R plays a neuroprotective role against METH toxicity (Nader et al., 2014).

The Mesolimbic Pathway

The mesolimbic dopamine (DA) system, often referred to as the reward pathway, plays an important role in mediating the acute rewarding effects of pleasurable stimuli, such as food, sex, drugs of abuse, and social interaction (Nestler and Carlezon, 2006). The mesolimbic system consists of dopaminergic projections from the ventral tegmental area (VTA) to the nucleus accumbens (NAc). Located in midbrain, the VTA consists primarily of DA neurons with axons that extend and synapse onto neurons in the NAc, located in striatum (Cameron et al., 1997). VTA dopaminergic neurons play a key role in motivation, reinforcement learning, and motor output (Graybiel et al., 1994; Cagniard et al., 2006). VTA also contains GABAergic neurons, which are thought to locally inhibit VTA dopaminergic neurons and may also project to the NAc (Van Bockstaele and Pickel, 1995). There is also a small population of VTA glutamatergic neurons that may provide excitatory regulation of the dopaminergic neurons (Yamaguchi et al., 2007). In

addition to drug addiction, the VTA has been shown to be essential for the development of 'natural addictions' which involve compulsive consumption of natural stimuli and include gambling, overeating, and sex addictions (Nestler and Carlezon, 2006).

The NAc contains primarily medium spiny neurons (MSNs), which are GABAergic and receive dopaminergic input from the VTA (Salgado and Kaplitt, 2015). Anatomically, the NAc consists of the central core region and the outer shell region, which differ morphologically and functionally. NAc core surrounds the anterior commissure (AC) and is in turn surrounded by the shell on the medial, ventral, and lateral sides (Fig.1-1) (Heimer et al., 1997). The core is thought to consist of a smaller density of cells, with relatively less dendritic branching and few multipolar neurons. The shell, on the other hand, is regarded as containing a denser population of fusiform and multipolar neurons with more dendritic spines on secondary and tertiary branches (Berendse and Groenewegen, 1990; Sazdanovic et al., 2011). Rodent morphology studies have yielded opposing results, however, with evidence suggesting the shell contains smaller neurons with fewer dendritic spines and branching (Meredith et al., 1989; Meredith et al., 1992).

Despite varying mechanisms of action, elevated DA levels in the NAc is a central component of the role of the mesolimbic system in the reward-reinforcement of drugs of abuse (Wise, 1998; Koob and Le Moal, 2001). For example, in the case of psychostimulants like METH and cocaine, increased DA transmission in the NAc results from the direct inhibition of DA uptake (Wise, 2004). Opiates, on the

other hand, achieve DA elevation by inhibiting GABAergic interneurons in the VTA, thereby disinhibiting VTA dopaminergic neurons (Howlett et al., 2004).

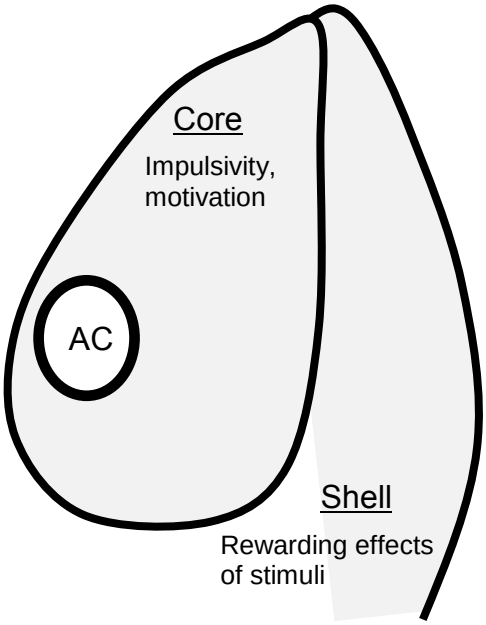

Figure 1-1. Nucleus accumbens.
The NAc core surrounds the anterior commissure (AC) and is involved in impulsivity and motivation. The NAc shell, which processes the rewarding effects is stimuli, is located lateral to the core. The shell is also implicated in addiction.

Functionally, the core and shell seem to serve different purposes. The core is vital to conditioned responses, impulsivity, and motivation (Maldonado-Irizarry and Kelley, 1995; Parkinson et al., 2000; Cardinal and Howes, 2005) while

the shell is more involved in the reinforcing properties of novelty, pleasurable substances, drug relapse, and feeding behavior (Parkinson et al., 1999; Alderson et al., 2001; Bossert et al., 2007; van der Plasse et al., 2012). The NAc shell is of special interest regarding substance abuse as it is thought to play a more significant role in the rewarding effects of drugs in comparison to the core (Ikemoto, 2007). Lesioning dopaminergic terminals in the NAc shell, but not core, reduces amphetamine (AMPH)-induced conditioned place preference (Sellings and Clarke, 2003). Additionally, rats learn to self-administer AMPH and cocaine into the NAc shell, but not the core (Ikemoto and Witkin, 2003). Chronic cocaine exposure impairs DA signaling in the NAc shell of self-administering rats much more dramatically than the core (Saddoris et al., 2016). Finally, the shell has also been implicated in METH-induced behavioral sensitization and withdrawal symptoms (Xu et al., 2011; Ren et al., 2015). For these reasons, we focused our studies on the NAc shell.

Tonic-Phasic Dopamine Model

Tonic and phasic release:

Current models of DA release posit DA to be released in two separate modes, driven by independent mechanisms that work together homeostatically (Wong et al., 2008). Phasic release is a transient episode of action potential-dependent burst firing that releases DA into the synapse to elicit a post-synaptic response. Tonic release is described as a slow, sustained release of lesser amounts of DA that diffuse into the extracellular space and generally do not elicit a strong post-synaptic response. Disruptions in the balance of tonic and phasic firing have been proposed to underlie the DA pathophysiology of multiple neurological disorders as well as the deleterious effects of substance abuse (Grace, 1991, 1995). This study will investigate phasic and tonic DA release in NAc using fast-scan cyclic voltammetry (FSCV), which uses a carbon-fiber electrode to measure extracellular DA concentrations.

The precise definitions of the terms “tonic” and “phasic” have changed slightly over time and their usage differs slightly in relation to different contexts. The tonic-phasic DA model was first proposed by Grace et al. and describes synaptic (phasic) and extra-synaptic (tonic) DA release to explain discrepancies seen between microdialysis and voltammetry studies (Grace, 1991). The term “tonic DA concentration” has been used to refer to the steady-state extracellular DA

concentration that is maintained by steady tonic DA release. Changes in this basal DA concentration occur slowly over minutes of time, such as that measured by microdialysis studies.

Past studies seeking to depict basal tonic DA concentrations in striatum have reported levels ranging from 1 nM to 2.5 µM (Atcherley et al., 2015). This wide range of concentrations has largely been attributed to the physical limitations of microdialysis and voltammetry techniques (Justice, 1993). More recently, Atcherley et al. used a novel method called fast-scan controlled-adsorption voltammetry (FSCAV), purported to give more direct measurements of tonic DA concentrations, and reported concentrations of 90 ± 9 nM DA in anaesthetized mouse NAc (Atcherley et al., 2015).

The usage of the term phasic DA release is more straight-forward and refers to the rapid vesicular release of vesicular DA into the synaptic space in response to an action potential. Phasic DA release concentrations as high as 1 µM have been reported using FSCV (Gonon, 1988; Garris et al., 1997). Further critique and comparison of DA-measuring techniques will take place in the GENERAL DISCUSSION section.

Tonic and phasic 'firing':

The definitions of tonic and phasic also incorporate the electrical activity profiles thought to underlie each mode of DA release. VTA dopaminergic neurons exhibit a 'pacemaking' axonal firing maintained by a slow depolarization (40-120 ms) of about 13 mV at 3-8 Hz (Grace and Bunney, 1984a). Consecutive depolarization events are associated with voltage-gated Ca^{2+} channel (VGCC)-mediated currents (Lambert et al., 2014). This low frequency firing intrinsically occurs at regular intervals and is influenced by GABAergic inputs from afferent connections and local circuitry (Grace and Bunney, 1983). These inhibitory controls result in dopaminergic neurons displaying a slow, irregular firing pattern that, in combination with spontaneous release events, contributes to extracellular DA concentrations. This non-phasic firing pattern, referred to in some of the literature as 'tonic firing' becomes more regular in *ex vivo* brain slices when GABAergic afferent inputs are lost (Grace and Bunney, 1985; Grace and Onn, 1989; Cohen et al., 2012).

Early studies on rats noted that only about half of the population of DA neurons in rat VTA are typically active, a phenomenon that was eventually attributed to robust GABAergic input from the ventral pallidum (VP) (Grace and Bunney, 1984a; Freeman and Bunney, 1987; Floresco et al.,

2001; Floresco et al., 2003). This constant inhibitory input is required to keep certain neurons in a 'non-firing state', and in the absence of inhibition, the neurons fire consistently in a 'control state'.

Overall tonic DA concentration in the NAc is maintained by the baseline activity of the VTA DA neuron population. The collective baseline electrical activity of the population, referred to as the population activity, may loosely be referred to in some papers as "tonic DA activity". Increases in tonic DA activity are thought to result from an increase in the total number of DA neurons that are in the control state. Some other possible factors that could modulate tonic DA levels are changes in firing rate, release probability, and vesicular content (Dreyer et al., 2010).

Phasic DA release results from burst firing events that typically involve 3-10 action potentials (5-15 mv) at 40-80 ms intervals (Grace and Bunney, 1984b). Phasic firing of DA neurons is driven by glutamatergic input from multiple brain regions. The most robust input noted comes from the brainstem, which becomes active in response to behaviorally relevant stimuli (Grace, 2012). Only neurons that are already in the control state, however, exhibit burst firing in response to glutamatergic signals from the brainstem (Mayer et al., 1984; Chergui et al., 1993). Therefore, it is postulated that the greater the number of neurons activated, the larger the resultant phasic DA signal (Floresco et al., 2003).

According to this model, tonic DA release would typically correlate with the amplitude of the phasic response. This relationship could change, however, if tonic DA levels rise disproportionately to population activity. This could result from augmented quantal size, increased spontaneous release, or slower DA reuptake rates (Grace, 2016). In this case, increased extracellular DA could cause a greater occupancy of D2 auto-receptors and subsequently attenuate the phasic DA release that results from burst firing (Floresco et al., 2003).

The ventral subiculum (vSub) of the hippocampus has been demonstrated to increase population activity of DA neurons by inhibiting VP afferents to the VTA (Lodge and Grace, 2006). Therefore, it is thought that the input from the vSub transmits information about the contextual relevance of a situation considering that the more ventral regions of the hippocampus are innervated by limbic inputs, particularly from the amygdala (French et al., 2003). For example, a situation with elevated an risk/reward ratio may result in less inhibition from the vSub and, therefore, allow for a more robust phasic DA signal in response to behaviorally salient stimuli (Schultz, 2016). While vSub activity increases tonic firing in DA neurons by inhibiting the VP, the basolateral amygdala (BLA), which is activated in response to stress, has been shown to

decrease DA neuron population activity potentially through glutamatergic inputs to the VP (LeDoux, 2000; Chang and Grace, 2014).

Historically, DA activity has been investigated in terms of firing patterns using single cell recording. Microdialysis originally provided the best means of measuring DA release. More recently, the development of FSCV has provided a means to measure DA concentration with sub-second temporal resolution and, therefore, capture synaptic release events. FSCV modeling of endogenous tonic firing involves single-pulse stimulations and multi-pulse stimulations under 20 Hz in frequency. Phasic burst-firing, on the other hand, is modeled using multi-pulse stimulations of at least 20 Hz (Ferris et al., 2013).

Functional interplay of tonic and phasic release:

Tonic DA release is thought to provide a baseline tone which dictates the local responsivity of DA receptors to phasic DA events originating from the VTA (Grace, 2012). The occupancy of D1R and D2R is highly dependent on the balance and synchronicity of tonic and phasic DA firing. Computational modeling of DA signaling predicts that synchronized phasic burst firing increases D1R and decreases D2R average occupancy relative to tonic firing. Phasic patterns consist of bursts during which D1R occupancy is high and intra-burst pauses during which occupancy of both receptors is relatively low.

Impact of Methamphetamine on Society

METH is a powerful sympathomimetic with a wide range of devastating health effects and high potential for abuse. It is a member of the AMPH class of psychostimulant drugs. METH is a methylated derivative of AMPH and shares much the same pharmacodynamics (Melega et al., 1995). As such, this study considers scientific findings on the actions of AMPH to be representative of similar actions exerted by METH. While METH is generally suggested to be more potent than AMPH, few studies have directly compared the two drugs.

METH is a large player in the global market for synthetic drugs. In the United States, the prevalence of METH abuse was estimated to be about 1.2 million individuals in 2012 according to the National Survey on Drug Use and Health (Volkow, 2013). It is estimated that there are 15-16 million METH users worldwide. AMPHs are the second most widely used illicit drug

worldwide, trailing only marijuana (UNODC, 2014). The economic strain of METH in the United States alone is staggering with estimated costs as high as $48.3 billion (RAND, 2009).

Acute METH exposure can cause rapid/irregular heartbeat, hyperthermia, hypertension, and convulsions. In the long-term, significant alterations to the DA system can lead to problems with anxiety, insomnia, violent behavior, psychosis, mood disorder, and of course addiction (Volkow, 2013). Although addiction and acute METH toxicity can be supportively managed, there are currently no medications that counteract the specific actions of METH (Volkow, 2013). To date, most clinical trials for pharmacological treatments have produced negative results. A recent expert review on METH addiction pharmacotherapy has indicated a need for new treatment targets and, thus, further understanding of the underlying molecular mechanisms of METH is needed (Ballester et al., 2017).

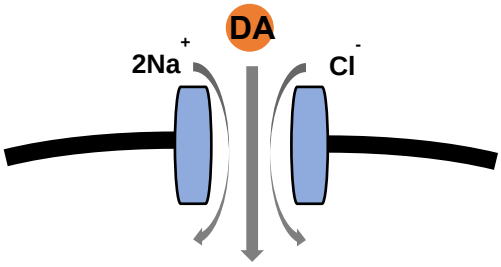

Figure 1-2. Transport of DA and METH through DAT.
DAT co-transports 2Na+ and Cl- along with DA using the Na2+ concentration gradient as a driving force. In the case of DA efflux, this transport mechanism acts in the opposite direction, transporting cytosolic DA into the synaptic space.

Methamphetamine Mechanism of Action

Methamphetamine-induced dopamine efflux:

METH exerts its main effects on the brain through its ability to greatly potentiate dopaminergic transmission. Currently, the most commonly accepted mechanism of action is that METH inhibits DA uptake through DAT by competing with DA for the binding site, resulting in elevated levels of DA in the synapse (Seiden et al., 1993; Sulzer, 2011). METH is also capable of reversing the transport direction of DAT (Jones et al., 1998) as well as entering dopaminergic terminals and causing release of DA from vesicles into the cytosol by disrupting VMAT-2 function (Fig. 2-1) (Sulzer et al., 1992).

Vesicular DA stores are depleted and DA is released from the pre-synaptic terminal via reverse directional activity of DAT. Electrophysiological studies suggest that this biphasic mechanism is concentration dependent with vesicular depletion requiring higher concentrations (10μM) than DAT inhibition (<10μM) when applied to mouse brain slices (Siciliano et al., 2014). This phenomenon, commonly referred to as DA efflux, is thought by many to account, perhaps exclusively, for the increases in extracellular DA levels that are central to METH-induced neurological and psychosomatic effects.

Methamphetamine action on vesicular dopamine:

METH has been demonstrated to have a high affinity for VMAT-2 and compete with DA and chemical VMAT-2 inhibitors for binding (Peter et al., 1994). There are two major hypotheses to explain the mechanism through which METH removes DA from vesicles into the cytosol. The first is that METH competes with DA for the uptake site on VMAT-2, referred to as *VMAT competition* and has also been suggested to be taken up into the vesicle as a VMAT-2 substrate (Sulzer et al., 2005). AMPH was known early on to accumulate in acidic organelles inside the cell, but this is likely due to its characteristics as a lipophilic weak base and to date there is no direct evidence of METH being transported as a VMAT-2 substrate (Mack and Bonisch, 1979). Nevertheless, METH is at least capable of reducing DA uptake into vesicles which can deplete vesicular DA levels over time as there is naturally a constant low-level leakage of DA out of synaptic vesicles (Floor et al., 1995; Pothos et al., 2000).

The second hypothesis to explain METH-induced vesicular DA depletion purports that the weak base activity of METH makes it membrane permeable and thus allows it to enter synaptic vesicles and bind protons. This *weak base hypothesis* predicts the alkalinization of the vesicular lumen and, therefore, the destruction of the pH gradient that drives DA uptake into the vesicle. These hypotheses are not mutually exclusive and are commonly accepted mechanisms of action to explain DA vesicle depletion in the presence of METH.

Methamphetamine action on the dopamine active transporter:

Like with VMAT-2, there are multiple proposed hypotheses to explain the mechanism of METH-induced DAT reverse transport. *Facilitated exchange diffusion* presumes that the DA binding site on DAT crosses the membrane to release DAT. After crossing, it is then available for

binding cytosolic DA and transporting it out of the cell. The underlying assumption of this hypothesis is that the substrate drives the transport process (Sulzer et al., 2005). According to this model, intake would occur much more frequently than efflux due the higher Na^+ concentration extracellularly (Bogdanski and Brodie, 1969). As a DAT substrate, METH would be taken into the neuron and increase the probability of the binding site being on the cytosolic side and, therefore, increasing the rate of DA efflux (Paton, 1973). The net result of this model would be a one-to-one exchange of DA out of the neuron for METH into the neuron.

The *channel-like transporter modes hypothesis* suggests that upon exposure to METH, transmembrane gradients drive a net flux of DA molecules through DAT in an ion channel-like conductance event (Sonders et al., 1997; Kahlig et al., 2005). This model allows for a greater than one-to-one exchange of DA for METH and thus a more potent mode of DA efflux. Khoshbouei et al. introduced a hypothesis that contends that DAT has an asymmetric structural conformation that transports DA bi-directionally, but strongly favors influx over efflux (Khoshbouei et al., 2004). In this model, METH causes secondary messenger events that result in DAT phosphorylation and a conformational shift that favors DA efflux. Most evidence points to protein kinase C (PKC) as the primary mediator of this pathway (Giambalvo, 1992a, b; Kantor and Gnegy, 1998). While multiple ideas have been proposed, the mechanistic details of METH-induced DA efflux remain to be fully elucidated.

There are several additional mediating factors that have been proposed to contribute to METH-induced extracellular DA elevation at large including MAO inhibition (Blaschko et al., 1937; Mantle et al., 1976), increased DA synthesis (Larsen et al., 2002), DAT internalization (Saunders et al., 2000), redistribution of VMAT-2 to endosomes (Brown et al., 2000; Brown et al., 2002), changes in intracellular Ca^{2+} (Haigh and Phillips, 1993; Mundorf et al., 1999), excitatory current conductance via DAT (Ingram et al., 2002), and activation of surface receptors such as trace amine-associated receptor 1 (TAAR1) (Cotter et al., 2015), α-2 adrenergic receptors (Ritz and Kuhar, 1989), and nicotinic acetylcholine receptors (nAChRs) (Liu et al., 2003).

Methamphetamine-induced vesicular dopamine release:

There is some evidence to support the less commonly considered hypothesis that METH causes an increase in vesicular DA release. Using *in vivo* single-unit recording of rat VTA DA neurons, Shi et al. showed that AMPH induces heightened excitatory bursting and overall firing

rate, which is masked by D2R auto-inhibition (Shi et al., 2000). The excitatory effect was itself shown to occur in a DA receptor-independent manner. Later studies using FSCV revealed the ability of AMPH to activate phasic DA transients in mice *in vivo* and suggested a mechanism involving facilitated vesicular DA release (Covey et al., 2013; Daberkow et al., 2013). These studies reported an increase in striatal evoked DA release following intraperitoneal injection (i.p.) of AMPH. Additionally, spontaneous DA transients were shown to increase in amplitude and frequency with AMPH exposure. Schmitz et al. revealed that AMPH has an indirect effect of up-regulating D2R auto-inhibitory activity in striatal mouse brain slices (Schmitz et al., 2001). Interestingly, pre-treating VTA dopaminergic neurons *in vivo* with tetrodotoxin, a voltage-gated Na^+ channel antagonist used to inhibit action potentials, prevents AMPH-induced tonic DA elevations in mice altogether (Covey et al., 2016).

There is disagreement, however, whether this is evidence of an AMPH-induced increase in vesicular DA release or simply an artificial result of DA uptake inhibition. DAT knockout (KO) mice show a complete absence of AMPH-induced increases in extracellular DA concentrations, implying that the effect is DAT-dependent and, therefore, likely results from prototypical efflux though DAT (Siciliano et al., 2014). One hypothesis put forth by Covey et al. attempts to reconcile these paradoxical findings by claiming that AMPH up-regulates vesicular release of DA from readily-releasable DA vesicle pools while exerting its vesicular depletion effects on reserve DA pools (Covey et al., 2013).

It is worth pointing out that since METH seems to block DAT at low doses and must be present in high doses to reverse DAT function, it is possible that a separate mechanism leading to increased vesicular release of DA may also be dose-dependent. Furthermore, such an effect may be masked by the amount of DA efflux and vesicular depletion seen with high doses. Nevertheless, this remains a highly contested topic in AMPH research, which carries with it very important implications as DA transients are critical in reward-based learning and drug reinforcement (Stuber et al., 2005; Steinberg et al., 2014). Moreover, Calipari et al. and Ferris et al. have suggested that goal-directed behavior is driven by the ratio of phasic DA release to baseline DA concentration, rather than simply the overall DA level (Calipari and Ferris, 2013). The second part of this study provides data in support of an increase in vesicular DA release in response to METH as well as a mediating function of pre-synaptic D2R.

Selenium and the brain

Se is a nutritionally essential trace element with a variety of biological functions. It has been implicated in antioxidant defense, inflammatory response, thyroid hormone metabolism, and fertility (Brenneisen et al., 2005; Moghadaszadeh and Beggs, 2006; Youn et al., 2008; Schomburg, 2011). Epidemiological studies have indicated a protective role for Se in cancer, HIV progression, age-related mortality, and neurodegenerative disease (Beck et al., 2003; Akbaraly et al., 2005; Rayman, 2005; Brigelius-Flohe and Banning, 2006). Se is particularly important for proper brain function, primarily through its antioxidant functions (Chen and Berry, 2003; Steinbrenner and Sies, 2013).

Selenoprotein transcription and expression:

Se primarily exerts its physiological functions through the actions of a family of proteins called selenoproteins, which contain Se in the form of the 21st amino acid, selenocysteine (Sec) (Reeves and Hoffmann, 2009). Selenoproteins are synthesized through a process that involves the re-programming of the UGA stop codon to instead cause the insertion of a Sec residue (Allmang et al., 2009; Donovan and Copeland, 2010). Selenoprotein mRNAs contain a stem-loop structure downstream from the UGA codon on the 3' untranslated region (UTR) called the Sec insertion sequence (SECIS) element. which is necessary for and controls the efficiency of Sec insertion (Latreche et al., 2009). The process also requires the recruitment of several proteins and factors, including a unique tRNA (Sec-tRNA$^{[Ser]Sec}$), the alternative elongation factor EFsec, and SECIS-binding protein 2 (SBP2) (Bulteau and Chavatte, 2015).

Selenoprotein production is largely dependent on the availability of dietary Se. Early studies with radioactive [^{75}Se]selenite labelling in rats revealed that under Se-deficient conditions, Se supply is preferentially retained in the brain, reproductive, and endocrine organs (Behne et al., 1988). It was also noted that expression of certain Se-containing proteins also seemed to be differentially affected by Se deficiency. It was eventually found that while GPx1 mRNA levels fall dramatically in response to Se deficiency, Sepp1 and iodothyronine deiodinase 1 (Dio1) mRNA levels were less affected by Se scarcity (Hill et al., 1992). Furthermore, protein levels decreased to a much greater extent than their respective mRNAs, suggesting regulation at the translational level. This suggests a 'hierarchy' in selenoprotein expression and a high priority for Se utilization in the brain. Indeed, multiple studies have revealed details of the 'hierarchy', as well

as multiple ways it is imposed by Se availability (Sunde and Raines, 2011). Additionally, selenoproteins undergo degradation through nonsense-mediated decay (NMD), a process to eliminate aberrant mRNA, in which some selenoprotein transcripts are more vulnerable to than others (Seyedali and Berry, 2014).

Neuroprotective role of Selenium:

Within the brain, an important role of Se is protecting against oxidative stress through reactive oxygen species (ROS) and reactive nitrogen species (RNS) scavenging (Spallholz, 1990). The brain is especially vulnerable to oxidative stress due to its high demand for oxygen and relatively low amounts of antioxidants (Rayman, 2012). Generally, Se has been shown to have a protective affect through selenoproteins against neurodegenerative disorders such as Alzheimer's disease (AD), Parkinson's disease (PD), Huntington's disease, and amyotrophic lateral sclerosis (ALS). While Se neuroprotection has largely been attributed to antioxidant capabilities of particular selenoproteins, other mechanisms include preventing Ca^{2+} influx and anti-inflammation via NF-$_K$B inhibition (Santamaria et al., 2005; Demirci et al., 2017; Kahya et al., 2017). Se may protect against glutamate-induced excitotoxicity, also by inhibiting NF-$_K$B (Savaskan et al., 2003).

While Se protects the brain from numerous sources of damage, high Se treatment can also be detrimental. Case studies on Se exposure have linked it to a multitude of motor symptoms including ataxia, paralysis, tremors, and hyperreflexia as well as mental conditions such as irritability, depression, and lethargy (Civil and McDonald, 1978; Ammar and Couri, 1981; Wilson et al., 1988). Pigs exposed to high Se levels develop paresis and bilateral lesions in brain stem motor nuclei (Wilson et al., 1983). Overall, not much research has been done on Se-induced toxicity.

Selenium and neurotransmission:

There is some evidence to suggest that Se status can cause changes to neurotransmission. While Se can decrease glutamatergic excitoxicity, not much has been revealed about how it influences glutamatergic transmission specifically. Interestingly, the seleno-organic GPx mimetic ebselen can both increase and decrease synaptic glutamate uptake rates when delivered at concentrations of 1 and 10 µM, respectively, in rat brain synaptosome preparations (Porciuncula et al., 2004). Treatment with 10 µM ebselen also showed an inhibition of H^+-ATPase activity,

potentially through oxidation of thiol groups on the proton. Ebselen can also inhibit glutamate uptake in rat cortical slices at 100 µM (Moretto et al., 2007). These effects could involve a redox modulation of one or more proteins involved in glutamate transport.

The ability of Se to influence neurotransmission may also involve the GABAergic system (Solovyev, 2015). Pitts et al showed that Sepp1-KO mice have a reduced number of GABAergic parvalbumin (PV)-interneurons in the inferior colliculus (IC). This is potentially caused by increased oxidative stress within these highly metabolically active cells. Another study showed that ablating selenoprotein synthesis in the forebrain of CamKII-Cre mice via conditional KO of the tRNA[Ser]^{Sec} gene, causes a reduction of PV interneurons in the HPC and cortex (Wirth et al., 2010). Interestingly, PV-interneurons were shown to express ApoER2, suggesting a potential role for Sepp1-ApoER2 interactions in protecting GABAergic neurons (Pitts et al., 2012). Genetic KO of both Sepp1 and the catabolic enzyme selenocysteine lyase (Scly) revealed further degeneration of GABAergic neurons and neurological dysfunction, including audiogenic seizures which may occur due to the loss of the PV-interneuron role in synchronicity (Byrns et al., 2014; Pitts et al., 2015).

The cholinergic (ACh) system is also vulnerable to loss of Se and selenoprotein function as SBP2-KO mice suffer from cholinergic neuron loss in striatum (Seeher et al., 2014). These results represent the importance of Se in the development and protection of the GABAergic and cholinergic system. Although these are not examples of direct interaction, the implication is that overall neurotransmission dysfunction may arise from loss of Se neuroprotection. While the exact underlying mechanisms remain unelucidated, they likely involve protection from oxidative stress.

Supplementing mice with selenite induces anti-inflammatory action via prostaglandin E1 receptor and improves mitochondrial function in hippocampal cells (Mendelev et al., 2012; Rehni and Singh, 2013). In rat striatum, selenite supplementation elevates cholesterol and total lipid levels in a dose-dependent manner (Zia and Islam, 2000). These various effects should be considered in any study concerning Se and neurotransmission. Although this study focuses exclusively on dopaminergic effects in the NAc, changes to other types of neurotransmission could also affect DA and vice-versa. Therefore, other neurotransmitters must be considered as potential mediators of the observed actions of Se.

Dopamine and Selenium

There is considerable evidence that Se modulates the dopaminergic system. Castano et al. reported that 2 weeks of Se deficiency caused an increase in DA turnover in the prefrontal cortex (PFC) of Wistar rats (Castano et al., 1997). The increase in DA turnover was accompanied by an increase in DOPAC turnover, an increase in TH activity, but not TH protein expression, and a decrease in GPx activity. Subsequent studies by the same investigators reported Se deficiency-induced increases in DA turnover in substantia nigra (SN) and hippocampus (HPC) (Castano et al., 1993; Castano et al., 1995). A few years later, Romero-Ramos et al. reported an increase in DA, TH mRNA, TH activity, DAT mRNA, and DAT activity in rat striatum following the same length of Se deficiency (Romero-Ramos et al., 2000).

The increase in DA turnover was hypothesized to be the result of reduced GPx activity, based upon previous reports that impairment of the glutathione (GSH) system can increase DA turnover. For example, human melanoma cells exhibit an increase in TH activity under conditions of GSH depletion and Cys deprivation (del Marmol et al., 1993; del Marmol et al., 1996). In rat PC12 cells, reduced levels of GSH causes inhibition of vesicular DA storage and a subsequent increase in DA turnover (Drukarch et al., 1996). Interestingly, the VMAT-2 inhibitor reserpine, which depletes vesicular DA stores, also causes increases in both DA turnover and TH mRNA production in midbrain dopaminergic cells (Spina and Cohen, 1989; Pasinetti et al., 1990).

While multiple studies have reported greater DA turnover caused by Se deficiency, similar results have also resulted from high levels of Se supplementation. Rasekh et al reported that i.p. injection with 3 mg/kg selenite caused an over-potentiation of DA activity that could be suppressed by pre-treatment with the D2R agonist quinpirole (Rasekh et al., 1997). It is possible, therefore, that excessive DA activity may mediate the neurotoxic effects of both Se deficiency and Se over-supplementation. Moreover, D2R auto-inhibition of DA release may underlie the interaction between Se and the DA system. This study seeks to contribute to a more thorough understanding of the relationship between Se and DA signaling.

Selenium neuroprotection against methamphetamine

The neurotoxic effects of METH are well-studied and have long been known to occur primarily at DA terminals in the striatum (Ricaurte et al., 1980; Wagner et al., 1980). METH causes neurotoxicity through the production of ROS at DA terminals (Cadet et al., 1998). This is thought

to result from excessive of DA auto-oxidation, which produces hydrogen peroxide (H_2O_2) and superoxide (O_2^-) (Cubells et al., 1994; LaVoie and Hastings, 1999).

Repeated METH exposure greatly depletes the DA system, eventually leading to increased anxiety and symptoms of psychosis, likely the result of neurodegeneration. Although oxidative stress caused by DA auto-oxidation is likely the main mediator of METH-induced neurotoxicity, the precise mechanisms underlying DA terminal-specific damage have not been fully characterized (Miyazaki and Asanuma, 2008).

Se has been shown to protect against the neurotoxic effects of METH, indicating a potential for selenoproteins to counter the molecular actions of METH (Imam et al., 1999; Kim et al., 1999). While Se supplementation protects against METH-induced toxicity, Se deficiency potentiates METH toxicity *in vitro* in SH-SY5Y cell cultures (Barayuga et al., 2013). Decreased GPx protein levels and activity are suspected mediators.

Multiple molecular processes have been proposed to underlie METH-induced neurotoxicity, which could also provide targets for the protective actions of selenoproteins. Mitochondrial dysfunction may play a role through the activation of caspase-dependent and -independent apoptotic cascades (Cadet et al., 2003). Mitochondria are present in nerve terminals and are vulnerable to H_2O_2-induced oxidative stress (Chinopoulos and Adam-Vizi, 2001). The selenoprotein glutathione peroxidase 4 (GPx4) and thioredoxin reductase 2 (TxnR2) are involved in regulating mitochondrial redox regulation and may protect against mitochondria-induced apoptosis (Reeves and Hoffmann, 2009).

The precise mechanisms through which Se protects against METH-induced neurotoxicity are not fully understood, although redox signaling is likely to be involved. It is also possible that selenoproteins may mediate the effects of METH on DA signaling, however, given the potential involvement of Se in DA transmission. Identifying the physiological effects of Se will help identify potential key targets of interest for therapeutic treatment of METH toxicity and abuse. The current study investigates the specific contributions of GPx and Sepp1 activity.

Glutathione Peroxidase

GPxs are a class of selenoenzymes responsible for reducing H_2O_2 and a variety of hydroperoxides by using GSH as a reductant, thus playing a significant role in protecting cells from oxidative stress (Ursini et al., 1995). GPx activity relies on a tetrad catalytic center that

contains one Sec residue (Epp et al., 1983). The main reaction involves a selenol group (-SeH), which interacts with H_2O_2 and becomes oxidized to form a selenic acid intermediate (-SeOH). Selenic acid is then reduced by 2 GSH molecules in a process that involves the formation of a glutathionylated selenol (Se-SG) intermediate. This process results in the formation of glutathione disulfide (GS-SG), eventually reduced by enzyme glutathione reductase, and two H_2O molecules (Toppo et al., 2009).

GPx1, the first selenoprotein identified, is a highly abundant peroxide scavenger considered to be the prototypical GPx (Rotruck et al., 1973; Lei et al., 2007). GPx1 primarily reacts with H_2O_2 as well as some soluble hydroperoxides (Flohe, 1988). Although GPx1-KO mice develop normally, they are susceptible to acute oxidative stress induced by paraquat injection, even when supplemented with dietary Se (Ho et al., 1997; Cheng et al., 1998). GPx1 expression is highly dependent on Se status, giving it a very low ranking in the selenoprotein 'hierarchy' (Sunde et al., 2009). Due to its antioxidant defense capabilities, GPx1 may play a role in protecting the brain against neurodegenerative processes. Post-mortem tissue studies have suggested GPx1 to play a neuroprotective role in Parkinson's disease (PD) and dementia with Lewy Bodies (DLB) (Powers, 2009).

GPx4 is another antioxidant enzyme with a broad substrate specificity compared to other GPxs that includes hydrogen peroxide. Its main substrates, however, are phospholipid hydroperoxides produced in membranes, which GPx4 reduces to their corresponding alcohols (Conrad et al., 2007). GPx4 also uses GSH as a reductant, despite lacking the GSH binding sites native to GPx1, and carries out a similar catalytic mechanism (Aumann et al., 1997; Ursini et al., 1997). GPx4 is less dependent on GSH as a reducing substrate, however, as it can also make use of protein thiols (Conrad et al., 2007).

GPx4-KO is embryonic lethal, highlighting the importance of GPx4 function (Yant et al., 2003). Interestingly, developmental retardation of the brain appears to be involved in the mid-gestation death of Gpx4-KO embryos (Ufer et al., 2008). Tamoxifen-inducible GPx4-KO mice die within 2 weeks of injection and suffer from HPC neuronal loss and astrogliosis (Yoo et al., 2012). Moreover, GPx4 is downregulated in an Alzheimer's disease mouse model that overexpresses the amyloid precursor protein (Yoo et al., 2010). Elevated lipid hydroperoxide by-products are a common trait amongst neurodegenerative diseases, further indicating the importance of GPx4 lipid hydroperoxide-reducing actions.

Glutathione Peroxidase interactions with methamphetamine:

GPx helps protect against METH-induced neurotoxicity through its peroxide scavenging capabilities. METHs neurotoxic effects are thought to result primarily from a sudden, dramatic increase in extracellular DA concentrations. In these conditions, auto-oxidation and metabolic breakdown via MAO both produce O_2, OH, and H_2O_2, causing oxidative stress (LaVoie and Hastings, 1999; Yoo et al., 2010; Halpin et al., 2014). GPx provides an important antioxidant defense against these ROS. As previously stated, METH appears to downregulate GPx expression and activity implying a special role of this selenoprotein.

GPx may also affect responses to METH at DA terminals, as H_2O_2 itself functions as a signaling molecule. H_2O_2 inhibits evoked DA release in mouse striatal slices through the activation of ATP-sensitive K^+ (K_{ATP}) channels (Avshalumov and Rice, 2003; Avshalumov et al., 2005). K_{ATP} channels couple metabolic activity to electrical activity by closing in response to an increase in the intracellular ATP/ADP ratio (Rubaiy, 2016). Depolarization induces Ca^{2+} influx via VGCCs, a preceding event of action potential generation and subsequent neurotransmitter release (Zamponi, 2016). K_{ATP} channel activation, on the other hand, generates polarization through K^+ outflow and attenuates neurotransmitter release (Kawano et al., 2009).

The mechanism of K_{ATP} channel suppression of DA release is proposed to result from endogenous H_2O_2 produced by AMPAR excitation, but can also be experimentally induced with exogenous H_2O_2 application. Specifically, this was shown to be mediated by K_{ATP} channels that have the sulfonylurea receptor 1 (SUR1) subunit, which are directly inhibited by the sulfonylurea drug glibenclamide (Hussain and Cosgrove, 2005). Therefore, GPx activity may mediate METH-induced increases in DA signaling by regulating an inhibitory control on DA release. Specifically, GPx may prevent the suppression of DA release by excess levels of H_2O_2 typically produced in the presence of METH. The first part of our study explores this possibility.

Role of Selenoprotein P in the Brain

Selenium delivery:

Sepp1, the second selenoprotein identified in animals, is a secreted glycoprotein and is unique amongst selenoproteins in both its structure and function (Herrman, 1977). Sepp1 contains 10 Sec residues, 1 on the larger N-terminal domain and 9 on the smaller C-terminal domain (Fig.

1-3). Sepp1 accounts for over 50% of the total Se in mouse and rat plasma (Burk and Hill, 1999; Hill et al., 2003; Reeves and Hoffmann, 2009). Its high Se content suggests it acts as a Se transporter and many studies have confirmed this role. For example, cells cultured in human serum depleted of Sepp1 experience reduced GPx activity, which is restored upon addition of Sepp1 to the media (Saito and Takahashi, 2002).

Sepp1 is mainly produced in the liver where it can then enter the bloodstream and deliver Se to different parts of the body (Burk and Hill, 2009). Sepp1 mRNA have been found in many different tissue types, including glia, and Sepp1 is presumed to be produced in low levels in these locations (Burk and Hill, 1994; Zhang et al., 2008). Genetic Sepp1 deletion decreases Se levels in many tissues in mice with the most profound effects seen in the brain and testes (Burk and Hill, 2009). Expression of Sepp1 itself is considerably sensitive to Se availability (Savaskan et al., 2007). Interestingly, Se deficiency induced by Sepp1 deletion increases Se levels in the liver in a gene-dose-dependent manner consistent with a drop in Se turnover caused by Sepp1 synthesis.

Se delivery to the brain involves endocytosis mediated by Sepp1 binding to the β-propeller domain of the surface protein Apolipoprotein E receptor 2 (ApoER2), expressed mostly in neurons (Kurokawa et al., 2014). The same Sepp1-ApoER2 interaction has been proposed to occur at the blood-brain barrier (BBB). In this scenario, the interaction allows Se to be transferred across the BBB and taken up by glia to be re-incorporated into Sepp1 and subsequently secreted to deliver Se to ApoER2-expressing neurons (Burk et al., 2014).

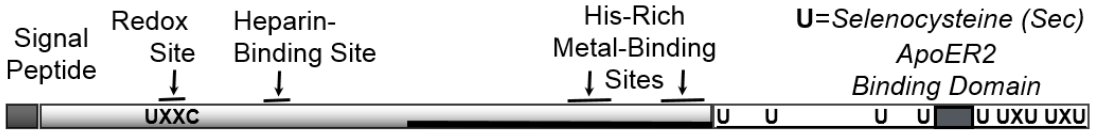

Figure 1-3. Sepp1 schematic diagram.
The N-terminal region of Sepp1 contains one Sec (U) residue within a UXXC thioredoxin motif with antioxidant properties. Also, on the N-terminal region are the heparin-binding site and the His-rich metal-binding sites. The C-terminal region contains 9 Sec residues, as well as the ApoER2 binding domain.

Antioxidant and other activity:

The N-terminal domain of Sepp1 contains 1 Sec residue in a thioredoxin-like redox motif which suggests it plays an antioxidant role as well (Fig. 1-3) (Arteel et al., 1998; Saito et al., 1999; Saito and Takahashi, 2002). The redox motif, which occurs at residues 40-43 and contains the

sequence Sec-XX-Cys, can carry out peroxidase activity (Fomenko and Gladyshev, 2003; Saito et al., 2004). The peroxidase activity of Sepp1 acts primarily on membrane hydroperoxides and uses thioredoxin as a reducing substrate (Saito and Takahashi, 2002; Takebe et al., 2002).

Sepp1 also has a heparin-binding domain comprised of residues 80-95 on the N-terminus (Herrman, 1977; Akesson and Martensson, 1991; Hondal et al., 2001), allowing binding to heparin glycoproteins. The heparin binding site is unique in its inclusion of histidine at basic residue sites and its sensitivity to pH (Chittum et al., 1996). These qualities, as well as the fact that Sepp1 does not bind heparin itself *in vivo*, but rather heparin sulfate proteoglycans, has led to the postulation that Sepp1 binds areas of inflammation under acidic conditions while remaining unbound at physiological pH (Burk and Hill, 2005).

The Sepp1 N-terminus also contains two histidine-rich regions (Arteel et al., 2000). These regions have also been theorized to play a role in Sepp1s heavy metal binding properties by providing a binding site. Sepp1 has been reported to bind metals such as copper, nickel, cadmium, and mercury presumably for detoxification (Yoneda and Suzuki, 1997; Sasakura and Suzuki, 1998; Sidenius et al., 1999). Sepp1 can also chelate zinc, which may play a role in cellular responses to METH (Chen and Berry, 2003; Aizenman et al., 2010).

Potential role of Sepp1-ApoER2 interactions

*ApoER2 influence on neural activity**:***

The focus of the current study on the role of Sepp1 in dopaminergic transmission is centered on interactions between Sepp1 and ApoER2. Sepp1 has been suggested to play a role in neurotransmission given that ApoER2 is important for synaptic transmission, long-term potentiation, and memory tasks (Weeber et al., 2002). ApoER2 has also been shown to be involved in dendritic spine formation in primary rat HPC cells (Dumanis et al., 2011). Interestingly, ApoER2 has been demonstrated to functionally associate with NMDARs (Beffert et al., 2005). Sepp1-KO mice perform poorly on spatial learning tasks, such as the Morris water maze, and display enhanced basal HPC synaptic transmission, reduced short-term plasticity, and absence of long-term potentiation in response to high-frequency stimulation (Peters et al., 2006). These alterations in synaptic plasticity and learning are typically attributed to the well-established effects of the ApoER2 ligand Reelin on NMDA receptor activity, but may also be influenced by a defect or loss of the Sepp1-ApoER2 interaction.

ApoER2 expression is most prevalent in the brain and testes, making it unique compared to other lipoprotein receptors that are highly expressed in multiple organs throughout the body (Nimpf and Schneider, 2000). ApoE itself is most abundantly expressed in the brain and is thought to mediate lipid transport for growth and injury repair in the brain (Weisgraber et al., 1994). Interestingly, certain ApoE alleles are major genetic determinants for risk of Alzheimer's disease (AD) (Liu et al., 2013).

ApoER2-mediated signaling:

ApoER2 is also known to bind several other ligands, mostly extracellular matrix proteins, to carry out a variety of functions. These include Reelin (involved in neuronal positioning during development, synaptogenesis and memory formation during adulthood) (D'Arcangelo, 2005; Lee and D'Arcangelo, 2016), thrombospondin-1 (involved in neuronal migration and survival) (Blake et al., 2008), F-spondin (involved in amyloid precursor protein processing) (Hoe et al., 2005), and clusterin (sperm maturation, subventricular zone neurogenesis) (Andersen et al., 2003; Leeb et al., 2014; Riaz et al., 2017).

Intracellularly, ApoER2 interacts with multiple proteins. The most investigated is the adapter protein Disabled-1 (Dab1), which binds ApoER2 on its C-terminal helix (Morimura and Ogawa, 2009). It is thought that Dab1 is recruited upon Reelin binding ApoER2 and is phosphorylated by either Src or Fyn kinases (Howell et al., 1997). These pathways have mostly been shown to mediate organizational effects through investigations into the role of Reelin in neurodevelopment. Dab1 activation can also increase surface localization of ApoER2 (Hoe et al., 2006).

Disabled-2 (Dab2) is thought to play a similar role to Dab1 in neurodevelopment and activates Src as well (Yang et al., 2002). It differs from Dab1, however, in that it can suppress the mitogen-activated protein kinase (MAPK) pathway and does not bind the very low density lipoprotein receptor (VLDLR) (Zhou et al., 2003). Dab2 also mediates ApoER2 internalization through direct binding at a separate site than that of Dab1 (Cuitino et al., 2005).

ApoER2 also binds other adaptor proteins and scaffolds, demonstrating a wide range of possible interactions within the cell. Interestingly, postsynaptic density protein 95 (PSD-95) is one such binding partner that forms a complex with ApoER2 that includes NMDA receptors (Beffert et al., 2005). The adaptor protein FE65 binds ApoER2 and forms multi-protein complexes. These

serve a range of functions, including cytoskeleton regulation and mediation of gene transcription events. The ability of ApoER2 to bind multiple adaptor proteins and scaffolds in combination with its internalization function, introduces a wide range of possibilities downstream from Sepp1-ApoER interaction.

Potential role in neurotransmission:

There is some evidence that presynaptic ApoER2 is involved in neuronal signaling (Barger, 2013). NMDAR phosphorylation occurs on the NR2A and NR2B subunits upon acute Reelin application to HPC slices in a Src-dependent manner (Hoe et al., 2006). Chronic Reelin administration results in increased AMPA receptor surface expression in HPC post-synaptic terminals (Qiu et al., 2006). While most studies addressing the involvement of ApoER2 in neurotransmission primarily focus on glutamatergic activity, there is some evidence to suggest a role in DA release. Activation of rat striatal presynaptic NMDA receptors stimulates DA release in a Ca^{2+}-dependent manner (Wang, 1991). Interestingly, ApoER2 is known to functionally associate with N-methyl-D-aspartate (NMDA) glutamate receptors (Beffert et al., 2005), which may be present on presynaptic DA terminals (Johnson and Jeng, 1991; Krebs et al., 1991).

One study on postmortem PD brain tissue revealed Sepp1 to be present in dopaminergic terminals in human striatum as well as cell bodies in midbrain (Bellinger et al., 2012) implying the possibility of Sepp1-ApoER2 interactions at these sites. Therefore, Sepp1-ApoER2 interactions have the potential to cause changes to dopaminergic terminals via ApoER2-induced cellular responses. The second part of this project explores this possibility in the context of dopaminergic responses to METH.

Investigative Focus

In this study, tonic and phasic DA release were individually interrogated using FSCV techniques as described in the METHODS section. Regarding tonic DA, changes in response to pharmacological agents is simply referred to as a change in tonic release. The change in extracellular DA concentration in response to METH is mainly referred to in this study as DA efflux, as this is considered the primary means of METH-induced DA elevation. There remains a possibility, however, that METH may also influence the mechanisms underlying tonic DA release separate from DA efflux. Experiments were focused around interplay between GPx activity and

H_2O_2-K_{ATP} channel inhibition of DA release, and the possibility of this mechanism to contribute to the METH response.

Transient increases in extracellular DA upon electrical stimulation will be referred to as evoked or phasic DA release. This study uses phasic release to explore the functional relationship between Se and dopaminergic transmission. Phasic DA release is also modulated by METH, although the extent to which these effects are dependent on striatal mechanisms is unclear. This study uses dietary Se and Sepp1-KO mice to tease apart these underlying mechanisms. Specifically, we hypothesized that Se plays a direct role in reducing the dopaminergic effects of METH. We sought to test this hypothesis with the following aims: First, we determined the effects of short-term Se deficiency (2 weeks) on dopaminergic transmission and modulation by METH. Next, we further investigated the involvement of Se using a chronic Se deficiency model. Finally, we investigated the specific role of Sepp1 using a Sepp1 KO mouse model.

CHAPTER 2: MODEL SYSTEM AND METHODS

Model System

The purpose of this study is to investigate DA transmission using the electrochemical technique fast-scan cyclic voltammetry (FSCV) that records extracellular DA concentrations. FSCV can be performed both in brain slices and in live animals. This study utilizes striatal brain slice preparation, which has the advantage of providing a simpler context of local circuitry for the interpretation of results. Conversely, it removes the findings from the context of the overall neural system thereby obscuring physiological relevance. While slice voltammetry is overall a useful technique for studying local control of DA release there are some additional caveats to consider during the interpretation of results.

First, electrical stimulation elicits synchronized firing of a local population of NAc DA terminals. Therefore, a change in phasic DA release is simply interpreted as the potential strength of that local population to release DA in response to depolarization. Thus, an advantage of *in vivo* studies is the ability to record striatal activity with or without stimulating the cell bodies in VTA. Contributing factors to changes in evoked release in slices could include characteristics such as quantal size, Ca^{2+} availability, or even D2R activity as described in the present study. Furthermore, DA release from striatal terminals has been linked to the level of excitability of the VTA-resident cell bodies (Ferris et al., 2013).

Two different models of dietary Se deficiency are used: short-term (2 weeks) and chronic. Short-term Se deficiency is expected to decrease the activity levels of some selenoproteins, although not necessarily expression levels as Se is preferentially retained in the brain. As previously noted, GPx activity decreased in rodent striatum following 15 days of Se deficiency (Romero-Ramos et al., 2000). This time-frame of Se deficiency should not induce neurodegeneration. Chronic Se deficiency on the other hand is likely to cause neurodegeneration and brain Se content levels have been reported to decrease to 56% of controls (Burk and Hill, 2009). Consequently, general selenoprotein expression should be decreased in chronic Se deficient mice.

Animal Care and Usage

The animals used in this study were C57/BL6 J sub-strain mice aged 3-5 months, housed at the JABSOM vivarium. Male and female mice were found to have no differences in basic METH response and were, therefore, pooled together into the control group. For all experiments beyond controls, only male mice were used. All care and experimental procedures were approved by the UH Manoa Institutional Animal Care and Use Committee and conducted in accordance with the National Research Council's *Guide for the Care and Use of Laboratory Animals*. Littermates were group-housed up to 5 in a cage on a light/dark cycle and allowed access to food and water *ad libitum*.

Dietary Selenium:

Mice were raised on standard lab chow estimated to contain 0.25 ppm Se. For Chronic Se deficiency studies, mice were put on Se-deficient Torula Yeast (TY) Diet (Teklad) immediately post-weaning. For short-term Se-deficient conditions, mice were raised on standard lab chow until 3 months of age, then changed to Se-deficient TY Diet for 2 weeks immediately prior to experimentation or brain harvest. Moderate Se TY Diet containing 0.25 ppm Se (Teklad) was also utilized for control comparison.

Husbandry:

In Sepp1 KO studies, due to the infertility of Sepp1 KO male mice (Olson et al., 2005), breeding pairs

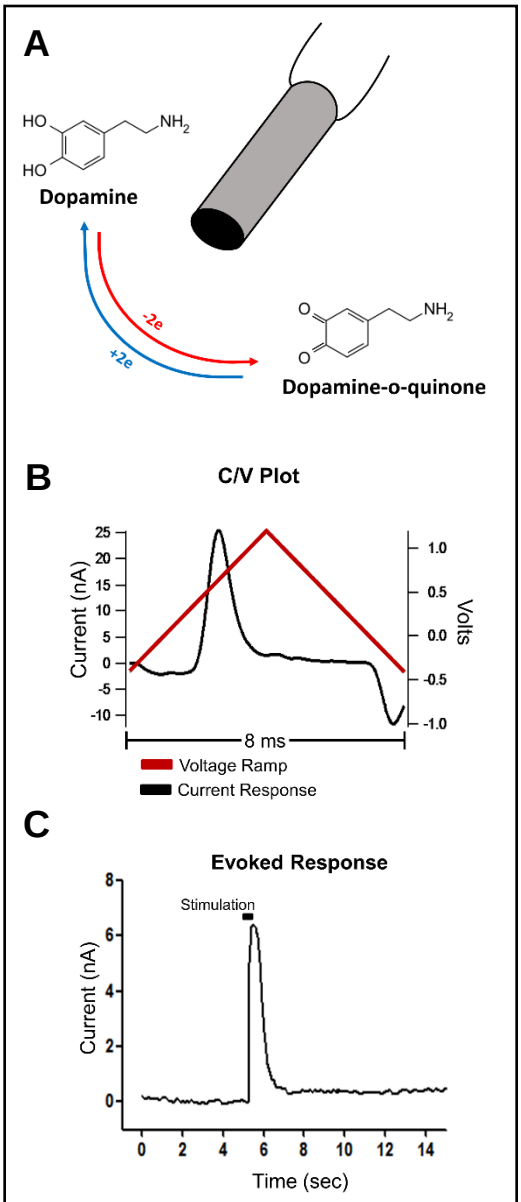

Figure 2-1. Fast-scan cyclic voltammetry. **A.** DA oxidation is induced, resulting in electron donation to a carbon-fiber electrode. **B.** C/V Plot showing current response to voltage ramp. DA oxidation occurs at 0.6V. **C.** Sample evoked DA response. Peak current values from C/V plots are taken at 10 Hz frequency. Stimulation elicits DA release, resulting in a large C/V plot peak. Current is converted to concentration following individual electrode calibration.

consisted of males heterozygous for Sepp1 deletion and female Sepp1 KO mice. Female breeders were raised on Se supplemented water containing 1mg/ml sodium selenite to support fertility.

Fast-scan Cyclic Voltammetry

Brain Slice Preparation:

Immediately following cervical dislocation without anesthesia, mouse brains were extracted and placed in ice-cold artificial cerebral spinal fluid (ACSF) consisting of: 130.00 mM NaCl, 3.50 mM KCl, 10.00 mM glucose, 24.00 mM $NaHCO_3$, 1.25 mM NaH_2PO_4, 1.50 mM $MgSO_4$, 2.00 mM $CaCl_2$ (Sigma), and bubbled with carbogen gas (95% O_2/ 5% CO_2). Coronal brain slices of 350 μm containing NAc were obtained using a Leica VT 1200 S vibrating blade microtome (Leica Microsystems). For some experiments, Ca^{2+}-free ACSF was made by replacing the 2.00 mM $CaCl_2$ with 1.00 mM EGTA (Sigma) as utilized in a previous study (Perez-Velazquez et al., 1994). Striatal slices were separated by hemisphere using a scalpel and placed into a slice incubation chamber containing oxygenated ACSF. Slices recovered at room temperature for 30 minutes, then transferred to a heated water bath at 33°C and allowed to equilibrate for at least 30 minutes prior to experimentation.

Voltammetric Recordings and Experimental Protocol:

For *ex vivo* FSCV experiments, brain slices were transferred to a slice recording chamber (Warner Instruments) and constantly perfused with oxygenated ACSF at 33°C at a flow rate of 3 mL/minute. For recordings, a carbon fiber electrode (CFE) was placed ~100 μm below the surface of the brain slice in the NAc shell using a Sutter MP-225 micromanipulator (Sutter Instrument) under the guidance of a microscope with a 10X objective lens (Nikon Corporation). The stimulating electrode was placed 100-200 μm from the tip of the CFE at the same depth of the CFE and a reference electrode was placed in the ACSF downstream from the slice. Extracellular DA concentrations were measured using a Dagan CHEM-CLAMP voltage clamp amplifier (Dagan Corporation). A command voltage (CV) was applied to the CFE and scanned linearly in a triangular waveform from -0.4 V to 1.2 V at a rate of 400 V/second (Fig. 2-1A). For stimulated DA release measurements, the CV was applied at a frequency of 10 Hz (every 0.1 seconds) and the resulting current response to each CV was measured to produce a cyclic voltammogram with a peak current response representing DA oxidation at its oxidation potential (~0.6V) (Fig. 2-1B).

The peak response occurred at the oxidation potential for DA, 0.6V, as previously reported (Yorgason et al., 2011). For non-stimulated DA release measurements, voltammograms were collected at a frequency of 0.5 Hz (every 2 seconds) in the absence of stimulation. Cyclic voltammograms were regularly referenced to confirm specificity of the current output to DA oxidation. Data were digitized using an NI-6221 analog-to-digital converter (National Instruments) and analyzed using the LabVIEW (National Instruments)-based software Demon Voltammetry (Yorgason et al., 2011).

DA release was evoked using a 10-pulse train of 0.5 ms stimulations (370 µA) at 20 Hz every 2 minutes using a WPI A365 Stimulus Isolator (World Precision Instruments) to simulate phasic DA release events (Ferris et al., 2013), with voltammograms collected for 1 minute epochs (Fig. 2-1C). After observing 30 minutes of stable baseline responses, METH was applied via perfusion in ACSF for 30 minutes, followed by washout with regular ACSF for another 30 minutes. In some experiments, other treatments were applied for at least 15 minutes prior to METH application and for total durations indicated in figures. To observe METH-induced DA efflux, DA release was first elicited via stimulation to confirm satisfactory placement of the electrodes near a population of DA terminals. Slices were then allowed to recover without stimulation for 30 minutes before beginning baseline recordings and, if stable baseline was observed, followed the same experimental timeline as in stimulated DA release experiments. Following washout of non-stimulated DA recordings, stimulated DA release was once again elicited to verify the sustained health and dopaminergic function of the selected area for the duration of the experiment. Data from experiments in which post-washout stimulation did not elicit DA release were not included in analysis.

Data Analysis:

Peak current heights were converted to DA concentrations using a conversion factor calibrated for each CFE. ACSF containing 10 µM DA•HCl was perfused into the slice chamber and the resultant current was recorded to yield the conversion factor (nA/µM) Multiple measurements taken from the current signal included signal amplitude, area under the curve (AUC), and rising slope.

Michaelis-Menten Analysis:

Data were also fit to a Michaelis-Menten-based curve-fitting model in the Demon Voltammetry software to provide further metrics of DA release and uptake: [DA]p, representing the average concentration of DA released per individual electrical stimulation pulse; Vmax, representing the maximal rate of uptake; Km, representing the apparent affinity of DA for DAT (Fig. 2-2) (Yorgason et al., 2011).

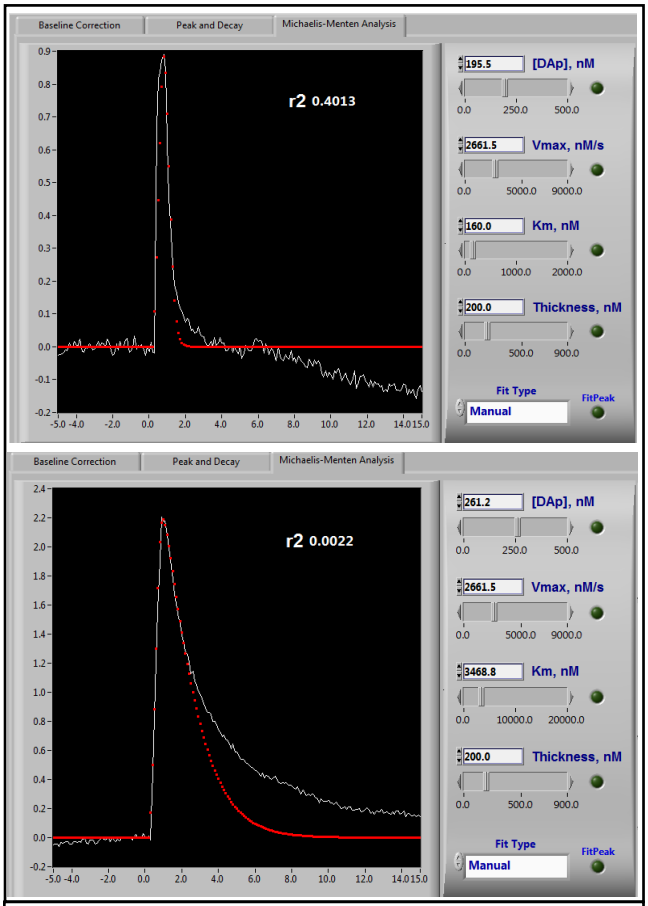

Figure 2-2. Curve-fitting model
The analytical model mathematically resolves the release and uptake components of the DA signal. Top panel: Baseline evoked DA signal with Vmax (maximal DA uptake rate) determined using Michaelis-Menten kinetics. Bottom panel: METH induces an increase in DA per pulse, [DA]p, representing vesicular release. METH also increases apparent Km, representing slower uptake rates.

For baseline recordings, the Km was adjusted to a default value of 160 nM in accordance with previous studies on the affinity of DA for DAT in rodent striatum (Wu et al., 2001). Vmax was measured at baseline and kept constant for the duration of experiments. Km was increased to model the slower DA signal decay exhibited upon METH application. Km was also used to monitor any potential effects on DA uptake rates by the various chemicals applied to the brain slices.

The limits of this model are that the variables generated are approximations made based upon some underlying assumptions. First, it is assumed that DAT is the primary mediator of DA uptake and that any other process of uptake that might occur is negligible. Second, saturation of total DAT must occur for an accurate measurement of Vmax, which may or may not occur from experiment to experiment. Finally, the diffusion of DA out of the synaptic release/uptake site is not accounted for and could occur due to DA overflow.

Electrode Fabrication and Calibration:

CFEs were produced by inserting a 7 µm diameter carbon fiber into a borosilicate glass capillary tube, OD: 1.2 mm, ID: 0.696 mm, L: 100 mm, (Hilgenberg) using negative air pressure. Carbon fiber-containing capillary tubes were then pulled on a David Kopf model 700B vertical pipette puller (David Kopf Instruments) and the protruding fiber cut to a length of 100 µm from the tip of the pipette. CFEs were calibrated by perfusing the electrode in the recording chamber with ACSF containing 10 µm DA•HCl (Sigma) and observing the maximum resultant current (nA) to produce a 'current to DA concentration' conversion factor. CFEs were backfilled with 3 M KCl.

Stimulating electrodes were pulled on a Sutter P-1000 Flaming/Brown micropipette puller (Sutter Instrument) using borosilicate glass capillary tubes, OD: 1.5 mm, ID: 0.86 mm, L: 100 mm, (Sutter Instrument) and the tips were broken to yield a 50 µm diameter opening. Stimulating electrodes were backfilled with ACSF.

Pharmacological Treatments:

Drugs and purified proteins were diluted in ACSF and delivered via perfusion during experiments. METH was used at a working concentration of 10 µM. Concentrations of other agents are indicated in the RESULTS sections.

The following chemicals were used: AM630 (Sigma, SML0327); Ebselen (Sigma, E3520); GBR 12909 (Sigma, D052); Glibenclamide (Sigma, G0639); Hydrogen peroxide (Certified ACS) (Fisher Scientific, H325); Mercaptosuccinate (MCS, Sigma, M6182); Quinpirole (Sigma, Q102); Rimonabant hydrochloride (Sigma, SML0800); RSL3 (MedChem Express, HY-100218A); Sulpiride (Sigma, S8010); WIN 55,212 mesylate salt (Sigma, W102). Stock solutions were made up in Milli-Q water at 10,000X concentration to minimize any potential effect on the osmolarity of ACSF chemical components. MCS was made to 100X and, therefore, dissolved in ACSF instead of water. Ebselen, glibenclamide, and RSL3 were dissolved in DMSO and vehicle control experiments completed due to the tendency of DMSO to damage neurons as high enough concentrations (Hanslick et al., 2009; Yuan et al., 2014).

Brain Harvest and Dissection

Harvest:

Mice were sacrificed via cervical dislocation and brains were immediately extracted and fresh-frozen. Upon removal from skull, one cut was made to split the brain into left and right hemispheres. Each hemisphere was immediately placed medial side down on a thin glass slide on top of powdered dry ice in a Styrofoam box and the cover closed to freeze the tissue. Protein was later extracted from right hemispheres for use in western blotting. All animal procedures were approved by the University of Hawaii Institutional Care and etc (IACUC, protocol number 742-10).

Dissection:

Prior to tissue lysis, ventral midbrain and ventral striatum were dissected for protein extraction. Dissection was performed at -20° C using a razor blade to make anatomical landmark-guided cuts. Cuts were made in the following order: 1) sagittal cut ~1/3 from midline and lateral portion removed, 2) horizontal cut (through rostral tip of corpus callosum and dorsal side of 4th ventricle) and dorsal portion removed, 3) coronal cut (through posterior side of interpeduncular fossa and posterior side of superior colliculus) and posterior portion removed, 4) 1mm anterior and parallel to 3rd cut and posterior portion containing ventral midbrain kept and stored separately, 5) coronal cut 60° from dorsal surface and 1mm posterior to the posterior end of the olfactory bulb and the anterior portion removed, and 6) 1mm posterior and parallel to 5th cut and the anterior portion containing ventral striatum kept and stored separately. All other brain parts were kept for future studies.

Protein Extraction:

Dissected brain parts were pulverized using the CryoGrinder kit (OPS Diagnostics). The ceramic mortar was placed on powdered dry ice along with a ceramic pestle and metal scooper, covered and allowed to equilibrate for 10 minutes. Next, the individual brain part was placed in the mortar and ground into powder using the pestle attached to a Black and Decker drill. One half of the powder was added to a tube containing 300 µL CelLytic MT Mammalisn Tissue Lysis/ Extraction Reagent (Sigma) containing 1:100 protease inhibitor cocktail (Sigma) while the other half was placed in an empty tube for future studies.

Lysis buffer with suspended tissue was sonicated with 20 one-second pulses at 5 Hz, separated by one second each, using a Fisher Sonic Dismembrator Model 100 (Fisher Scientific). Samples were then centrifuged at 14,000xg for 10 minutes at 4°C. Supernatant was collected and stored at -80°C for western blotting.

Western blotting

Tissue lysate samples containing 40 µg of protein were separated on 4-20% gradient polyacrylamide TGX gels (BIO-RAD, 5671094) via electrophoresis and transferred to 0.45 µm pore size Immobilon-FL polyvinylidene difluoride membranes (Millipore, IPFL00010). Membranes were incubated in PBS-based blocking buffer (LICOR, P/N 927) for 1 hour and then probed with primary antibodies for 1.5 hours, followed by washing with PBS containing 0.01% Tween 20 (Fisher Scientific, BP337) (PBS-T). Blots were incubated with infrared fluorophore-bound secondary antibodies in the dark, washed again with PBS-T, and analyzed using the Odyssey Imaging System (LI-COR Biosciences).

Antibodies:

Primary antibodies used for western blotting were: rabbit anti-TH (Cell Signaling, 2792); rabbit anti-DAT (Millipore, AB2231); rabbit anti-VMAT-2 (Millipore, AB 1598P; goat anti-GPx1 (R&D Systems, AF 3798); rabbit anti-GPx4 (Epitomics, 3649-1); mouse anti-αTubulin (Invitrogen, 62204).

Secondary antibodies used for western blotting were LI-COR IRDye highly cross-adsorbed antibodies optimized for use with the Odyssey Imaging System: 680LT donkey anti-mouse (926-68022), 80CW goat anti-mouse (926-32210), 680LT donkey anti-rabbit (925-68023), 800CW goat anti-rabbit (926-32211), 800CW donkey anti-goat (926-32214).

Sepp1 Protein Purification

Sepp1 protein was purified from WT C57/BL6 mouse serum using an antibody affinity column previously prepared by Suguru Kurokawa in the Berry lab. Monoclonal Sepp1 antibody (9S4) was coupled to AminoLink Plus Coupling Resin (Pierce) and applied to a 10 mL serological pipette.

Serum was first diluted 1:2 in chilled PBS and centrifuged at 14,000 g for 10 minutes at 4°C and the supernatant containing protein collected. Supernatant was run through the column, followed by a brief rinse with PBS. Next, 1 M NaCl was applied to the column, followed by another PBS rinse. 50 mM glycine pH 2.5 was then run through the column to remove Sepp1 from its bound state and the eluate collected in 1 mL fractions in tubes containing 1 M Tris pH 8.0. Fractions were tested for protein content by adding 5 µL of eluate to 10 µL drops of Bradford Assay Reagent to observe color change to blue indicating the presence of protein. After all fractions were collected, column was rinsed with PBS until wash out reached a pH of at least 7.4.

The fraction from each elution that contained the most protein was selected and used to produce concentrated Sepp1 for experimentation. Fractions were concentrated to 1 mL of stock protein using a Vivaspin Centrifugal Concentrator (Sartorius). The Sepp1 concentration was calculated from the absorbance at 280 nm measured using a NanoDrop ND-1000 Spectrophotometer (Thermo Scientific). The stock concentration was 3.6 µM.

Sepp1 mutants were generated as previously described and provided by Dr. Kurokawa at Osaka Ohtani University (Kurokawa et al., 2014). The full-length all-Cys mutant is full-length Sepp1 with Sec residues changed to Cys residues. The N-terminal fragment (NT) mutant is an all-Cys Sepp1 N-terminal peptide lacking the C-terminal region. The Δ234-237 mutant is a full-length all-Cys Sepp1 with an essential region of the ApoER2 binding domain deleted, thus it is unable to bind ApoER2.

Data Analysis and Statistics

For phasic DA release experiments, peak DA oxidation currents were extracted from individual voltammograms occurring at a 10 Hz frequency. These values were plotted over time to monitor DA release in response to stimulation and uptake via DAT. Baseline measurements are current averages for the duration of baseline (30 minutes) and converted to DA concentration. Statistical comparisons were made using the peak signal in response to the first stimulation after adding METH, which was typically the largest peak. Data for tonic DA release varied in time course from experiment-to-experiment. Therefore, the maximum current during the entire METH exposure (30 min) was extracted and used for comparison, unless a specific time-point was noted.

Data are represented as mean ± SEM in data graphs. Single replicates were taken from separate biological specimens. One-way ANOVA was used for between-subject group comparisons. Tukey's multiple comparisons test was used for post-hoc analysis. Otherwise, unpaired t-test was used to compare sets of 2 groups. The following criteria were used for significance: at $p < 0.05$ (*), $p < 0.01$ (**), $p < 0.001$ (***), and $p < 0.0001$ (****)
All statistical analysis was executed in GraphPad Prism 6 software (GraphPad Software, Inc.).

CHAPTER 3: SHORT-TERM EFFECTS OF SE DEFICIENCY ON THE DOPAMINE SYSTEM

Abstract

Mice put in a Se-deficient diet exhibit reduced amount of METH-induced DA efflux, which can be potentiated by the GPx mimetic ebslen. GPx enzymatic activity inhibition also reduced DA efflux. The suppressive effect of GPx inhibition in DA efflux can be partially reversed by K_{ATP} channel blockade and CB1R antagonism. These results suggest that GPx4 inhibition can reduce DA efflux through mechanisms involving elevated H_2O_2 and lipid-peroxide-induced endocannabinoid signaling.

Introduction

Short-term (15 day) dietary Se restriction has been shown to affect DA turnover rates in the rodent brain, indicating that Se plays an important role in the DA system (Romero-Ramos et al., 2000). Se also protects against METH-induced neurotoxicity in cell and rodent models, presumably through antioxidant defense (Kim et al., 1999; Barayuga et al., 2013). We used FSCV to investigate the role of dietary Se on phasic DA release and uptake. We also measured action potential-dependent and -independent DA responses during METH challenge to reveal the mediating role of Se in METH-induced DA efflux. GPx is a potential mediator of the protective effects of Se and may affect the physiological response to METH though its influence on redox balance (Spanos et al., 2013). We used pharmacogical agents to evaluate the contributions of GPx activity to dopaminergic METH responses and explore possible underlying mechanisms of such interactions. Futhermore, we investigated the mediating role of K_{ATP} channel activity and the endocannabinoid system.

Methods

Male C57/BL6 J-background wild-type mice (aged 3-5 months) were placed on a Se-deficient diet lasting 2 weeks to be compared to control mice fed a Se-sufficient diet. The 2-week period was chosen in order to restrict selenoprotein activity without causing long-term neurodegenerative effects (Castano et al., 1997). FSCV was performed in live NAc brain slices

as described in the METHODS section to measure phasic and tonic DA events before and during 30 minutes of 10 μM METH application.

Phasic DA release was measured through the detection of transient increases in extracellular DA concentration on a sub-second timescale following electrical stimulation every 2 minutes. DA uptake was evaluated using Michaelis-Menten analysis of the transient DA signal. Extracullar DA concentration was also measured continuously in the absence of stimulation to detect METH-induced DA efflux. METH was delivered to slices via perfusion with ACSF after 30 minutes of stable baseline recording for both phasic and tonic DA measurements.

The GPx mimetic ebselen was applied to slices of Se-deficient mice in order to restore GPx activity and evaluate its effect on METH-induced DA efflux. GPx inhibitors MCS and RSL3 were also utilized to investigate a potential role of GPx activity. To evaluate the role of Ca^{2+} influx, which controls DA release and is affected by redox signaling, METH responses were recorded in the presence of Ca^{2+}-free ACSF. Glibenclamide was also used to inhibit K_{ATP} channels, another moderator of DA release and potential target of GPx activity (Avshalumov and Rice, 2003).

The endocannabinoid system, which was recently suggested as an essential mediator of METH-induced DA efflux, was manipulated using the non-specific CB receptor agonist WIN55,212-2 (WIN55) and the CB1R antagonist rimonabant (RIMO) (Covey et al., 2016). Finally, protein was extracted from ventral midbrain and ventral striatum for western blot analysis of DA machinery and selenoprotein expression levels.

Results

Effects of se-deficiency on phasic dopamine release and uptake:

Upon testing for an impact of Se-deficiency on DA neurotransmission, FSCV did not uncover any major changes in phasic DA signaling in Se-deficient mice at baseline or during METH application. The average DA concentration evoked by stimulation reached an average maximum of ~1.1 μM in slices from control mice. Evoked DA release in brain slices from Se-deficient mice reached an average of ~0.8 μM, a slight downward trend (Fig. 3-1A, B). METH application caused an immediate spike in evoked DA release that decreased with each successive stimulation back to baseline levels. Evoked DA concentrations reached an average spike of ~1.5 μM in both experimental groups in the presence of METH (Fig. 3-1C, D). METH-induced spikes

were also calculated as a percent increase over baseline. This metric was also unchanged by Se deficiency (Fig. 3-1E).

Basal DA uptake rate, represented by the Michaelis-Menten constant Vmax, was not affected by dietary Se restriction (Fig. 3-1F). The apparent affinity of DA for DAT, represented by the Michaelis-Menten constant Km, was set to 160 nM at baseline. This value increased during METH application, representing the magnitude of METH-induced DA uptake inhibition. Apparent Km was not changed in slices from Se-deficient mice compared to controls (Fig. 3-1G, H). Western blot analysis of DAT and VMAT-2 expression revealed no changes in ventral midbrain or ventral striatum (Fig. 3-2B, C).

Protein expression changes in Se-deficient mice:

Protein expression levels were measured in brain lysates of ventral midbain, which contains the VTA-resident dopaminergic cell bodies, and the ventral striatum, which contains the DA terminal-containing NAc. Western blot anaylsis revealed that TH expression was unchanged by Se deficiency, although a downward trend was detected in the ventral striatum of Se-deficient mice (Fig. 3-2A). DAT and VMAT-2 expression were also unchanged (Fig. 3-2B, C). Expression of GPx1 trended towards a decrease in the brains of Se-deficient mice (Fig. 3-2D). GPx4 expression was significantly reduced in the ventral midbrain of Se-deficient mice, while again trending towards a decrease in ventral striatum (Fig. 3-2E).

Se deficiency changes the tonic response to methamphetamine:

Upon addition of METH, extracellular DA concentration quickly rises due to DA efflux and remains elevated for the duration of METH application in slices from control animals (Fig. 3-3A). The maximum increase in DA concentration from baseline reached an average of 12.19 µM in slices from control animals, yet was reduced to a 3.33 µM increase in slices from Se-deficient mice (Fig. 3-3B). The total amount of DA efflux was calculated by measuring the area under the curve (AUC) of the DA response for the duration of the METH application. Total DA efflux was also significantly reduced by Se deficiency (Fig 3-3C).

Involvement of glutathione peroxidase:

GPx activity was pharmacologically increased in Se-deficient brain in response to the GPx mimetic ebselen. Ebselen caused and increase in extracellular DA concentration, followed by a more robust increase when METH was added (Fig. 3-3D). The maximum change in DA concentration caused by METH was compared to both the orignial baseline (pre-ebselen) as well as the heightened values measured just before METH exposure. Ebselen-treated slices from Se-deficient mice displayed a significantly higher change in DA concentration than non-treated slices from Se-deficient mice when data was compared to the original baseline and trended towards an increase when compared to the ebselen-adjusted baseline (Fig. 3-3E). Ebselen also caused an upward trend in total DA efflux (Fig. 3-3F).

To investigate whether inhibition of GPx activity would cause the opposite effect of ebselen, GPx inhibitors were added to control slices for 15 min prior to METH. The GPx1 inhibitor MCS caused a downward drift in extracellular DA and decreased the response to METH (Fig. 3-4A). Maximum DA concentration (compared to the MCS-adjusted baseline) and total DA efflux were reduced by MCS treatment (Fig. 3-4B, C).

MCS reduces evoked DA release in dorsal striatum (Avshalumov et al., 2005). Therefore, evoked DA was measured in the current study to confirm a similar effect in the NAc. MCS quickly reduced evoked DA release by ~25%, followed by stable recording (Fig. 3-4D, E). When compared to the MCS-reduced baseline, neither peak phasic DA release nor percent increase were changed by MCS treatment (Fig. 3-4F).

In contrast to MCS, the GPx4 inhibitor RSL3 (0.5 μM) did not affect basal tonic DA levels (Fig. 3-4G). Remarkably, RSL3 greatly reduced the tonic response to METH with the average DA increase reaching only 2.8 μM, ~25% of that seen in controls (Fig. 3-4G, H). Total DA efflux was also reduced by RSL3 to ~15% of the control response (Fig. 3-4I). Since RSL3 is an inducer of apoptosis, its effects on phasic DA signals were measured to confirm the viability of slices (Yang et al., 2014). RLS3 did not affect evoked DA release or uptake, ruling out cell death as an underlying cause of the reducing effect on DA efflux (Fig. 3-4J, K).

Mediating role of K_{ATP} channels:

K_{ATP} channels reduce spontaneous DA release events by inhibiting Ca^{2+} influx via VGCCs (Rice et al., 2011). K_{ATP} channels can also be activated by H_2O_2. Since a reduction of

GPx activity will cause an increase in H_2O_2 levels and reduces the tonic DA response to METH, we investigated whether this effect is mediated Ca^{2+} influx. First, we evaluated the contribution of Ca^{2+} influx to METH-induced extracellular DA concentration elevations by exposing slices from control mice to METH under conditions of zero extracellular Ca^{2+}. Removal of extracellular Ca^{2+} reduced the increase in DA concentration in response to METH (Fig. 3-5A). Average peak DA concentration and average total DA efflux were reduced compated to (Fig. 3-5B, C).

Next, we used the K_{ATP} channel inhibitor glibenclamide to investigate whether K_{ATP} channel blockade would attenuate the effect of Se deficiency and RSL3 on METH responses by up-regulating Ca^{2+}-dependent DA release. Interestingly, in slices from control animals glibenclamide (3 μM) decreased the response to METH (Fig. 3-6A). Maximum change in DA and total DA efflux were both reduced by glibenclamide treatment (Fig. 3-6B, C). When Se-deficient brain slices were treated with glibenclamide, the METH response was raised (Fig. 3-6D). The Maximum change in DA concentration was significantly higher than non-treated slices from Se-deficient mice and total DA efflux was was also raised, but did not reach statistical significance (Fig. 3-6 E, F).

Glibenclamide was also added prior to RSL3 to slices from control animals to investigate if K_{ATP} channel blockade could also have a reversal effect on RSL3 suppression of METH-induced DA efflux. This resulted in a small response to METH that peaked at around 8 minutes before gradually declining (Fig. 3-6G). For this reason, maximum DA concentrations were compared to slices exposed to RSL3 only at the 8 minute mark. Glibenclamide partially reversed the suppressive effect of RSL3 on DA efflux (Fig. 3-6H, I).

Modulation by cannabinoid receptor activity:

METH-induced increases in striatal DA levels is dependent on CB1 receptor activation as the CB1R antagonist RIMO completely blocks METH-induced DA efflux *in vivo* (Covey et al., 2016). Covey et a. proposed that METH-induced CB1R activity inhibits GABAergic interneurons located in the VTA to promote DA neuron firing. We investigated the possibility of striatal CB1R involvement in METH-induced DA efflux using our *in vitro* brain slice technique. RIMO (1 μM) added to slices from control animals prior to METH exposure resulted in no change in the METH response (Fig. 3-7A). WIN55, a CB1R and CB2R receptor agonist, caused

an increase in basal DA levels, yet significantly reduced the METH response (Fig. 3-7A). The maximum change in DA concentration and total DA efflux were both significantly reduced compared to controls (Fig. 3-7B, C).

Since the WIN55 blockade of METH-induced DA efflux implies a suppressive effect of CB receptor activity, we next investigated whether RSL3 prevents DA efflux through CB receptor activation. Adding RIMO prior to RSL3 resulted in an increase in DA concentration in response to METH (Fig. 3-7D). Similar to glibenclamide, this spike in DA concentration peaked at 8 minutes, so we compared DA levels at this timepoint. The maximum change in DA concentration and the total DA efflux were both increased by RIMO treatment (Fig. 3-7E, F).

Conclusions and Discussion

Contrasting results in phasic and tonic release:

Overall, there were no measured effects of Se deficiency on phasic DA signals. Despite reports of increased DA turnover with 2 weeks of dietary Se deficiency (Romero-Ramos et al., 2000), evoked DA was not affected. Past studies utilized microdialysis and HPLC, however, which may account for contrasting findings and will be further elaborated on in the GENERAL DISCUSSION section. Accordingly, basal uptake rates and expression of DA-related proteins were unchanged, revealing no neuroadaptive or degenerative effects.

Se protects against METH-induced neurotoxicity, purportedly by reducing oxidative stress caused by DA auto-oxidation (Yu et al., 2015). As Se deficiency reportedly potentiates METH-induced neurotoxicity, this suggests it may also cause an increase in DA efflux, and thus increase auto-oxidation. Our results point to the opposite, however, as METH-induced DA efflux was reduced by Se deficiency. VMAT-2 expression did not change in response to Se deficiency, which would have suggested a change in vesicular DA levels. Instead these results suggest a change in vulnerability to METH within the Se-deficient mouse striatum.

Glutathione peroxidase regulates basal release:

We have identified GPx activity as playing a mediating role. The first evidence was that ebselen caused an upward drift in tonic DA levels, possibly due to decreased ROS. In contrast, MCS caused a decrease in tonic DA levels. Take together, this data indicates that H_2O_2 inhibits tonic DA release.

Since H_2O_2 suppresses evoked DA release by activating K_{ATP} channels and consequently inhibiting Ca^{2+} influx, a similar mechanism may decrease tonic DA release (Avshalumov and Rice, 2003). This suppressive role was theorized to be carried out by H_2O_2 produced downstream from AMPAR activation as demonstrated *in vivo*. AMPAR-induced H_2O_2 generation is unlikely to contribute to the present pre-METH tonic results, however, as glutamatergic afferents are cut off in brain slices and no electrical stimulation occurred. Nevertheless, MCS likely causes general H_2O_2 elevation that can activate K_{ATP} channels. Interestingly, K_{ATP} channels can inhibit T-type VGCCs, which would disable the 'pacemaking' depolarization in DA terminals that drives tonic release (Perez-Reyes and Lee, 2014).

K_{ATP} channel inhibition with glibenclamide had no direct effect on tonic DA release, implying that K_{ATP} channels may be widely inactive. Indeed, this has been reported to be the case in DA neurons in brain slices (Roper and Ashcroft, 1995; Liss et al., 1999). This seems to cast some doubt over whether ebselen-induced increases in extracellular DA can be attributed to the H_2O_2-K_{ATP} channel pathway. If K_{ATP} channels are already inactive, reducing H_2O_2 would have no effect on their activity. Therefore, it is possible that reduced H_2O_2 may increase tonic DA release through an alternative mechanism. Nevertheless, GPx activity has been demonstrated to have a bi-directional effect on tonic DA release, likely through H_2O_2 regulation.

Glutathione peroxidase modulates the response to methamphetamine:

The GPx mimetic, ebselen, recovered DA efflux in slices from Se-deficient micewhile GPx inhibition reduced efflux in control slices. Surprisingly, treating control slices with the GPx4-specific inhibitor RSL3 dramatically suppressed METH-induced DA efflux. One concern regarding this result is that RSL3 induces cell death via ferroptosis (Yang et al., 2014). In order to rule out cell death as an underlying cause of the decreased tonic response to DA, we measured the effect of RSL3 on evoked DA release in control slices. RSL3 did not change the amplitude or uptake kinetics of evoked DA release, ruling out terminal degeneration as a contributing factor. These data suggest an inhibitory effect of both H_2O_2 and lipid peroxides on the changes in DA efflux in response to METH.

K_{ATP} channels reduce dopamine efflux:

While the role of K_{ATP} channels in mediating GPx influence on basal tonic release is not completely clear, it appears to be crucial for METH-induced DA efflux. K_{ATP} channel blockade prevented the inhibitory effect in Se-deficient and RSL3-exposed slices. In contrast to baseline conditions, METH elevates H_2O_2 levels in rodent striatum (Yokoyama et al., 1997). Therefore, K_{ATP} channels are likely activated in the presence of METH, with a stronger effect in the Se-deficient striatum. Therefore, the present findings indicate that H_2O_2-K_{ATP} activation may underly the reduced DA efflux in Slices from Se-deficient mice and slices exposed to RSL3. It is worth noting that DAT blockade via GBR 12909 reduces METH-induced DA efflux, presumably by limiting the number of channels through which DA can leave the cell (Hedges, unpublished). RSL3 did not affect DA uptake kinetics, however, implying no effect on DAT.

The findings further suggest that increased tonic DA release is partially responsible for METH-induced increases in extracellular DA levels. Our collaborators at BYU previously showed that lidocaine blockade of Na^+ channels, which prevents action potential-dependent release, had effect on DA efflux suggesting that membrane potential and Ca^{2+} influx are not involved (Hedges, unpublished). As the current study shows, however, removal of extracellar Ca^{2+} reduces DA efflux. Therefore, while Ca^{2+} influx is not necessary for DA efflux, it does potentiate it. Combined with the inhibitory effect of K_{ATP} channels, the overall implication is that depolarization increases METH-induced DA efflux. Whether this depolarization causes an increase in vesicular tonic DA release remains an interesting prospect for future studies. Alternatively, METH has been proposed to act through phosphorylation events initiated by intracellular Ca^{2+} elevation, such as PKC reversal of DAT function (Kantor and Gnegy, 1998).

Cannabinoid receptor activity reduces dopamine efflux:

The present study also elucidates a mediating role of the endocannabinoid system. CB1R antagonism by RIMO did not change METH-induced DA efflux, implying that CB1Rs are already in a constitutively low activation state. RIMO also caused a similar effect as glibenclamide in reversing RSL3 suppression of DA efflux. This suggests that RSL3 suppresses the METH response partly by activating CB1R. This is further supported by the fact that the CB receptor agonist WIN55 prevented METH DA efflux similarly to RSL3.

These results are in contrast to a previous study showing CB1R activity is necessary for AMPH-induced DA elevation *in vivo*. Covey et al. argued that activation of CB1R on GABAergic interneurons disinhibited VTA DA neurons, subsequently increasing DA release into the striatum (Covey et al., 2016). Since our experiments were carried out in NAc brain slices, however, the effect we have seen is restricted to the level of the striatum. The location of the responsible CB1R could be on presynaptic DA or GABAergic terminals.

RSL3-mediated CB receptor activation is likely achieved through a change in endocannabinoid production or metabolic balance. The simplest explanation is that inhibition of GPx4 by RSL3 results in increased lipid peroxides, which increases production of a CB1R activating endocannabinoid such as AEA or 2-AG. Lipid peroxides can inhibit FAAH, which in turn leads to a decrease in AEA breakdown (Clapper et al., 2009; Maccarrone et al., 2009). AEA can also be up-regulated by application of exogenous H_2O_2 to isolated primary mouse hepatocytes (Siegmund et al., 2006).

Sidlo et al. found that WIN55 suppresses evoked striatal DA release through a mechanism involving the suppression of GABAergic transmission (Sidlo et al., 2008). This permits H_2O_2 production and subsequent K_{ATP} inhibition of DA release. Interestingly, this mechanism seems to run in parallel to our finding that WIN55 suppresses DA efflux. Since WIN55 initially caused a slight elevation in tonic DA levels, it might act to relieve GABAergic inhibition of DA terminals. Then once METH is applied, this effect is overpowered by H_2O_2-K_{ATP} suppression of DA release. This model would require GABAergic synapses on to both presynaptic DA terminals and MSN postsynaptic membranes.

The simplest explanation is that CB1R located on DA terminals acts to inhibit METH-induced DA efflux (Wenger et al., 2003; Kofalvi et al., 2005).

Experimental limitations:

The findings of the present study are complicated by a few observations. First, glibenclamide unexpectedly exerted the opposite effect in slices from control animals from slices from Se-deficient mice, reducing METH-induced DA efflux rather than causing an increase. This could be due to a differential change in membrane excitability between control and slices from Se-deficient mice and further investigation is warranted.

There are also some caeveats in intepreting ebselen experiments. Ebselen significantly increased the METH-induced DA release above the pre-ebselen baseline, but not above post-ebselen DA levels. DA efflux following ebselen and METH may have reached a maximal 'ceiling' comparable to METH-induced efflux in slices from control animals. While our results indicate that ebselen is a tonic DA up-regulator, the depiction of the role of GPx in DA efflux is not quite as clear.

Ebselen is a lipid-soluble organoselenium compound that enters the cell to reduce ROS through a similar mechanism as GPx: the selenol residue of ebselen becomes oxidized by H_2O_2 and is subsequently reduced by 2 GSH molecules, resulting in GSH dimerization with the GSH units connected via a disulfide bond (Azad and Tomar, 2014). Ebselen has also demonstrated a wide range of effects within the cell which may complicate the interpretation of experimental results. These effects are consequences of antioxidant function and include: Na^+/K^+-ATPase inhibition that disrupts the resting memebrane potential; inhibition of PKC, which may downregulate DA uptake through DAT phosphorylation; and increasing cytosolic Ca^{2+} to increase spontaneous DA release (Azad et al., 2014; Azad and Tomar, 2014).

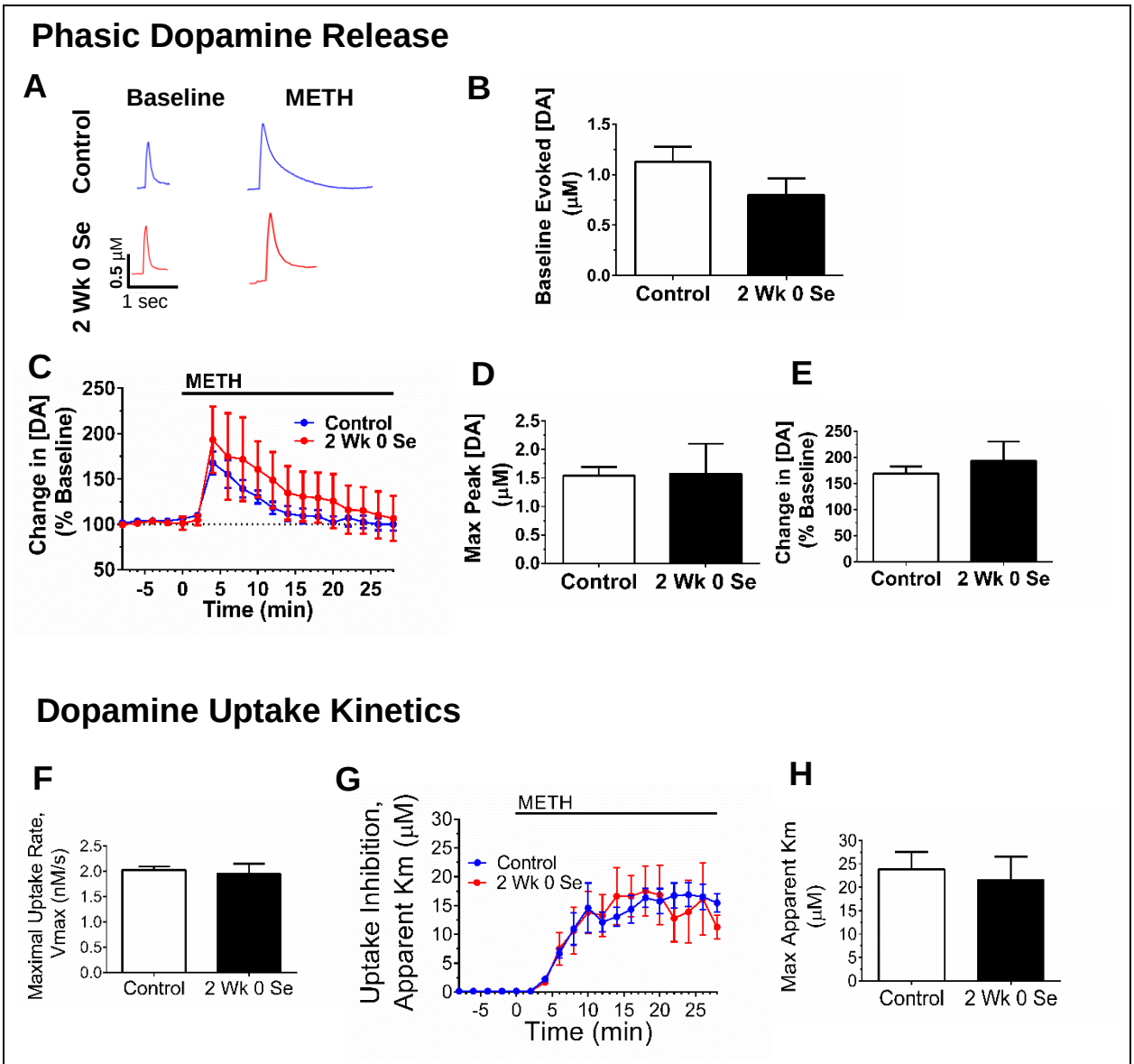

Figure 3-1. Following dietary Se deficiency (2 weeks) did not change phasic DA release and uptake kinetics. **A.** Sample traces of basal evoked DA release and peak response following application of 10 µM METH to brain slice of male C57 WT mice, aged 3-5 months. **B.** Se deficiency (2 weeks) does not alter basal evoked DA release compared to controls (1.126 ± 0.1476, n=16 and 0.7997 ± 0.1603, n=4, respectively, P = 0.31). **C, D, E.** Short-term Se deficiency does not affect augmentation of evoked DA release (n=8 for controls and 4 for Se deficiency). **F.** No differences in basal DA uptake rates (Vmax) were observed (n=19 and 4) (P>0.05). **G, H.** METH-induced uptake inhibition (Km) was also unchanged between groups (n=8 and 4) (P>0.05).

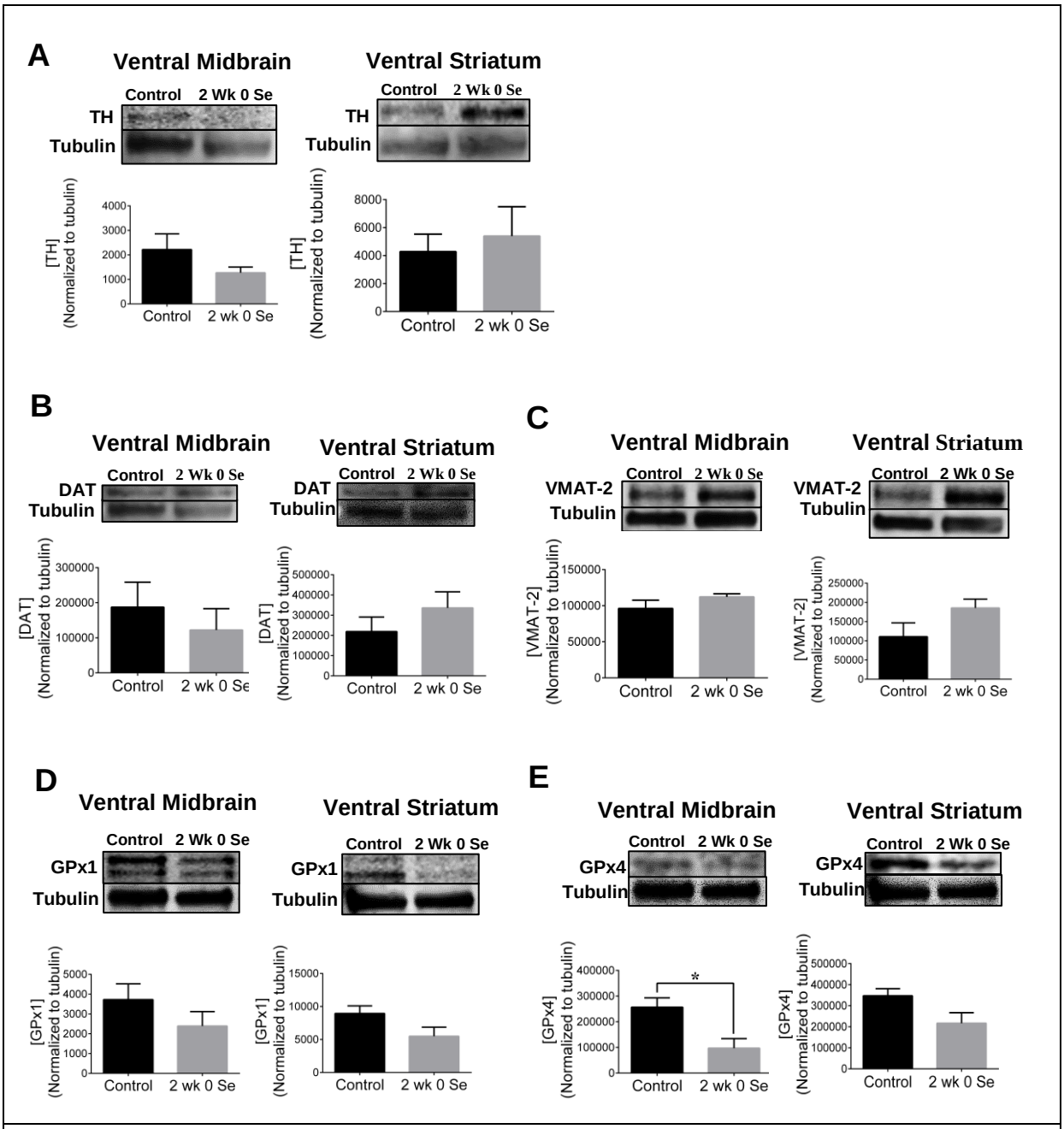

Figure 3-2. Western blot analysis of brain lysates from ventral midbrain and ventral striatum.
A, B, C. Western blot revealed no significant changes in the expression of TH, DAT, or VMAT-2 in male C57 WT mice, aged 3-5 months (n=4, 4) (P>0.05). **D, E.** GPx protein measurement via western blot showed a downward trend in expression of GPx1 and GPx4 in ventral midbrain (n=4 and 4, P = 0.26 and 0.02, respectively) and ventral striatum (n=4 and 4, P = 0.10 and 0.07, respectively) of Se-deficient brain lysates. GPx4 expression was significantly reduced in ventral midbrain (*P* = 0.02).

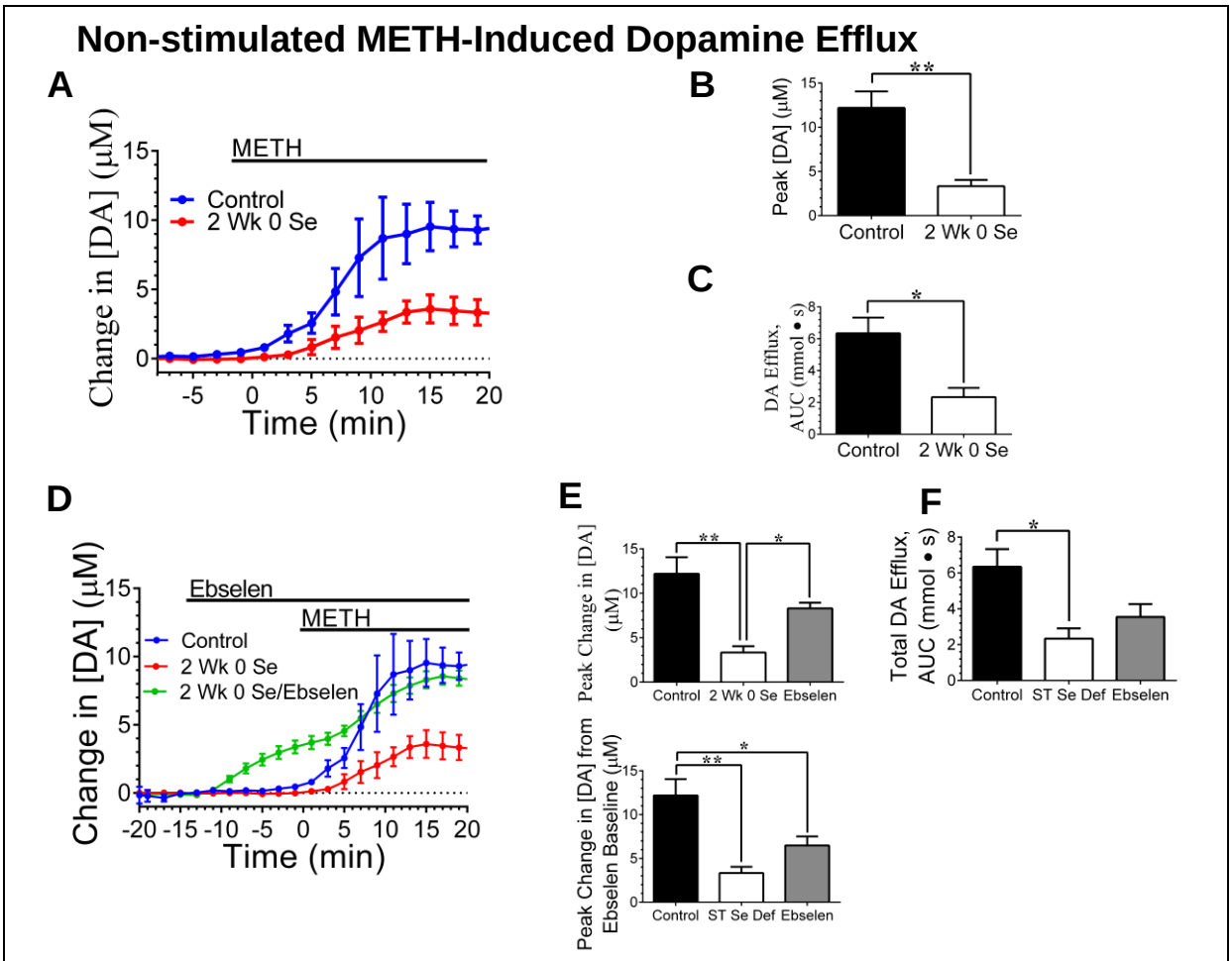

Figure 3-3. Short-term Se deficiency caused a reduction in METH-induced DA efflux that could be partially reversed by the GPx mimetic ebselen.

A. Time course graph showing increased extracellular DA concentration upon exposure to 10 µM METH in the absence of electrical stimulation in male C57 WT mice, aged 3-5 months. **B.** The maximum change in DA concentration caused by METH-induced DA efflux was greater in Se sufficient (12.19 ± 1.87, n=3) mouse brain slices than in slices from Se-deficient mice (3.33 ± 0.72, n=4; $P = 0.004$). **C.** Area under the curve (AUC) of the non-stimulated METH response was also reduced by Se deficiency (2335 ± 573.0, n=4 compared to 6344 ± 983.6, n=3 for controls; $P = 0.013$). **D** Treating Se-deficient brain slices with ebselen (3 µM) for 15 minutes prior to METH increases DA efflux. **E.** Ebselen treatment increased the maximum response in short-term Se-deficient brain slices when compared to the original baseline (n=4 and 3, respectively, P=0.02), but not when data was normalized to the increased baseline caused by ebselen (n=4 and 3, respectively, P=0.003). **F.** Total DA efflux was also increased by ebselen treatment, although statistical significance was not reached by one-way ANOVA (n=4 and 3, respectively, P=0.02).

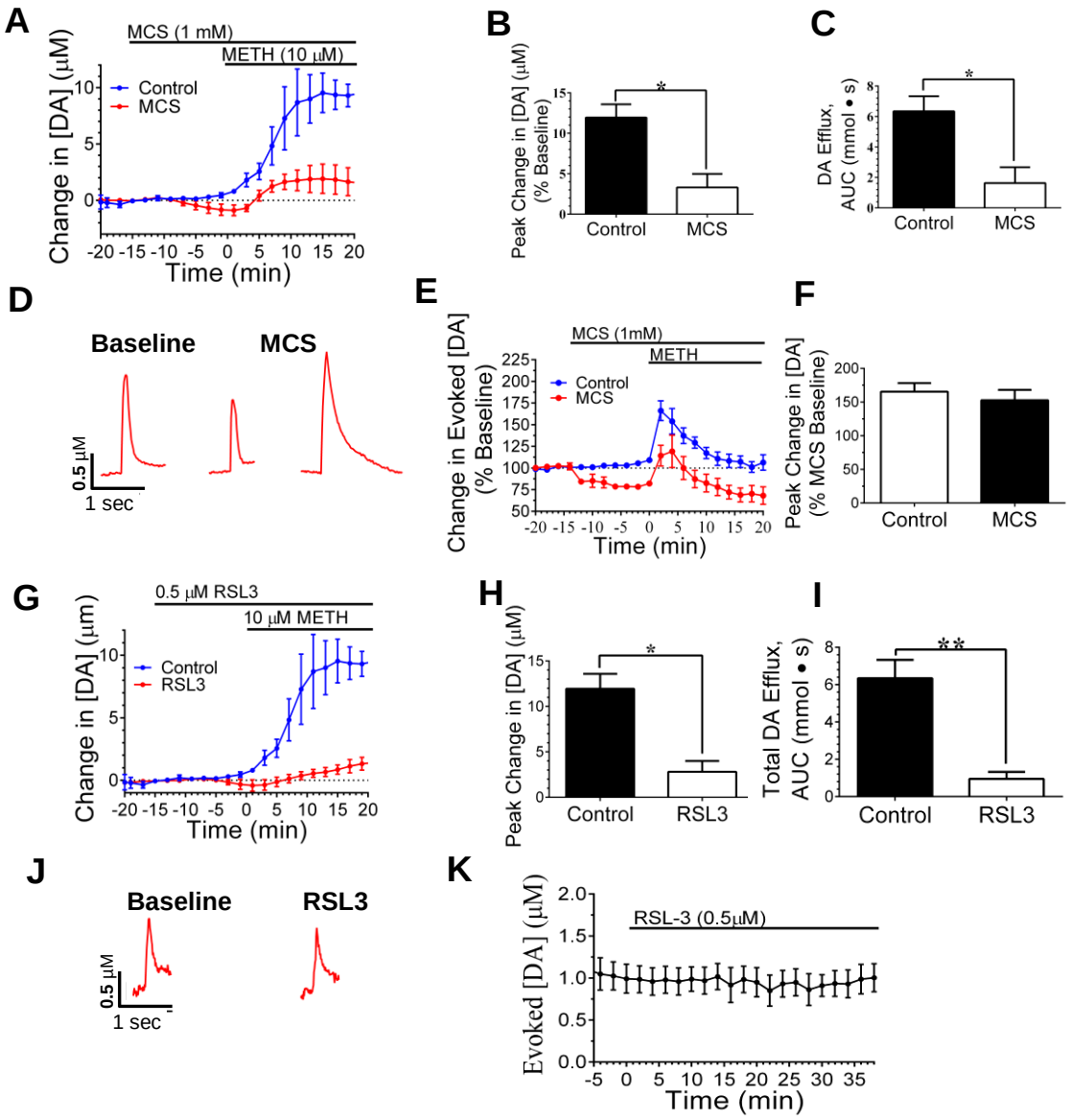

Figure 3-4. Inhibition of GPx activity reduced METH-induced DA efflux.
A. Pre-treatment with the GPx1 inhibitor Mercaptosuccinate (MCS) (1 mM) caused a decrease in baseline tonic DA levels as well as a reduction in the amount of DA efflux in response to METH in male C57 WT mice, aged 3-5 months. **B, C.** Maximum increase in DA concentration, compared to MCS-adjusted baseline (n=3 and 3), and total DA efflux (n=3 and 3) were significantly reduced by MCS (P = 0.0210 and 0.0302, respectively). **D.** Sample traces of phasic DA release after application of MCS and METH to slices from control animals. **E.** MCS decreased evoked DA release in response to METH. MCS also caused an increase in evoked DA release in response to METH, similarly to controls. **F.** MCS did not affect the max percent increase in evoked DA in response to METH (n=8 for controls and 3, P=0.26). **G.** Pre-treatment with 0.5 μM RSL3, GPx4 inhibitor, suppressed DA efflux in response to METH. **H, I.** Maximum DA concentration and total DA efflux were greatly reduced by RSL3 (n=3 and 3, P = 0.0106 and 0.0068, respectively). **J, K** RSL3 was added to slices from control animals with no changes in DA release or uptake.

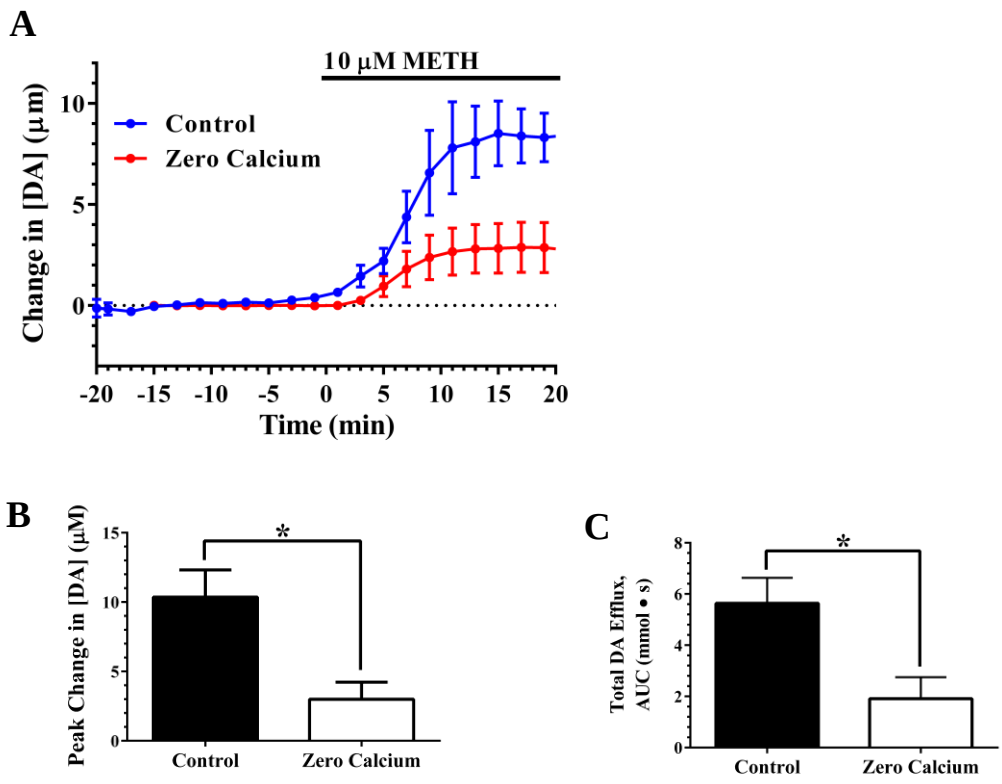

Figure 3-5. Zero extracellular Ca^{2+} conditions reduced METH-induced DA efflux.
To evaluate the role of calcium influx in mediating METH-induced DA efflux, we perfused brain slices from male C57 WT mice, aged 3-5 months with calcium-free ACSF before and during METH exposure. **A.** The absence of extracellular calcium resulted in a reduction in METH-induced DA efflux. **B, C.** Maximum DA concentration and total DA efflux were significantly decreased by zero calcium conditions (n=3 and 3, *P* = 0.0266 and 0.0120, respectively).

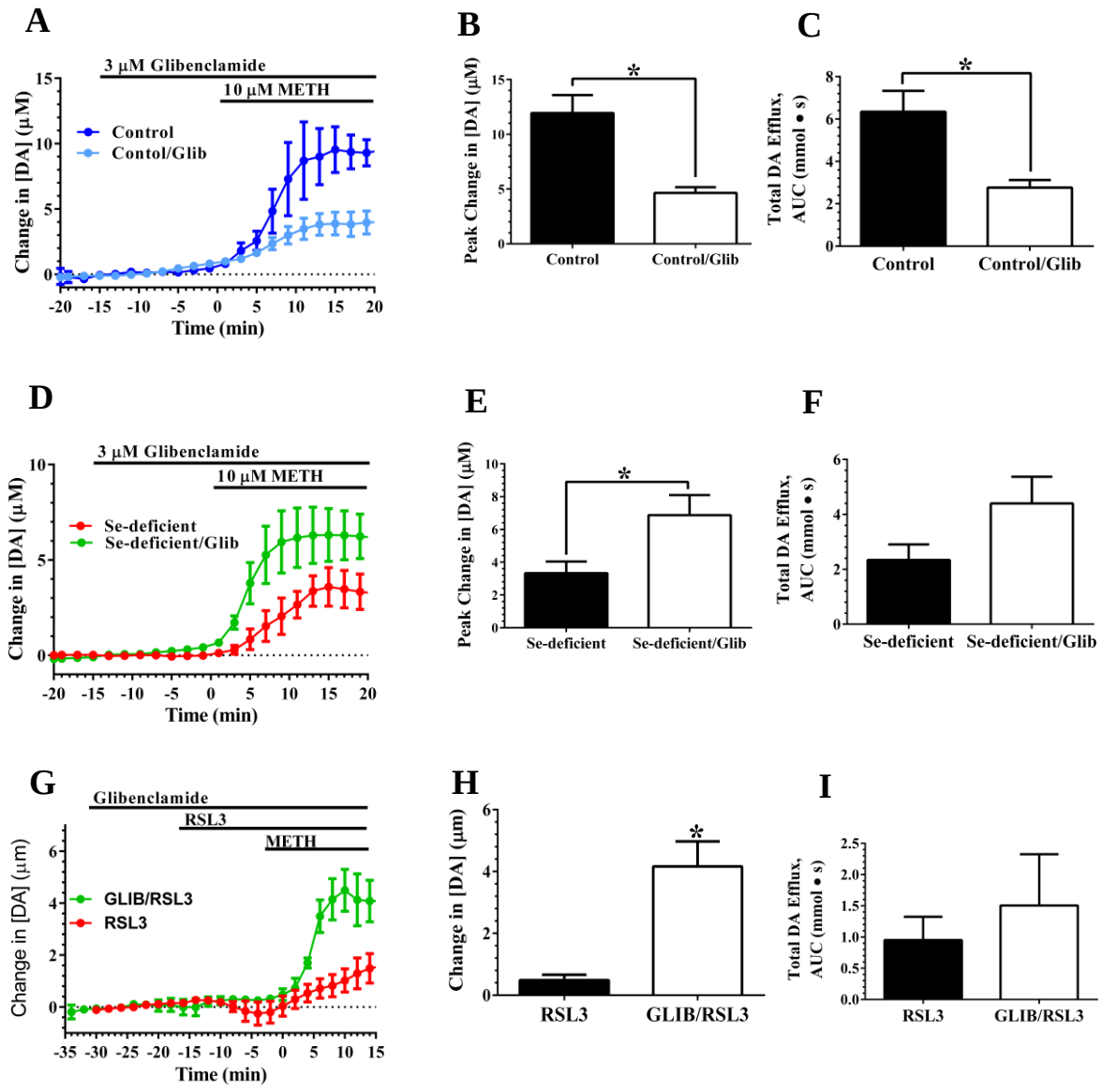

Figure 3-6. Se deficiency and RLS3 reduction of METH-induced DA efflux was potentiated by K_{ATP} channels.

A. The K_{ATP} channel blocker glibenclamide (3 µM) reduced METH-induced DA efflux in slices from male C57 WT mice, aged 3-5 months. **B, C.** Maximum DA concentration (n=3 and 3, P=0.002) and total DA efflux (n=3 and 3, P=0.02) in response to METH were significantly decreased by K_{ATP} channel blockade in slices from control animals. **D.** Glibenclamide treatment increased the DA response to METH in slices from Se-deficient mice. **E, F.** Maximum concentration was raised by glibenclamide in slices from Se-deficient mice (n=3 and 3, P=0.0130), while total DA efflux was increased, but did not reach significance (n=3 and 3, P=0.12). **G.** Glibenclamide caused a METH response in RSL3-treated slices. Comparisons were made at the 8-minute mark when the response to METH was greatest in slices treated with glibenclamide and then RSL3 prior to METH. **H, I.** Glibenclamide increased the maximum DA concentration (n=3 and 3. P=0.0164) in response to METH in RSL3-exposed slices, but not total DA efflux (P=0.38).

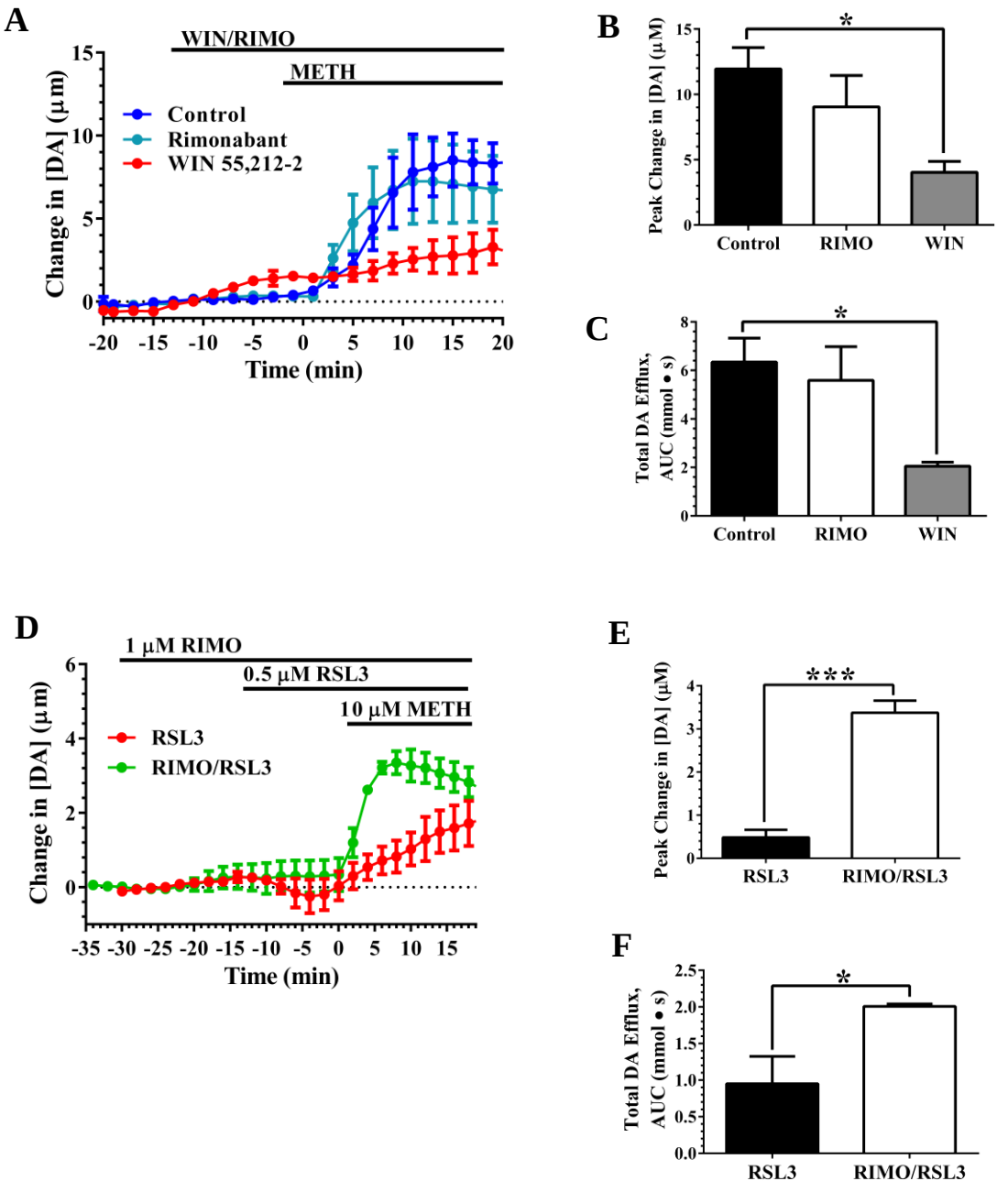

Figure 3-7. METH-induced DA efflux was reduced by CB1/CB2 agonism while CB1 receptor antagonism partially reversed RSL3 blockade of DA efflux.

A. Pre-treatment with the CB1/CB2 agonist WIN 55, 212-2 (10 µM) reduced DA efflux while the CB1 antagonist Rimonabant (1 µM) had no effect on slices from male C57 WT mice, aged 3-5 months. **B, C.** Maximum DA concentration and total DA efflux were reduced by WIN (n=3 and 3, P=0.01 and 0.01, respectively). **D.** Pre-treatment with RIMO partially reversed the RSL3 blocking effect on DA efflux. **E.** Measurements taken at 8 minutes after the beginning of METH application showed RIMO significantly increased maximum DA concentration increases in response to METH in Slices from Se-deficient mice (3.38 ± 0.28, n=3 compared to 0.49 ± 0.18, n=3; *P* = 0.0009). **F.** Total DA efflux was also increased by RIMO (2007 ± 33.34, n=3 compared to 951.0 ± 372.3, n=3; *P* = 0.048).

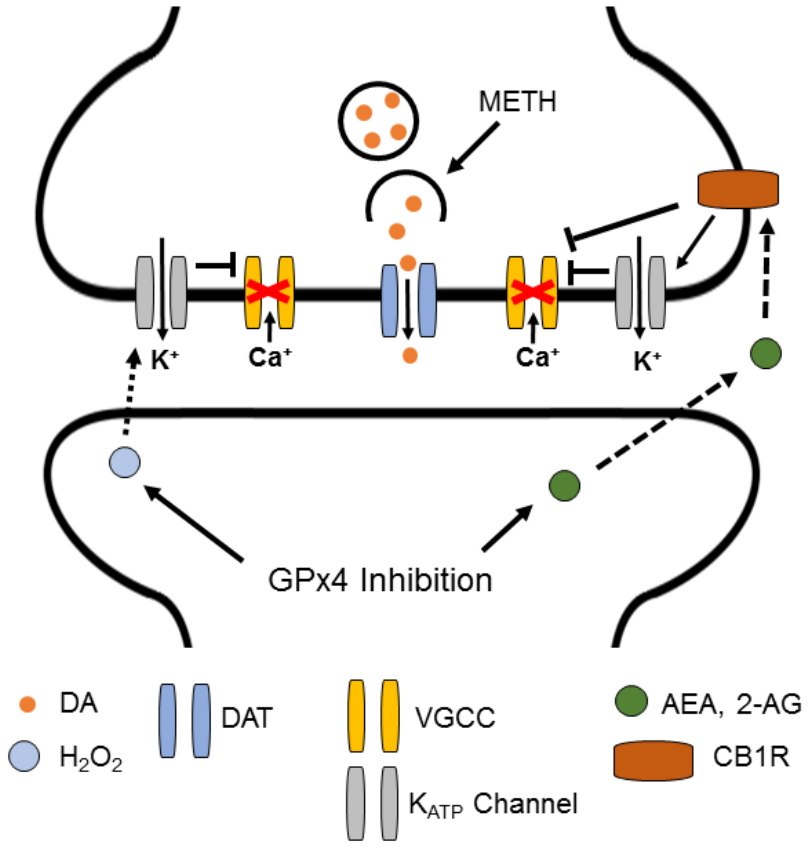

Figure 3-8. Model for GPx4 inhibition causing reduced METH-induced DA efflux.
RSL3 inhibition of GPx4 activity may reduce DA efflux through two separate pathways that converge to inhibit Ca^{2+} influx. The first proposed pathway is that loss of GPx activity will increase H_2O_2 levels, which is exacerbated by METH exposure. H_2O_2 then activates ATP-sensitive K^+ channels (K_{ATP} channels) to inhibit Ca^{2+} influx via voltage-gated calcium channels (VGCCs) to inhibit DA efflux. The second proposed pathway involves GPx4 inhibition causing lipid peroxidation that leads to production of an endocannabinoid (AEA or 2-AG). The endocannabinoids then act on cannabinoid receptor 1 (CB1R) located on DA pre-synaptic terminals. CB1R can activate K_{ATP} channels and inhibit VGCCs, leading to inhibition of DA efflux.

CHAPTER 4: THE EFFECTS OF CHRONIC SELENIUM DEFICIENCY ON THE DOPAMINE SYSTEM

Abstract

Chronic Se-deficient mice have reduced basal DA uptake rates, but no change in basal release. In response to METH, chronic Se deficiency causes reduced DA efflux compared to Se-sufficient mice. METH also caused an increase in phasic DA release in chronic Se-deficient mice that can be attributed to increased DA vesicular release.

Introduction

Although Se is preferentially retained in brain during chronic dietary Se deficiency, METH-induced neurotoxicity of DA neurons is exacerbated by Se deficiency and attenuated by Se supplementation (Behne et al., 1988; Kim et al., 1999; Barayuga et al., 2013). While there has been little investigation into the effects of chronic (11-13 weeks) Se deficiency on DA transmission, one study revealed an increase in K^+-induced DA release in mouse striatum measured via microdialysis (Watanabe et al., 1997). However, we did not observe increased DA release with short-term (4-5 weeks) Se deficiency. Possible long-term functional changes in dopaminergic neurons due to increased oxidative stress could explain the discrepency between short- and long-term Se deficiency. Previous work in the Bellinger lab demonstrated that chronic Se deficiency decreases DAT and VMAT-2, but not TH (data not shown). We investigated the effects of chronic Se deficiency on DA release and uptake.

Methods

Mice were raised on an Se deficient diet from weaning as described in the METHODS chapter. Brain slices were made at 3-5 months of age. FSCV was performed as previously described to depict changes in phasic and non-phasic DA release at baseline and in response to METH.

Results

Phasic dopamine release:

Baseline evoked DA peaks in brain slices from chronically Se-deficient mice trended towards a decrease compared to Se-sufficient control mice (Fig. 4-1A, B). When METH was applied, slices from chronic Se-deficient mice displayed a larger percent increase over baseline (211 ± 16.7%) of evoked DA release compared to controls (165 ± 12.8%), although peak DA concentrations evoked were not different (Fig. 4-1C-E). Kinetic modeling was used to derive the release rate constant dopamine per pulse DAp, which corrects for uptake to give an estimate of the amount of vesicular DA release. Slices from chronic Se-deficient mice exhibited a 141% average increase over baseline, implying an increase in vesicular DA release in response to METH (Fig. 4-1F). Se-sufficient slices, on the other hand, showed only a slight average increase of 107 ± 5.6% in DAp in response to METH (Fig. 4-1G-I). Similar to evoked DA concentration measurements, maximum DAp was comparable between the groups.

Dopamine uptake kinetics:

Michaelis-Menten kinetic analysis showed decreased DA uptake, represented by Vmax, in slices from Se-deficient mice, with average rates reduced by half compared with slices from control animals (Fig. 4-2A). When slices were treated with METH, slices from Se-deficient mice exhibited less inhibition of DA uptake (apparent Km) compared to controls (Fig. 4-2B, C).

Methamphetamine-induced dopamine efflux:

Non-stimulated DA release in response to METH was greatly reduced in slices from Se-deficient mice (Fig. 4-3A). The average maximum increase in DA concentration in the presence of METH was considerably lower in Se-deficient mice (3.080 µM) compared to controls (11.95 µM) (Fig. 4-3B). Total DA efflux measurements yielded a similarly large difference between the groups (Fig. 4-3C).

Conclusions and Discussion

Baseline evoked dopamine is unchanged by chronic selenium deficiency:

While past studies found increased DA turnover rates with Se deficiency (Romero-Ramos et al., 2000), our results did not reveal a change in the magnitude of action potential-driven DA

release events and may in fact indicate a decrease. Although our findings do not corroborate past studies, discrepancies may be due to the technical differences between FSCV and microdialysis. Specifically, FSCV has a much faster (sub-second) temporal resolution compared to microdialysis (tens of minutes), a difference that will be further discussed in the GENERAL DISCUSSION chapter. Our data suggests a lack of global change in the potential of the striatal DA system to respond to any given phasic firing event.

Comparable baseline phasic release concentrations may be reflective of comparable DA terminal densities or, perhaps, more directly a comparable availability of readily-releasable vesicular DA stores, despite increased oxidative stress. Similar dopaminergic density is further suggested by the fact that western blot analysis did not reveal a change in TH expression in chronic Se-deficient mice. However, there may be a change in TH activity without a change in TH expression. Indeed, Castano et al. reported increased DA turnover in PFC of Se-deficient rats that was accompanied by increased TH activity, but not TH expression. Such possibilities warrant further characterization of the physical characteristics of striatal DA terminals in chronic Se deficiency.

Chronic selenium deficiency impairs basal dopamine uptake:

The reduced Vmax observed in slices from Se-deficient mice indicates an impaired DA uptake, and is consistent with the reduced DAT expression found in ventral midbrain. DAT expression in ventral striatum trended towards a decrease, but was not statistically significant. This could be due to DA terminals making up a much smaller percentage of overall protein in striatum, compared to DA cell bodies, which make up a large percent of protein in the VTA. DAT may have reduced functionality in addition to reduced expression. H_2O_2 can inhibit DA uptake via DAT (Huang et al., 2003), and may be present in higher amounts in the Se-deficient striatum.

Methamphetamine increases vesicular dopamine release in chronically selenium deficient striatum:

In contrast to the results of our short-term Se deficiency study, chronic Se deficiency increased phasic DA release in response to METH. Moreover, the slices from chronic Se-deficient mice exhibited an increase in vesicular DA release in addition to reducing DA efflux,

indicating a biphasic modulation of DA release. In slices from control animals, vesicular release may be masked by the much larger output of the DA efflux mechanism. Additionally, DA efflux depletes vesicular DA stores, further decreasing the capacity for evoked DA release. As METH produces a smaller amount of DA efflux in slices from Se-deficient mice, however, vesicular DA stores should remain intact for longer, allowing for the observation of increased vesicular release.

Chronic selenim deficiency reduces methamphetamine-induced dopamine efflux:

The decreased amount of DA efflux in slices from Se-deficient mice may be the result of a reduction in overall striatal DA terminal density. The impaired antioxidant defense of the Se-deficient brain could lead to chronic oxidative stress-induced neurodegeneration in the striatum. This possibility is obscured by the result that TH expression did not change. Alternatively, the loss of GPx activity may be responsible for reducing METH-induced DA, as suggested in the previous chapter. Indeed, GPx expression is reduced in the Se-deficient brain, particularly in the ventral midbain, which contains the dopaminergic cell bodies that project to NAc.

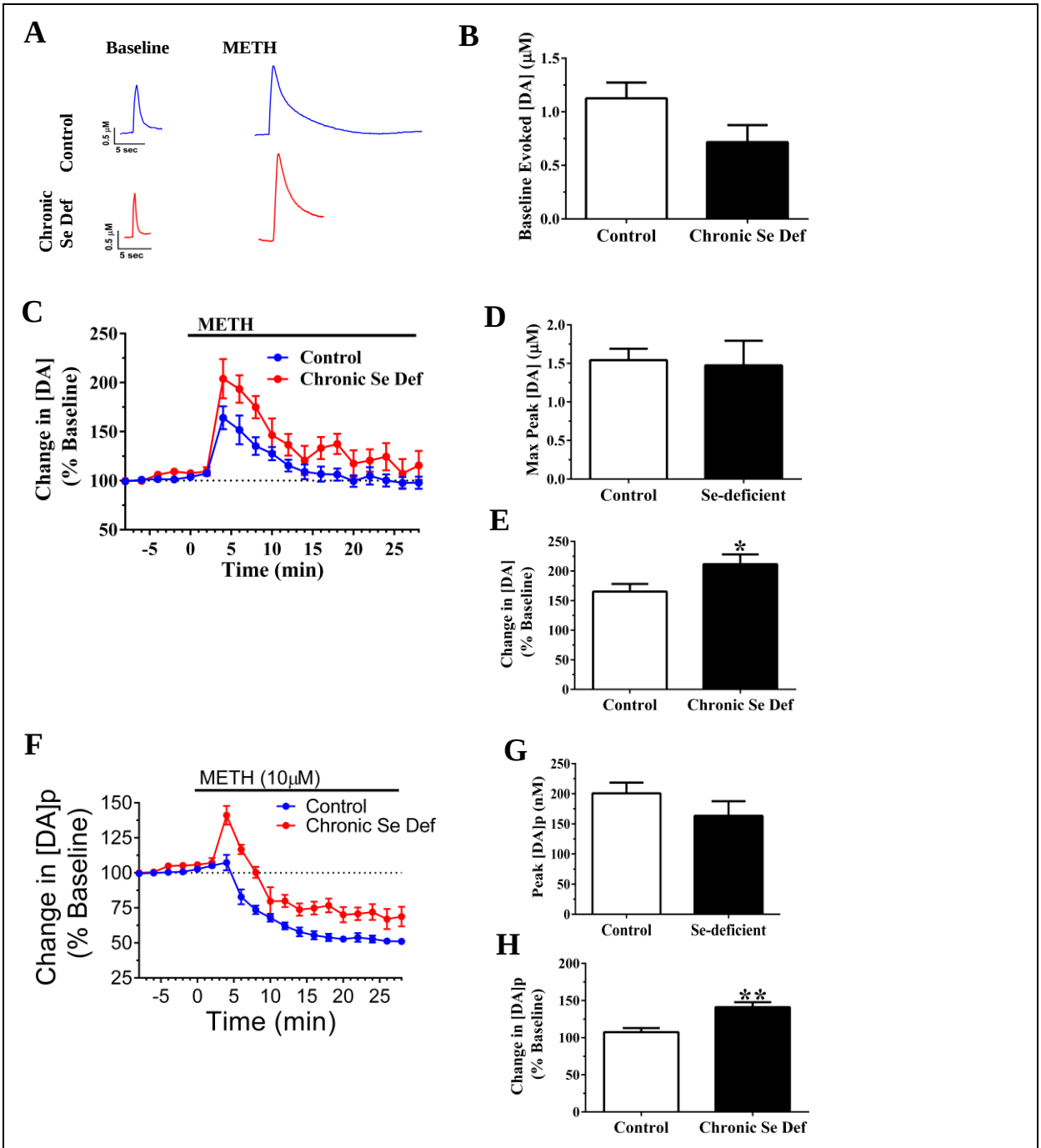

Figure 4-1. Chronic Se deficiency augmented the phasic DA response to METH.
A. Sample traces of baseline and (10 µM) METH-amplified phasic DA responses in slices from control animals versus slices from mice (Male C57 WT, aged 3-5 months) raised on a Se-deficient diet from weaning age (~21 days). **B.** Baseline evoked DA concentrations trended towards a decrease in Slices from Se-deficient mice (0.69 ± 0.16, n=7) compared to controls (1.126 ± 0.1476, n=16) (P = 0.102). **C.** Evoked DA release in slices from Se-deficient mice increased about 200% over baseline in response to METH. **D, E.** While the max evoked DA response was unchanged by chronic Se-deficiency, the percent increase over baseline was significantly higher than controls (211.5 ± 16.7, n=7 compared to 165.4 ± 12.80, n=8; P = 0.045). **F**. Dopamine released per pulse, [DA]p, was unchanged at baseline, but increased in response to METH in Slices from Se-deficient mice. **G**, **H.** Like extracellular DA concentration, max [DA]p was unchanged (P>0.05) while the percent increase over baseline was augmented by chronic Se deficiency (141.1 ± 6.7, n=7 compared to 107.4 ± 5.583, n=8; P = 0.002).

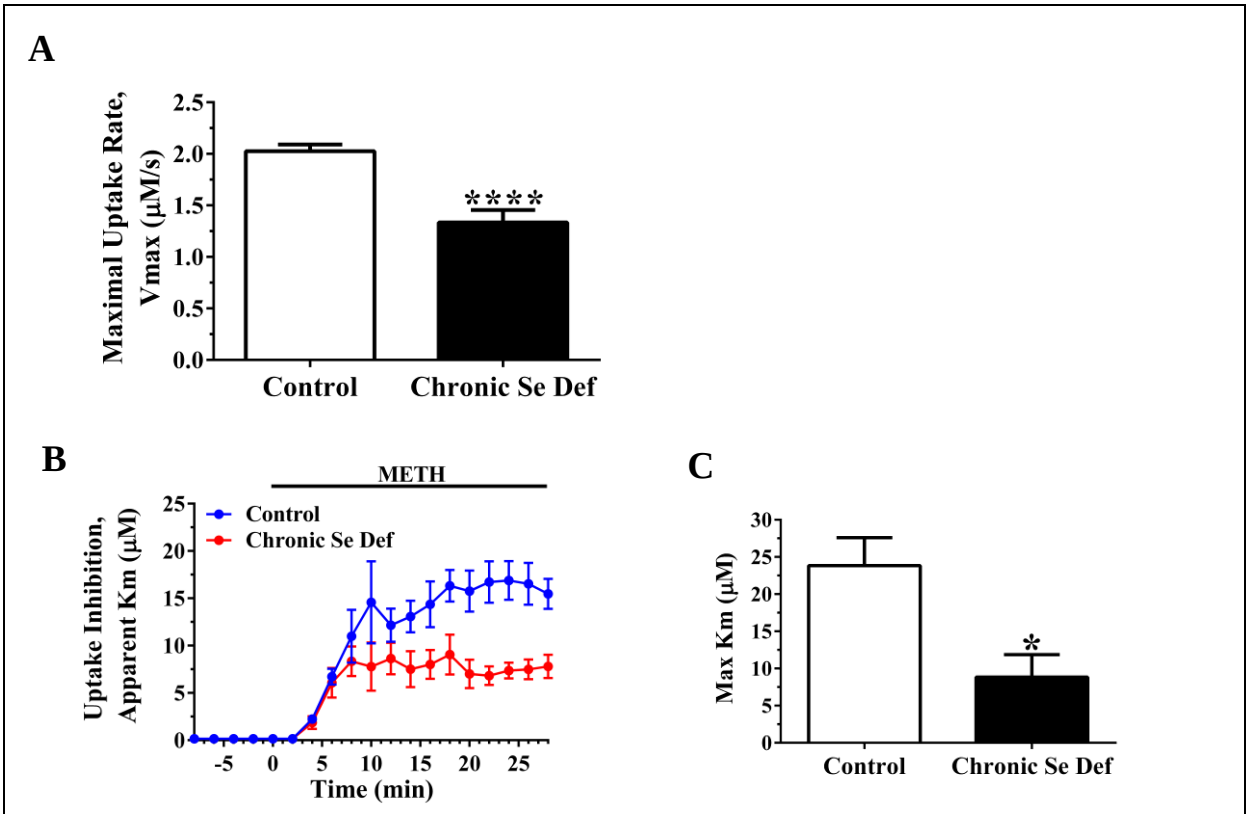

Figure 4-2. Chronic Se deficiency reduced basal DA uptake rates and attenuated METH inhibition of DA uptake.

A. Baseline DA uptake rates, Vmax, measured before METH (10 µM) exposure were lower in slices from Se-deficient male C57 WT mice, aged 3-5 months (1334 ± 122.0, n=8) than in slices from control animals (2026 ± 64.66, n=19) ($P < 0.0001$). **B**. Time course graph depicting changes in uptake inhibition, represented by apparent Km, in response to METH. Apparent Km, inversely proportional to the affinity of DA for DAT, was set to 160 nM at baseline and increased as METH inhibited DA uptake. **C.** Average peak Km values of slices from control animals (23830 ± 3764, n=8) were more than twice as high as for Slices from Se-deficient mice (8850 ± 3008, n=4) (P = 0.0276).

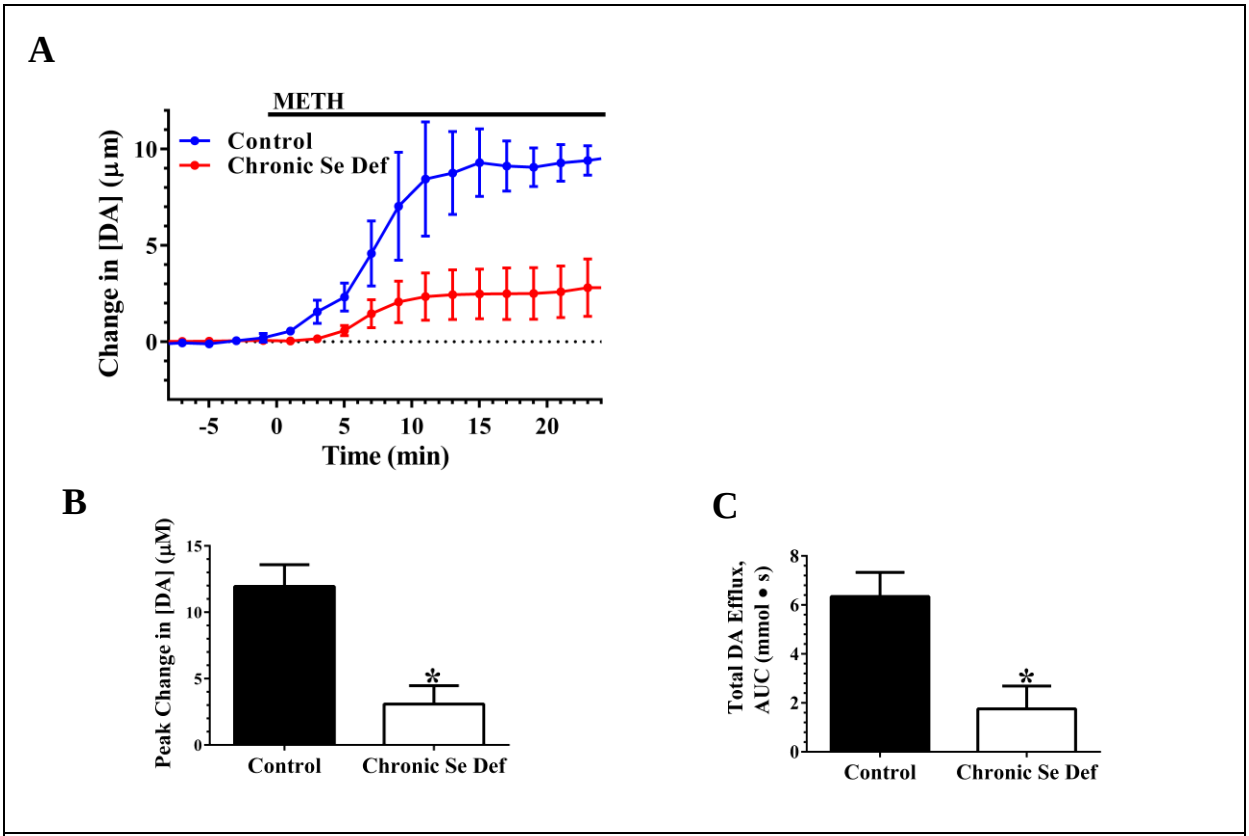

Figure 4-3. Chronic Se deficiency reduced METH-induced DA efflux.
A. Time course showing reduced DA efflux in slices from Se-deficient male C57 WT mice, aged 3-5 months in the presence of METH (10 µM). **B, C.** Maximum change in DA concentration (n=3 and 3, P=0.0143) and total DA efflux were both reduced by chronic Se deficiency (n=3 and 3, P=0.0278).

CHAPTER 5: THE ROLE OF SELENOPROTEIN P IN ACTION POTENTIAL-DEPENDENT DOPAMINE RELEASE

Abstract

Sepp1-KO mice have reduced baseline phasic DA release and uptake rates. In response to METH, phasic release was significantly potentiated due to increased DA vesicular release. METH-induced vesicular DA release is masked by D2R auto-inhibition in WT mice, which may be dysfunctional in Sepp1-KO mice. METH-induced vesicular DA release could be prevented in Sepp1-KO mice by application of purified Sepp1 protein acting on ApoER2 to promote D2R function.

Introduction

The work carried out in the previous chapters revealed a role of Se in modulating dopaminergic transmission and the response to METH in the mouse NAc, while highlighting the role of the selenoprotein GPx. Notably, we reported an increase in exoctotic DA release in the chronic Se-deficient NAc. We next investigated the potential role of the Se transport selenoprotein, Sepp1, using a Sepp1-KO mouse model. Since Sepp1 is responsible for delivering Se to the brain, we predicted the dopaminergic phenotype of Sepp1-KO mice to be similar to that seen in mice raised on a Se-deficient diet. Multiple studies have described the similarities in the neurological impairments caused by genetic Sepp1 deletion and dietary Se deficiency, including similar reductions in brain Se levels (Burk and Hill, 2009). Although there are no studies of Sepp1-induced signaling to date, Sepp1 has recently been confirmed to interact with ApoER2 in order to mediate Se transport across membranes (Burk et al., 2007; Olson et al., 2007; Burk et al., 2014). ApoER2 can also initiate signaling cascades leaving open the possibilty that Sepp1 can induce changes in the cell in addition to Se delivery (Reddy et al., 2011).

In this chapter, we describe the effects of Sepp1 deletion on the mesolimbic mouse DA system revealed through FSCV interrogation of brain slices. We also explore the vulnerability of Sepp1-KO mice to METH-induced increases in vesicular DA release and the ability of the Sepp1 protein to rescue this phenotype potentially through interaction with ApoER2. Finally, we describe the contributory role of D2R auto-inhibition of DA release in mediating the Sepp1-KO mouse response to METH as well as the rescue effect of Sepp1 protein.

Methods

To investigate the dopaminergic phenotype of Sepp1-KO mice, we measured phasic and tonic release as descibed in the METHODS section. C57/BL6 Sepp1-KO mice raised on standard lab chow with no Se supplementation were used. Male and female mice showed similar responses to METH (data not shown) and were, therefore, pooled together. For all other experiments on Sepp1-KO including pharmacological agents and Sepp1 protein application, male mice were used. DA release was evoked by 1-, 2-, and 10-pulse stimulations to test the level of responsiveness to varying degrees of stimulation. The early rising slope was also derived from 10-pulse-elicited response as an indicator of vesicular release, as the signal should be less affected by uptake through DAT.

Purified Sepp1 protein and mutants were applied to slices for 30 minutes prior to METH to investigate the effect of Sepp1 activity. For information on generation and descriptions of the mutants, refer to the METHODS section. The D2R agonist quinpirole (30nM) and D2R antagonist sulpiride (600nM) were added to characterize the role of D2R auto-inhibition in METH-induced changes in phasic DA release.

Results

Changes in Basal Phasic DA Release in Sepp1-KO Mice:

To investigate the responsiveness of DA terminals to varying degrees of stimulation, we first performed a progression of pulse stimulations: 1-pulse, 2-pulse, and 10-pulse. Sepp1-KO slices released lesser amounts of DA on average (0.1512 ± 0.0462 µM, n=5) than WT slices (0.5054 ± 0.1456 µM, n=5) following a 1-pulse stimulation ($P = 0.0490$) (Fig. 5-1A, B). 2-pulse stimulation trended towards significance ($P = 0.0513$) between Sepp1-KO slices (0.2184 ± 0.0499 µM, n=5) and WT slices (0.6269 ± 0.1713 µM, n=5) (Fig. 5-1A, C). The ratio of 2-pulse response over the 1-pulse response was greater in Sepp1-KO slices (1.558 ± 0.0977 µM, n=5 compared to 1.264 ± 0.0444 µM, n=5 for WT mice) representing a greater increase in DA release from 1 to 2 pulses ($P = 0.0256$) (Fig. 5-1C). In response to a 10-pulse stimulation train, Sepp1-KO slices had reduced DA release (0.4800 ± 0.1197 µM, n=4) compared to WT slices (1.399 ± 0.3666 µM, n=3) ($P = 0.0418$) (Fig. 5-1A, D) and there was no difference in the 10/1 pulse ratio between the groups ($P = 0.8999$) (Fig. 5-1D).

The average basal evoked DA release in Sepp1-KO slices (0.4731 ± 0.06796 µM, n=13) in response to 10-pulse stimulation trains taken from the baseline of ensuing experiments was about half the amount measured in WT slices (1.126 ± 0.1476 µM, n=16) (P = 0.0009) (Fig. 5-1E). The early rising slope of the baseline evoked DA release events was similarly reduced in Sepp1-KO slices (0.5546 ± 0.1387 µM/ms, n=6 compared to 1.416 ± 0.1197 µM/ms, n=4 in WT mice) (P = 0.0024) (Fig. 5-1F). The early slope represents the rate of DA release during the rising phase of the evoked response and is less affected by DA uptake. Baseline [DA]p was reduced in Sepp1-KO slices (87.29 ± 8.247 nM, n=13) to about half the level of WT slices (184.2 ± 19.69 nM, n=16) (P = 0.0003) (Fig. 5-1G). All three measurements of basal evoked DA release yielded significantly smaller values in Sepp1-KO slices in similar proportions.

Changes in protein expression in Sepp1-KO mice:

Western blot analysis revealed no differences in TH expression between groups (Fig. 5-2A). There was also a decrease in DAT expression in Sepp1-KO ventral striatum, with a downward trend in ventral midbrain (Fig. 5-2B). Interestingly VMAT-2 expression was increased in Sepp1-KO ventral midbrain, with an upward trend detected in ventral striatum as well (Fig. 5-2C). D2R expression was not changed in Sepp1-KO mice (Fig. 5-2D).

Changes in METH-induced DA release in Sepp1-KO mice:

We further employed FSCV to examine whether Sepp1-KO mice have an altered response to METH. Sepp1-KO slices and WT slices both exhibited an immediate increase in the phasic DA response post-METH application (Fig. 5-3A, B) that was reduced in Sepp1-KO slices (0.9173 ± 0.1452 µM, n=6) compared to WT slices (1.542 ± 0.1490 µM, n=8) (P = 0.0127) (Fig. 5-3C). Phasic DA signals gradually drifted back down towards baseline levels, an effect that was slower to occur in Sepp1-KO slices (Fig. 5-3B). Although the maximum response was lower in Sepp1-KO slices, the percent increase over baseline (292.9 ± 27.08 %, n=6) was nearly double that of WT slices (163.1 ± 11.81 %, n=8) (P = 0.0004) (Fig. 5-3D). The dramatic effect of Sepp1 deletion on evoked DA release in response to METH contrasted with non-stimulated DA efflux induced by METH, which was unchanged in Sepp1-KO slices (Fig. 5-3D, E). It is worth noting that while Sepp1KO slices displayed smaller evoked DA signals and a disproportionately larger

fold-increase with METH than controls, the peak phasic concentrations displayed by each group were comparable.

We used the Michaelis-Menten modeling application to depict changes in DA uptake in Sepp1-KO mice. Vmax was reduced in Sepp1-KO slices (1206 ± 86.56 µM/s, n=27) indicating slower basal DA uptake rates compared to WT slices (2026 ± 64.66 µM/s, n=19) ($P < 0.0001$) (Fig. 5-4A). METH elicited comparable increases in apparent Km in both WT (23830 ± 3764 nM, n=8) and Sepp1-KO slices (14611 ± 2215 nM, n=6) indicating similar levels of DA uptake inhibition, although there was a downward trend in the Sepp1-KO slices ($P = 0.0778$) (Fig. 5-4B, C).

There has been some debate over whether METH causes an increase in vesicular DA release in addition to the widely accepted mechanism of DA efflux (Siciliano et al., 2014). Recent publications have argued that AMPH causes increases in action potential-driven DA release as demonstrated by *in vivo* FSCV experiments (Covey et al., 2016). In response to METH, Sepp1-KO slices exhibited an initial increase in [DA]p that gradually decreased in amplitude towards baseline with successive stimulations (Fig. 5-5A). WT slices, by contrast displayed a slight increase that quickly dropped below baseline, likely due to vesicular depletion. The average percent increase over baseline [DA]p was greater in the Sepp1-KO slices (171.9 ± 11.86 %, n=6) than in WT controls (112.9 ± 3.139 %, n=8) ($P < 0.0001$) (Fig. 5-5B). To test whether reduced Se levels may have caused long-term neurodegeneration to affect these results, we supplemented some Sepp1-KO mice with Se water (1mg/mL) immediately post-weaning. Se-supplemented Sepp1-KO mice exhibited an equal increase in [DA]p as non-supplemented Sepp1-KO mice (data not shown), further implicating the role of Sepp1 protein.

Ability of Sepp1 Protein to Prevent METH-induced Increases in Vesicular DA Release:

To evaluate whether the increase in [DA]p in Sepp1-KO mice in response to METH was a direct effect of the loss of Sepp1 activity, we added 100 pM Sepp1 protein to brain slices via perfusion for 30 minutes immediately prior to METH application. Sepp1 protein by itself did not change DA release or uptake in either WT or Sepp1-KO slices. However, Sepp1 suppressed the METH-induced increased in vesicular DA release in Sepp1-KO slices without altering the response to METH in WT slices (Fig. 5-6A, B). The maximum percentage increase of [DA]p in

Sepp1-exposed Sepp1-KO slices (118.2 ± 7.276 %, n=4) was significantly lower than non-exposed Sepp1-KO slices (171.9 ± 11.86, n=6) (112.9 ± 3.139 %, n=8) (P = 0.0097) (Fig. 5-6C).

Although the accepted primary function of Sepp1 is to deliver Se, it has other functions including possible cell signaling via ApoER2. To examine which function of Sepp1 is involved, we first utilized a full-length (FL) all-cys Sepp1 mutant in which the 10 Sec residues have been changed to Cys residues, and is therefore unable to supply Se. Application of the FL all-Cys Sepp1 mutant to Sepp1-KO slices resulted in a robust suppression of the METH-induced vesicular DA release (106.0 ± 1.680 %, n=3) (Fig. 5-6D, E).

Next, we added to slices an N-terminal domain fragment (NT) of the all-Cys Sepp1 mutant, which resulted in a [DA]p (146.5 ± 21.66, n=3) response to METH similarly to non-exposed Sepp1-KO slices (Fig. 5-6D, E). The ineffectiveness of the NT mutant implies that the region of Sepp1 responsible for suppressing METH-induced increases in [DA]p is located on the C-terminal domain.

The ApoER2 binding site is in the C-terminal domain, suggesting the possibility that interaction of Sepp1 with ApoER2 is a contributing factor (Kurokawa et al., 2014). To explore this possibility, we used an all-Cys Sepp1 mutant in which an essential region (residues 234-237) for ApoER2 binding is deleted eliminating the ability of Sepp1 to bind ApoER2. The ApoER2 domain mutated peptide (Δ234-237) did not significantly reduce the METH-induced [DA]p increase (127.2 ± 8.245 %, n=3), demonstrating that Sepp1-ApoER2 interactions attenuate the METH response in Sepp1-KO slices (Fig. 5-6D, E). Dunnett's test following one-way ANOVA revealed a significant reduction in the [DA]p response to METH only following pre-application with the FL all-Cys mutant (Fig. 5-6F).

Role of Dopamine Receptor 2:

AMPH has an excitatory effect on DA release that is masked by D2R auto-inhibition (Shi et al., 2000). Therefore, the substantial increase in [DA]p induced by METH in Sepp1-KO mice may be due to D2R dysfunction. To see if increasing D2R activity would prevent the METH-induced [DA]p increase in Sepp1-KO mice, we applied the selective D2R agonist quinpirole to Sepp1-KO and WT slices for 15 minutes prior to and for the duration of METH exposure. Quinpirole activates presynaptic D2R to increase auto-inhibition of vesicular DA release to reduce evoked DA responses measured through FSCV. Exposure to 30nM quinpirole caused a

similar decrease in evoked DA release in WT and Sepp1-KO slices (45.88 ± 2.833 % of baseline signal, n=3 and 41.61 ± 3.856, n=3, respectively) (Fig. 5-7A, B).

In response to METH, [DA]p increased in both WT and Sepp1-KO slices following quinpirole application, but did not reach original baseline levels in either group (Fig. 5-7C). The maximum [DA]p reached in Sepp1-KO slices as a percentage of original baseline pre-quinpirole treatment was in stark contrast to the increase seen without quinpirole application (Fig. 5-7D). Quinpirole application did not significantly change the eventual maximum percentage change in [DA]p in response to METH in WT mice (Fig. 5-7D). Moreover, the WT and KO slices treated with quinpirole exhibited similar percent increases in [DA]p during METH application.

To block D2R auto-inhibition, we added the selective D2R antagonist sulpiride to further investigate the role of D2R in METH-induced changes in DA release. Addition of sulpiride (600 nM) resulted in comparable increases in evoked DA signals over baseline in Sepp1-KO (139.8 ± 6.146, n=7) and WT (148.5 ± 4.580, n=4) slices (Fig. 5-8A, B). Sulpiride caused an increase in [DA]p WT mice (429.3 ± 131.4, n=3) in the presence of METH (Fig. 5-8C, D). Sulpiride with METH did not further increase [DA]p in Sepp1-KO slices significantly above levels observed with METH alone (184.3 ± 21.54 % increase over baseline, n=3 and 176.3 ± 10.41 %, n=6, respectively) (Fig. 5-8C, D). In the presence of sulpiride, the [DA]p increase in response to METH was also significantly larger in WT than in Sepp1-KO slices (Fig. 5-8D).

Since sulpiride antagonism of D2R auto-inhibition resulted in an [DA]p in response to METH, we tested if it could prevent the Sepp1 protein from reducing the response in Sepp1-KO mice. We added sulpiride to Sepp1-KO slices prior to and during Sepp1 application as well as during METH exposure. Sulpiride prevented the suppressive action of Sepp1 protein, resulting in roughly a doubling of [DA]p (203.4 ± 23.87 %, n=4, $P = 0.0069$ when compared to just Sepp1-applied Sepp1-KO slices via unpaired t-test) once METH was added (Fig. 5-8E, F, G).

Conclusions and Discussion

Sepp1-KO mice have reduced basal phasic DA release:

All three measurements of basal evoked DA release yielded significantly smaller values in Sepp1-KO slices in similar proportions, indicating that genetic deletion of Sepp1 reduces the magnitude of phasic DA release. Altered vesicular content or distribution may be a possibility to account for the reduced basal release, considering that VMAT-2 expression was increased in

Sepp1-KO mice. It is possible that the vesicular DA was not necessarily present in the readily-releasable pool of vesicles (Covey et al., 2013). This will be further elaborated on in the GENERAL DISCUSSION section. Another explanation for decreased phasic release is that the Sepp1-KO mice could have fewer DA terminals due to neurodegeneration or aberrant neurodevelopment. Indeed, DAT expression was reduced in the relevant brain regions of Sepp1-KO mice, suggesting fewer DA terminals. TH expression was not changed in the same brain regions of Sepp1-KO mice, however, implying similar levels of DA synthesis. However, TH is expressed in both nerve terminals and cell bodies. Neurodevelopmental changes in the DA system of Sepp1-KO mice is plausible as the Sepp1 binding partner ApoER2 is heavily involved in migration of DA neurons during development (Sharaf et al., 2013; Sharaf et al., 2015).

The 2/1 pulse response ratio was greater in Sepp1-KO slices, representing a greater increase in evoked release. The ratios for both groups were less than 2, indicating that the amount of DA released from the 2nd pulse in the 2-pulse train is less than the amount released from the 1st pulse. D2R auto-inhibition is partially responsible for this phenomenon (Moquin and Michael, 2009; Anzalone et al., 2012) Therefore, the greater 2/1 ratio of the Sepp1-KO mice suggests a less robust D2R auto-inhibitory effect. Also, the 10/1 pulse response ratios were equal between the groups.

Sepp1 protein prevents METH-induced vesicular release in Sepp1 KO mice:

Sepp1-KO mice exhibited a dramatic increase in [DA]p in response to METH, indicating an increase in vesicular DA release, that was prevented by application of purified Sepp1 protein. Moreover, the effect is Se-independent as the full-length all-Cys mutant was as equally effective as the intact Sepp1. The all-Cys N-terminal fragment was not effective, however, implying that the C-terminal domain is necessary (Saito and Takahashi, 2002). The Δ234-237 mutant was also ineffective, revealing that proper function of the ApoER2 binding site on Sepp1 was necessary for this preventative effect.

Together, these results strongly suggest that Sepp1 acts through ApoER2-mediated signaling. Furthermore, the ability of sulpiride to block the suppressive effect of Sepp1 protein in Sepp1-KO slices suggests that Sepp1 signaling may engage pre-synaptic D2R to limit increases in vesicular DA release caused by METH.

ApoER2 interacts with different scaffolds and adaptor proteins, such as Dab1, which promotes ApoER2 surface expression. ApoER2 is also known to undergo internalization in response to ligand binding (Cuitino et al., 2005). Interestingly, the adaptor protein CIN85 binds to Dab1 and has been suggested to mediate internalization of various membrane receptors, including D2R (Fuchigami et al., 2013). This further suggests that ApoER2 may be able to influence D2R surface expression. ApoER2 is also known to associate with NMDARs. NMDAR activation on active pre-synaptic striatal DA terminals promotes DA release in a Ca^{2+}-dependent manner (Wang, 1991). Therefore, NMDAR internalization via ApoER2 activation is another prospective mechanism for Sepp1.

Implications for METH mechanism of action:

The ability of quinpirole to prevent the large METH-induced increase of [DA]p in Sepp1-KO mice implicates impaired D2R activation or function in Sepp1-KO mice in the METH-linked increase in vesicular DA release. This is an important finding that suggests that METH can directly increase evoked DA release independent of DAT inhibition, but that this increase is normally masked by D2R auto-activation. This is also contingent upon D2R auto-inhibition acting fast enough after METH application to inhibit the first evoked release. Interestingly, Shi et al. reported that AMPH causes an excitation in VTA DA neurons, which is masked by D2R activation via AMPH-elevated DA concentrations (Shi et al., 2000). The excitatory action of AMPH was reported to be driven by adrenergic afferents onto VTA cell bodies. Our current findings, however, suggest that METH can increase vesicular DA release through a mechanism localized to the striatal environment. While we have shown that D2R masks this effect as well, further investigation into how METH causes the increased vesicular DA release is warranted. The proposed mechanism of D2R dysfunction masking METH-induced vesicular DA release in Sepp1-KO mice, in a manner reversible by Sepp1 protein, is summarized in Figure 5-9.

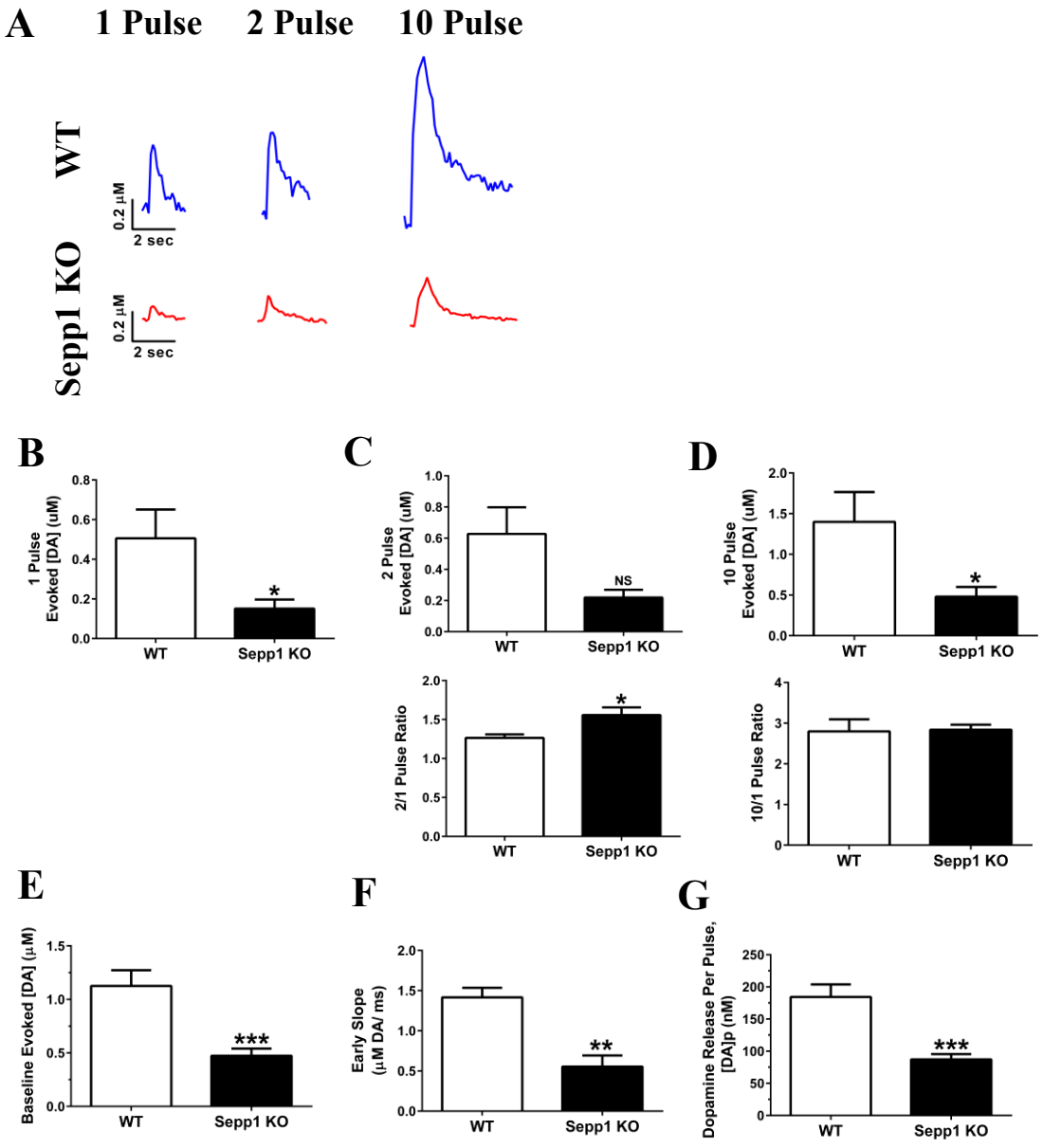

Figure 5-1. Deletion of Sepp1 results in reduced evoked dopamine responses in the nucleus accumbens.

A. Representative traces from male C57 WT mice and C57 Sepp1 KO mice, aged 3-5 months. DA signals evoked by 1-, 2-, and 10-pulse stimulations. **B, C.** 1-pulse (n=5 and 5, $P < 0.05$) stimulation elicited greater concentrations of DA from WT mice than from Sepp1 KO mice. 2-pulse stimulation caused in upward trend in Sepp1 KO mice (n=5 and 5, P=0.051). The ratio of 2-pulse-elicited responses (n=5 and 5, $P < 0.05$) to 1-pulse-elicited responses was greater in Sepp1 KO mice. **D.** 10-pulse stimulation induced greater DA release in Sepp1 KO mice (n=5 and 5, $P < 0.05$). The ratio of 10-pulse to 1-pulse responses was unchanged between the groups (n=5 and 5, P=0.9). **E.** Average baseline phasic DA release (evoked by 10-pulse stimulation trains) taken from all experiments was reduced in Sepp1 KO mice compared to WT (n=5 and 5, $P < 0.001$). **F.** The early rising slope of the baseline phasic signals was also reduced in Sepp1 KO mice (n=5 and 5, $P < 0.01$). **G.** Concentrations of vesicular DA released per individual stimulation pulse, [DA]p, estimated using a kinetic modeling system was decreased in

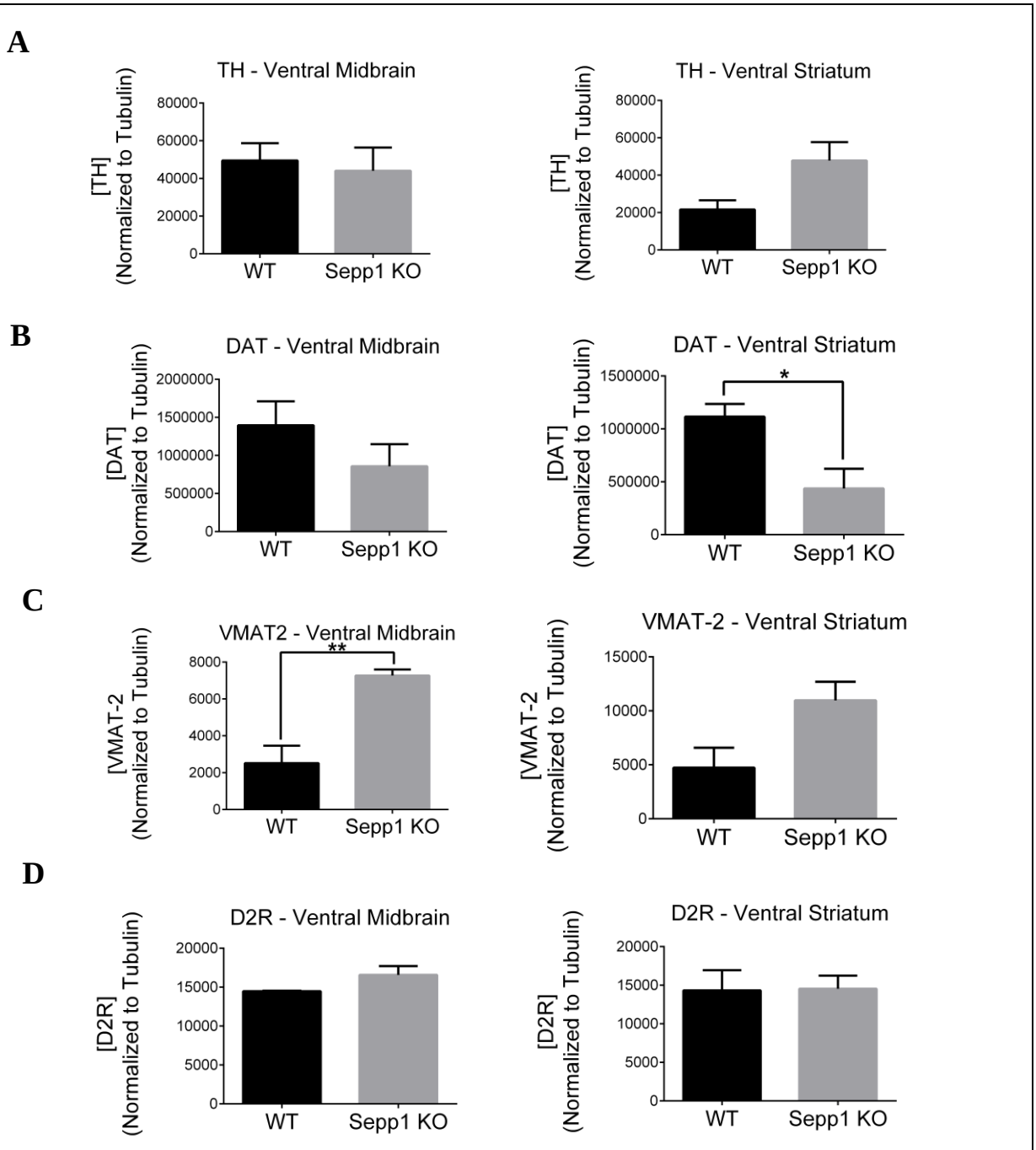

Figure 5-2. Western blot revealed Sepp-KO mice have reduced DAT and increased VMAT-2 expression in both the ventral midbrain and ventral striatum.

A. TH expression trended toward in an increase in ventral midbrain of male C57 WT mice and C57 Sepp1 KO mice, aged 3-5 months (n=3 and 3) (P=0.0561), while no changes were seen in ventral midbrain. **B.** DAT expression was significantly decreased in Sepp1-KO ventral striatum (P=0.0377) with no change in ventral midbrain (n=3 per group) (P>0.05). **C.** VMAT-2 expression was increased in Sepp1-KO ventral midbrain (P=0.0091) and trended up in ventral striatum (P=0.0694) (n=3 per group). **D.** No changes were seen in D2R expression (n=3 per group) (P>0.05).

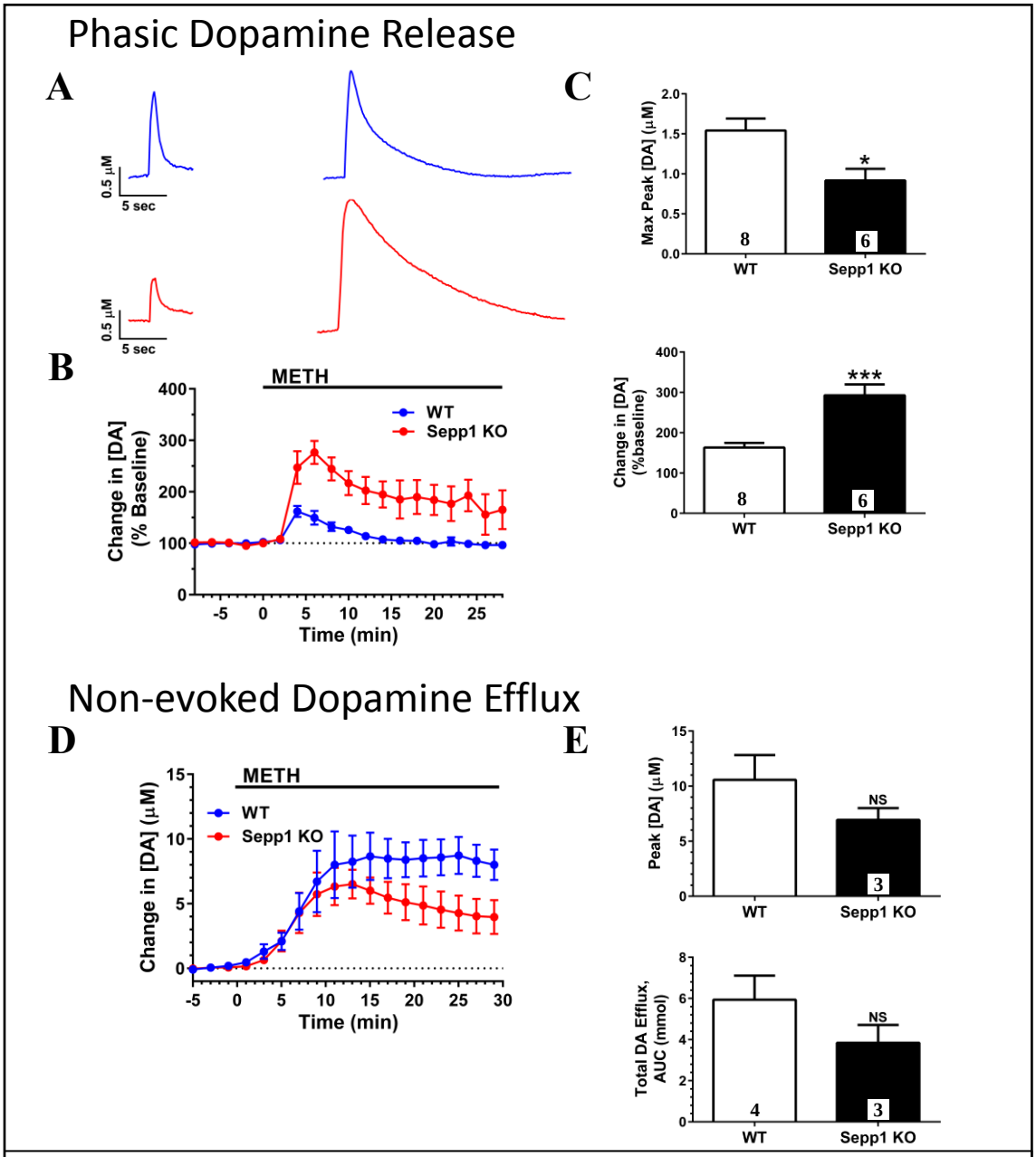

Figure 5-3. Increased phasic dopamine release induced by methamphetamine was greater in Sepp1 KO mice than wild-type controls, with no effect on dopamine efflux. **A.** Representative traces from male C57 WT mice and C57 Sepp1 KO mice, aged 3-5 months. Phasic DA signals at baseline and in response to 10µM METH. **B.** Time course of phasic DA release (elicited every 2 minutes) showing percent increases over baseline. **C.** WT mice displayed higher peak phasic DA responses to METH ($p < 0.05$). Sepp1 KO mice displayed greater percent increases in phasic DA release over baseline levels compared to WT mice ($p < 0.001$). The 'n' for each group is shown in the graph columns. **D.** Time course of DA efflux (non-stimulated) in the presence of METH measured as an increase in extracellular DA concentration over baseline levels. **E.** Maximum non-simulated DA concentrations and total DA efflux, measured as area under the curve (AUC) of the complete time course response, were not different between the groups (P>0.05).

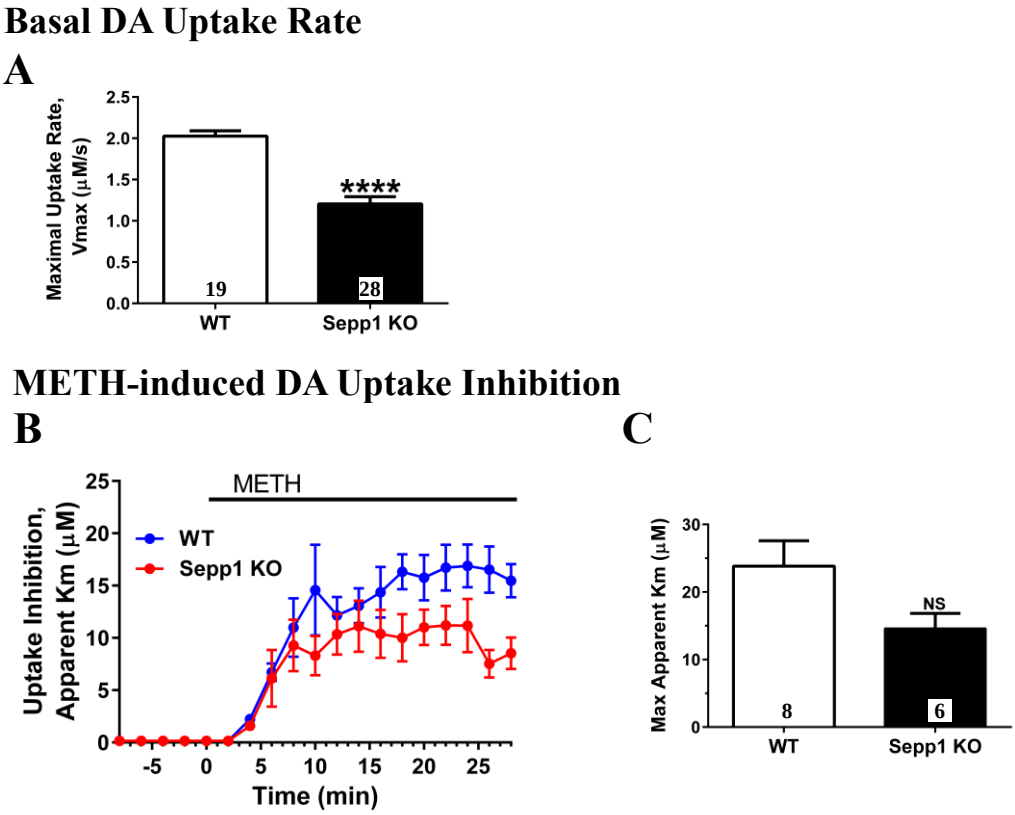

Figure 5-4. Sepp1 KO mice had reduced maximal DA uptake rates with no change in METH-induced DA uptake inhibition compared to controls.
A. Max DA uptake rates, calculated as Vmax using Michaelis-Menten kinetic modeling, were lower in Sepp1 KO mice ($p < 0.0001$). Male C57 WT mice and C57 Sepp1 KO mice, aged 3-5 months were used. Vmax was calculated for each subject at baseline and held constant for the duration of the experiment. **B.** Time course of apparent Km, representing the affinity of DA for DAT. Km was set to 160 nM at baseline an increased in response to METH (10 μM) as DA uptake was inhibited. **C.** No differences in maximum Km reached in the presence of METH were observed between groups ($P>0.05$).

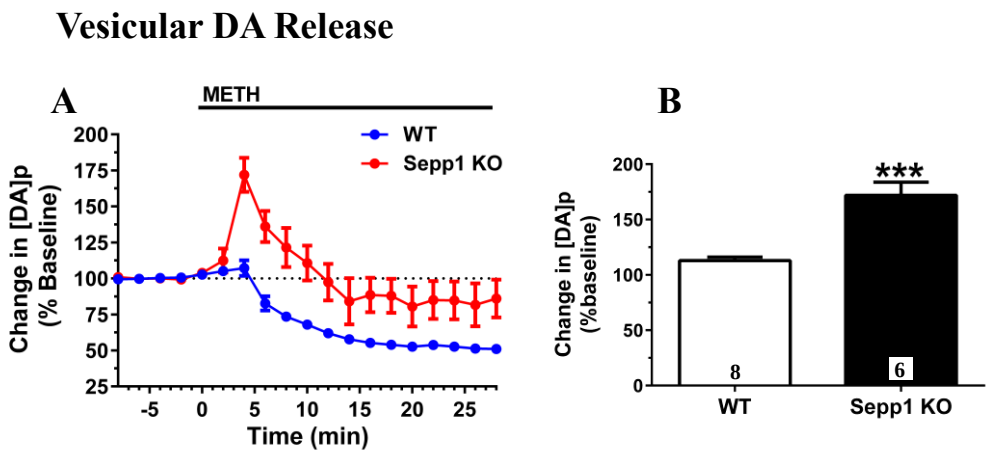

Figure 5-5. METH caused an increase in vesicular DA release in Sepp1 KO mice. **A.** Time course of vesicular DA release in response to METH (10 µM) from male C57 WT mice and C57 Sepp1 KO mice, aged 3-5 months. Vesicular DA release is measured by the Michaelus-Menten kinetic factor [DA]p, representing the average concentration of DA released per stimulation pulse. METH induced a slight increase in [DA]p in WT mice before dropping below baseline. Sepp1 KO mice exhibited a substantial increase in [DA]p upon METH application which took longer to drop below baseline. **B.** Sepp1 KO mice displayed a greater percent increase in [DA]p (171.9 ± 1.86 %) compared to WT mice (112.9 ± 3.14 %) ($P < 0.001$).

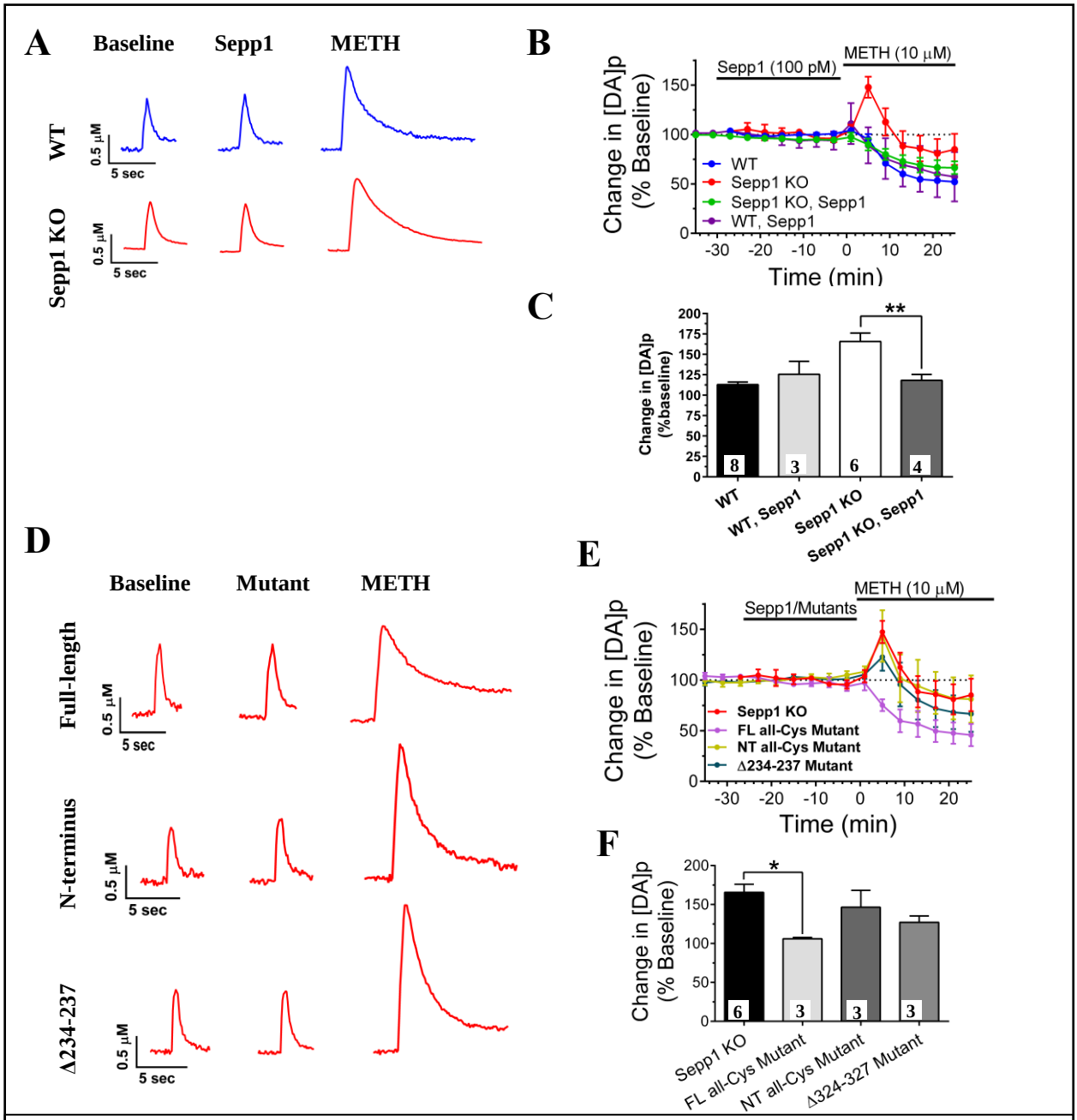

Figure 5-6. Sepp1 protein prevented METH-induced increases in vesicular DA release by acting through ApoER2 receptors.

A. Representative traces showing METH (10 µM) responses in Sepp1 KO and WT brain slices pre-treated with Sepp1 protein. **B.** Time course of [DA]p showing no change upon Sepp1 protein exposure and absence of a METH-induced increase in [DA]p in Sepp1 KO mice pre-treated with Sepp1 protein. **C.** Sepp1 protein reduced the [DA]p response to METH in Sepp1 KO mice to the level of WT mice ($P < 0.01$). Sepp1 treatment had no effect on the WT response. **D.** Representative traces of Sepp1 KO mice when treated with various Sepp1 mutants (100 pM) prior to being exposed to METH. **E, F.** Pre-treatment with a full-length all-Cys Sepp1 mutant lacking Se was successful in preventing the METH-induced [DA]p increase in Sepp1 KO mice ($P < 0.05$). Treatment with an all-Cys N-terminal region Sepp1 peptide lacking the C-terminus, however, did not prevent the increase in [DA]p in response to METH. The Δ234-237 Sepp1 mutant that is unable to bind ApoER2 also did not reduce the [DA]p response.

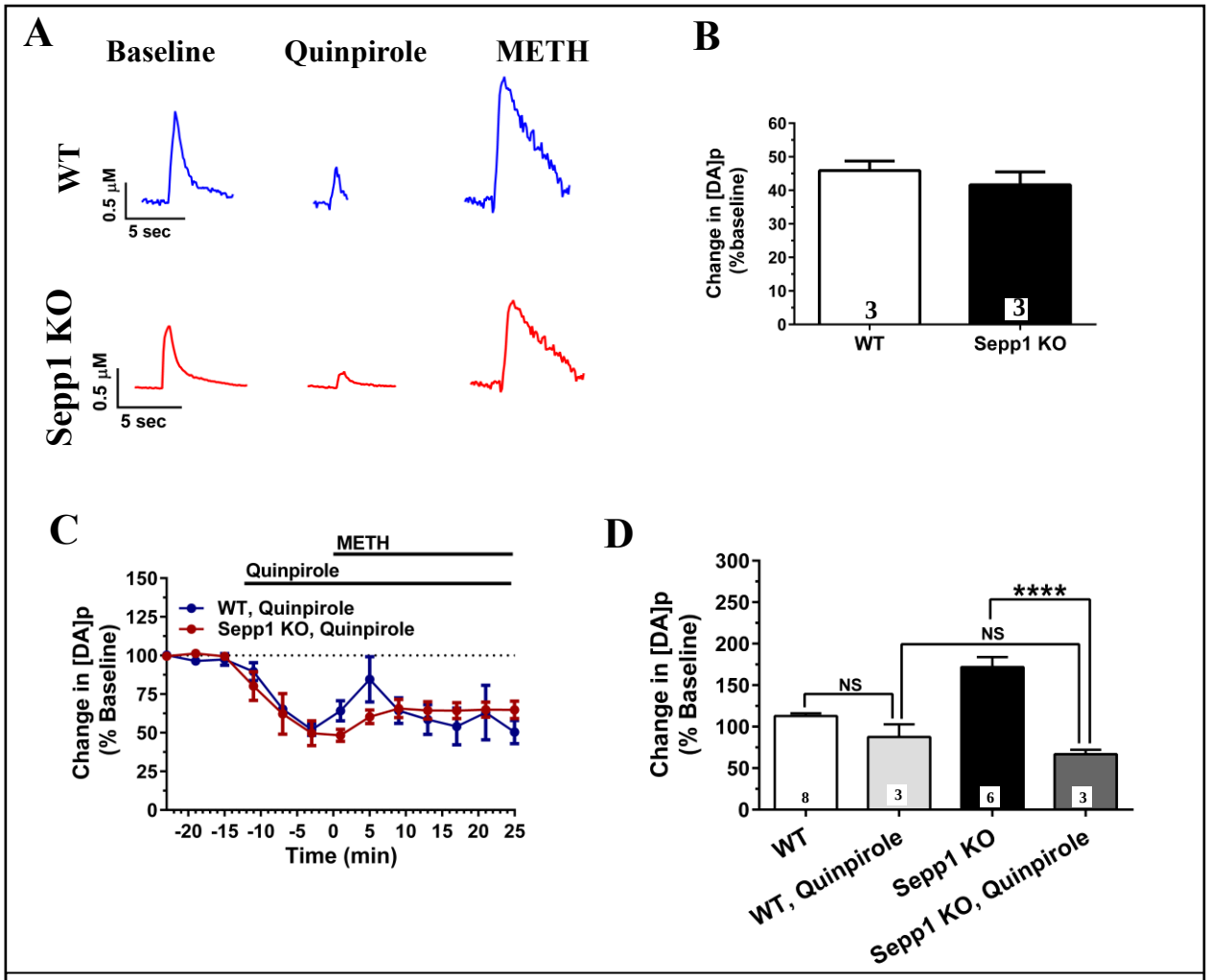

Figure 5-7. D2R activation prevented the METH-induced increase in vesicular dopamine release Sepp1 KO mice.

A. Sample traces of quinpirole-enhanced D2R auto-inhibition of evoked DA release from male C57 WT mice and C57 Sepp1 KO mice, aged 3-5 months. **B.** Quinpirole (30 nM) reduced basal DA release in WT and Sepp1 KO mice similarly. **C, D.** Quinpirole silenced the METH-induced increase in [DA]p above baseline levels in Sepp1 KO mice. WT and Sepp1 KO mice had comparable responses to METH

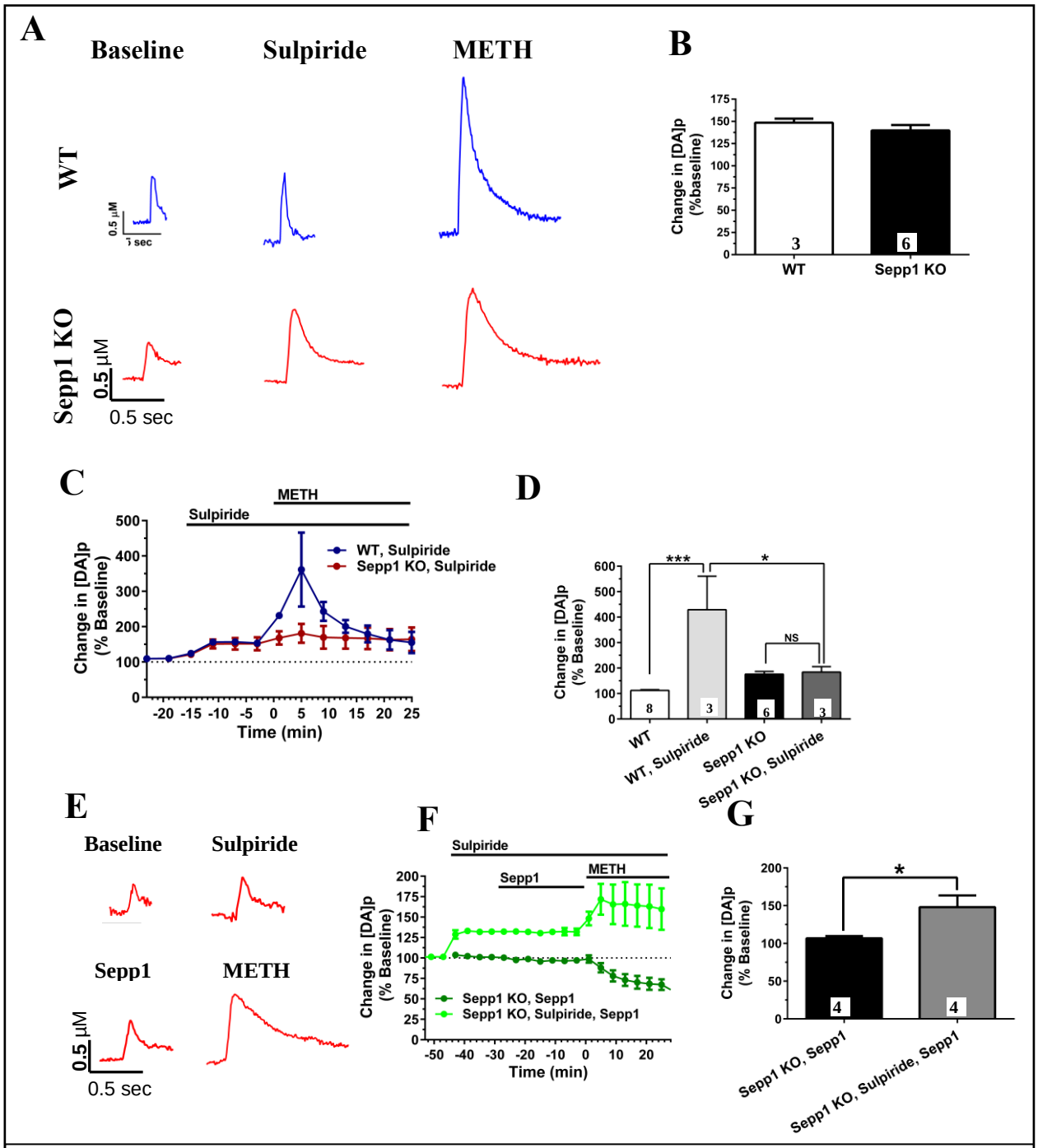

Figure 5-8. D2R antagonism unmasked an increase in vesicular dopamine release in wild-type mice and prevented the Sepp1 rescue in Sepp1-KO mice.

A. Sample traces showing sulpuride (600 nM) reduction of D2R auto-inhibition and subsequent response to METH from male C57 WT mice and C57 Sepp1 KO mice, aged 3-5 months. **B.** Sulpiride increased the baseline evoked DA release in WT and Sepp1 KO mice similarly. **C, D.** Pre-treatment with sulpiride caused a dramatic increase in [DA]p in WT mice while resulting in no changes to the METH response in Sepp1 KO mice. **E.** Sample traces showing the ability of sulpiride to prevent METH-induced vesicular DA release in Sepp1 KO mice. **F, G.** Sulpiride prevented the ability of Sepp1 protein to prevent the METH-induced increase in [DA]p in Sepp1 KO mice.

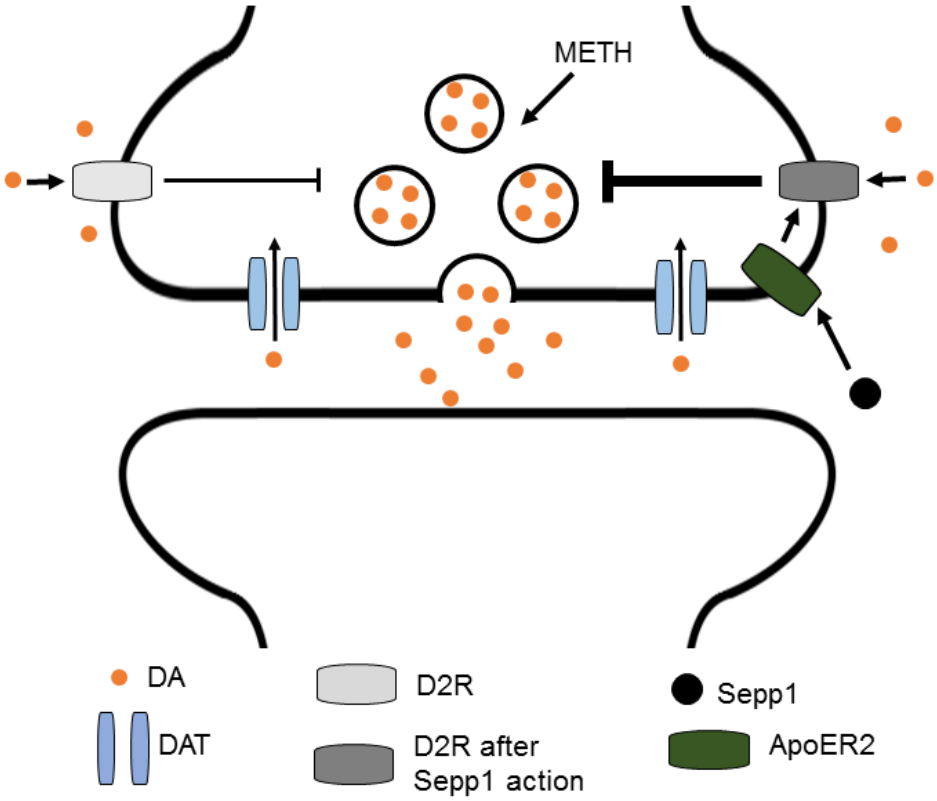

Figure 5-9. Proposed model for Sepp1 restoration of D2R function in Sepp1-KO mice.
The proposed mechanism is that Sepp1-KO mice have lower functioning pre-synaptic dopamine receptor 2 (D2R) compared to WT mice. D2R expression did not change suggesting a change in receptor kinetics or intracellular signaling. Phasic release of DA does not typically overflow out of the synaptic cleft due to uptake by DAT. When METH induces DA efflux, however, D2R become occupied by extra-synaptic DA overflow, thus allowing the D2R deficiency in Sepp1-KO mice to be observed. This D2R dysfunction unmasks the ability of METH to increase DA vesicular release. When Sepp1 is applied, it interacts with apolipoprotein e receptor 2 (ApoER2) to increase D2R function. This could be caused by an increase in D2R surface expression or cross-talk between ApoER2 and D2R intracellular signaling pathways.

CHAPTER 6: GENERAL DISCUSSION

Summary of Research Findings

The current study characterizes the influence of Se on dopaminergic transmission in the NAc through study of the impact of short-term and chronic Se deficiency. We found that short-term (2 weeks) Se deficiency reduced METH-induced DA efflux from acutely isolated NAc slices, potentially due to reduced GPx activity leading to increased levels of H2O2. This effect occurred in the absence of impact of short-term Se deficiency on phasic DA release. Application of a GPx mimetic increased tonic DA release and potentiated the METH-induced DA efflux. Direct inhibition of GPx activity had the opposite effect, instead reducing DA efflux, consistent with the Se-deficiency condition. Thus, our findings implicate GPx as playing a mediating role in the tonic dopaminergic response to METH. Furthermore, K_{ATP} channels seem to be involved in the suppression of the METH response by both 2-week Se deficiency and GPx4 inhibition. In addition, the endocannabinoid system may be involved as CB receptor activation reduced DA efflux. CB1R antagonism partially reversed GPx4 inhibition of DA efflux. H_2O_2 and lipid peroxides may be mediating players as described in detail in Figure 3-8.

Chronic Se deficiency reduced basal DA uptake rates and DAT expression, consistent with long-term Se deficiency leading to neurodegeneration. Moreover, the tonic response to METH was reduced to a degree like that seen in NAc slices from short-term Se deficiency mice. In contrast to the short-term Se deficiency condition, however, METH surprisingly increased vesicular DA release in NAc slices from chronically Se-deficient mice.

Lastly, we investigated DA release from Sepp1-KO slices to compare the impact of loss of the Se transport selenoprotein to the Se-deficiency condition. Sepp1-KO slices also exhibited strongly augmented METH-induced vesicular DA release, potentially due to dysfunctional D2R auto-inhibition. The augmentation METH-induced vesicular DA release in Sepp1-KO slices was prevented both by application of Sepp1 protein and a D2R agonist. D2R antagonism blocked the Sepp1 rescue effect, implying that Sepp1 acts through D2R activity. The Sepp1 rescue effect is dependent upon on the ApoER2 binding domain.

These findings highlight the ability of METH to regulate action-potential DA release independently of METH-induced DA efflux. Furthermore, we provide evidence of Sepp1-

induced changes in DA terminals that may involve intracellular signaling. Our proposed mechanism is explained in Figure 5-9.

Selenium-dopamine interactions in the striatum

Comparison of previous studies:

In previous studies, Se deficiency lasting 15-30 days increased DA metabolic turnover in the striatum (Romero-Ramos et al., 2000). These studies utilized microdialysis to measure changes in extracellular DA concentrations, which were accompanied by increases in TH and DAT activity. The authors postulated that the increase in DA turnover was a cellular adaptation to compensate for decreased DA vesicular storage caused by low GSH content. Our FSCV investigations did not reveal any changes in stimulated release of DA in NAc slices from Se-deficient C57/BL6 mice for a similar period, which likely would have been affected by a change in vesicular DA storage. Therefore, the increased DA turnover seen *in vivo* cannot be attributed to an effect specific to the NAc alone. The underlying cause could be an increase in the number of DA neurons in the active control state and, thus, greater contribution to tonic DA levels.

Potential Long-term Changes in Vesicular DA storage:

Several studies have reported a Se-deficiency induced increase in striatal DA turnover, but only one study by Watanabe et al. investigated Se deficiency lasting for 3-4 months (Watanabe et al., 1997). This study reported an increase in high K^+-induced DA release measured by microdialysis in mouse striatum. Since extracellular concentration of the DA metabolite DOPAC was not changed, however, the authors ruled out increased DA synthesis during the stimulation period. These data combined with our finding of METH-induced vesicular DA release suggest greater amounts of vesicular DA in chronic Se-deficient and Sepp1-KO striatum as an alternative underlying factor.

The potential for increased vesicular DA is complicated by the fact that the increase in evoked DA release in our study only occurred in the presence of METH. In contrast, baseline evoked DA release was slightly lower in slices from chronic Se-deficient mice and much lower in Sepp1-KO mice. One possible explanation is provided by a study by Covey et al. on the differential effects of AMPH on vesicular DA pool types (Covey et al., 2013). The study was based on the idea that neurotransmitters reside in distinct populations of vesicles that differ in

physical characteristics and function: the reserve pool, the recycling pool, and the readily-releasable pool. The authors of the study postulated that AMPH depletes reserve DA vesicular pools to drive reverse-transport while up-regulating the readily releasable pool to increase vesicular release.

This assertion is based on the idea that separate pools of DA-containing vesicles contribute exocytotic release in response to electrical stimulations of varying duration (Rizzoli and Betz, 2005). The stimulation protocol used in our study should activate the readily-releasable pool and, therefore, our results would suggest that the readily-releasable pool is up-regulated by METH in the NAc of chronically Se-deficient mice and Sepp1-KO mice more so than controls.

Implications for the Mechanism of Action of Methamphetamine:

GPx-mediation of the Tonic METH Response:

Inhibiting GPx enzymatic activity attenuates the rise in extracellular DA caused by METH exposure. Inhibition of GPx1 with MCS caused a decrease in tonic DA release while also blunting the tonic METH response. Inhibiting GPx4 activity with RSL3 caused a much stronger suppression of the tonic METH response, but did not change the tonic DA release baseline. This implies that H_2O_2 and lipid peroxidation both reduce the effect METH.

Correlating these findings to behavioral studies would help reveal the direct implications of this finding *in vivo*. On the one hand, it would appear that the Se-deficient brain is less vulnerable to the mechanism of METH-induced DA efflux. As previously mentioned, however, phasic DA transients are strongly implicated as a causative factor in addiction (Steinberg et al., 2014). Reduced amounts of DA efflux would cause less occupation of pre-synaptic D2R and allow greater DA release in response to incoming signals. It would be interesting to see whether Se deficiency changes the immediate behavioral response to METH or drug-seeking behavior following a chronic METH regimen.

Role of calcium:

One of the main implications of our study is that the tonic METH response is partially dependent on Ca^{2+} influx, which can be inhibited by K_{ATP} channels. This is supported by our finding that removal of extracellular Ca^{2+} reduces the tonic METH response. While this pathway was shown to inhibit action potential-driven DA release, the midbrain afferents are transected

during preparation of NAc slices, thus excluding VTA-originating action potentials from playing a role in our study. Moreover, blocking Na^+ channels with lidocaine did not alter the METH efflux in NAc brain slices (Hedges, unpublished personal communication). Thus, K_{ATP} channel activity likely reduced the METH response by preventing a Ca^{2+} influx-induced increase in intracellular Ca^{2+} levels. This mechanism may underlie the attenuation of the tonic response by both GPx inhibition and Se deficiency.

METH-induced reverse transport of DA can be inhibited in PC12 cells by PKC inhibition and intracellular Ca^{2+} chelation (Kantor et al., 2001). PKC inhibition also prevents DA efflux in rat striatum while having no effect on the inward uptake of DA (Kantor and Gnegy, 1998). AMPH can activate L-type VGCCs by inducing DAT-mediated depolarization as a DAT substrate (Cameron et al., 2015). Therefore, the reduced METH potency under zero extracellular Ca^{2+} conditions may be due to a loss of L-type VGCC activity. METH-induced L-type VGCC activity could work to enhance vesicular DA release. METH-induced Ca2+ influx could also contribute to a recent and compelling model of DA efflux in which it is posited that CaMKII signaling leads to DAT phosphorylation (Fog et al., 2006). The effect of METH may be concentration-dependent, however, as 50 µM concentrations inhibit L-type VGCCs in SH-SY5Y cells (Andres et al., 2015). Interestingly, CaMKII may also mediate METH-induced neurotoxicity (Chen et al., 2016).

Role of Endocannabinoids:

The endocannabinoid system can modulate the influence of the H_2O_2-KATP channel on evoked DA release through CB1 receptor activity. Sidlo et al proposed that activation of CB1 receptors on GABAergic terminals suppresses $GABA_A$ receptor activity to enhance H_2O_2 generation (Sidlo et al., 2008). We have confirmed a similar general effect in relation to tonic DA release by showing that broad CB receptor agonism via WIN55 increases striatal tonic DA levels. Whether this increase is mediated by changes in GABergic signaling warrants further investigation. The inability of CB1R antagonist RIMO to affect basal DA levels implies an absence of basal endocannabinoid activity under normal conditions.

Although WIN55 caused an increase in basal DA levels (Fig. 3-7A), it prevented the tonic DA response to METH similarly to RSL3. The attenuation by RIMO of the suppressive effect of RSL3 indicates that RLS3 may activate CB1 receptors. This would imply that high lipid

peroxidation causes elevated levels of a CB1 activator when METH is added. This could occur by suppressing a counter-endocannabinoid mechanism, such as clearance or metabolism, that is usually able to limit endocannabinoid levels in response to METH under normal conditions. Such a mechanism could involve preventing breakdown of AEA by FAAH. GPx4 is responsible for reducing the lipid peroxide 12-HPETE which in turn is capable of inhibiting FAAH (Sutherland et al., 2001; Maccarrone et al., 2009). Therefore, elevated 12-HPETE levels caused by GPx4 inhibition could potentially prevent AEA catabolism to up-regulate CB1R activity. In future studies, direct detection of each of these changes in DA terminals would be of particular interest.

RSL3 could also cause a more direct effect by facilitating release of endocannabinoids in the presence of METH. Maccarrone et al. showed that chemically disrupting lipid rafts stimulates 2-AG production and increases CB1R activity in mouse striatal slices (Maccarrone et al., 2009). Therefore, the combination of METH-induced oxidative stress and GPx4 inhibition may induce this same mechanism. Interestingly, Premasekharan et al. depicted the disruption of lipid rafts through iron-mediated lipid peroxidation (Premasekharan et al., 2011). This may account for the distinct effect of RSL3 since GPx4 inhibition leads to lipid peroxide-induced cell death in an iron-dependent fashion (Imai et al., 2017).

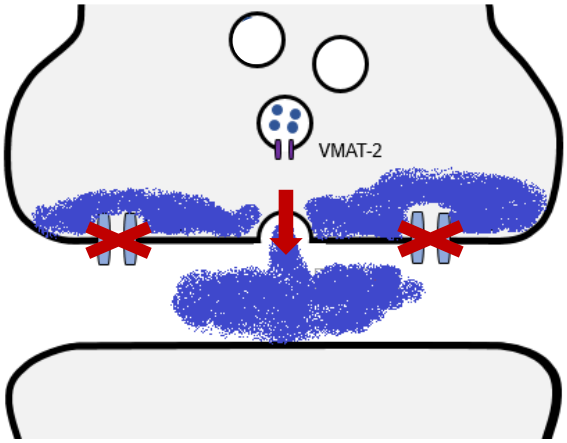

Figure 6-1. Model of Neurotoxicity in Chronic Se Deficiency.
DA is leaked out of pre-synaptic vesicles and becomes built up in the pre-synaptic terminal as reverse-transport via DAT is inhibited. When this DA auto-oxidizes within the terminal, there is greater oxidative stress to the cell. Additionally, a greater amount of vesicular DA release into the synapse occurs, leading to further oxidative stress.

Implications for METH-induced neurotoxicity:

The results of the present study may describe a physiological mechanism through which Se affects DA transmission to protect against METH-induced neurotoxicity. First, the reduced DA efflux in the conditions of Se deficiency and GPx inhibition provide and interesting possibility. Presuming that VMAT-2 inhibition still occurs, our findings imply that DA, after leaking out of pre-synaptic

vesicles, becomes built up within the terminal as reverse-transport through DAT is inhibited. Auto-oxidation of this built up DA may be more toxic for the DA terminal as it will occur within the cell as opposed to in the extracellular space, thus increasing oxidative stress. Second, the increased vesicular DA release caused by METH under conditions of chronic Se deficiency and Sepp1 deletion implies a greater amount of DA release into the synapse following action potentials. This could, in turn, cause greater oxidative stress via DA auto-oxidation. This proposed model for neurotoxicity is described in Figure 6-1.

Experimental Limitations:

Fast-scan cyclic voltammetry measurements:

One major limitation of this study is that tonic DA levels can only be measured differentially in relation to baseline levels. While FSCV can quantify the increase in tonic DA when METH is added, it is unable to measure the absolute concentration of extracellular DA. This has the potential to complicate some experimental findings as the baseline tonic DA level may influence the magnitude of the METH responses. For example, a higher basal tonic release in 2-week Se-deficient striatal slices could account for the decreased response to METH, as the local system is closer to reaching maximum DA release capacity. This is possible considering that microdialysis indicates higher extracellular DA concentrations in Se-deficient mice (Romero-Ramos et al., 2000). Since these microdialysis studies were performed *in vivo*, however, increased DA transients may also contribute to the elevations observed. The present study was performed in brain slices containing DA terminals transected from cell bodies, however, and are not affected by action potentials originating from the soma. Nevertheless, interpretation of the data collected via FSCV in this study would benefit from complementary microdialysis experiments.

Michaelis-Menten modeling:

While the benefit of FSCV lies primarily in its ability to measure rapid changes in DA release and uptake, there are some caveats to its use to study phasic DA signaling. Analysis of uptake kinetics relies on a mathematical model that in turn is based upon the assumption that DA uptake via DAT occurs according to Michaelis-Menten enzyme kinetics. Therefore, to accurately measure Vmax, the concentration of DA released upon stimulation must be high enough to

saturate DAT activity, a state called "DA overflow". Generally, Vmax is reliable when concentrations surpass the baseline Km value, which is approximately 160-200 nM in mice (Ferris et al., 2013). Saturation might not occur under some conditions, however, and must be considered (Yorgason et al., 2011). Complementary experiments could involve a more direct assay of DAT-mediated DA uptake in NAc dopaminergic terminals.

The modeling also assumes that DAT uptake is primarily responsible for the clearance of DA from the extracellular space and, therefore, the falling phase of the evoked DA response. While this is widely accepted to be the case in striatum, it may not always be the case in other areas of the brain (Hoffman et al., 2016). For example, the norepinephrine transporter (NET) carries out some DA uptake activity in mouse frontal cortex (Moron et al., 2002). Therefore, this underlying assumption must be reconsidered for prospective experimentation outside the striatum.

In the present study, METH-induced DA uptake inhibition was modeled by increasing Km while keeping Vmax fixed. Addition of a drug known to change DAT surface expression levels would require adjustment of Vmax values while keeping the Km constant. Therefore, the validity of the Km values reported in this study are contingent upon DAT levels remaining approximately constant for the duration of METH exposure. While METH has been suggested to cause DAT internalization, conflicting reports have emerged indicating no change or an increase in DAT surface expression (Kahlig and Galli, 2003; German et al., 2012; Wheeler et al., 2015). Moreover, most of the studies reporting DAT internalization are based on a timescale beyond the experimental design of the present study.

In our modeling, we set the baseline Km to 160 nM according to past studies that have determined DA affinity for DAT in mice. Se deficiency was not suspected to change the baseline affinity of DA for DAT in the current study, but it remains a possibility. DAT binding affinity has been suggested to change due to altered DAT phosphorylation states (Samuvel et al., 2008). H_2O_2 can inhibit DAT activity, but no change in Km occurs as a result (Huang et al., 2003). While there is no apparent mechanism through which Se deficiency could change DA affinity for DAT, such an effect should be experimentally ruled out to further validate the current findings.

Future Directions:

Our study has identified several potential interactions between selenoproteins and NAc DA terminals in the context of METH exposure. Future studies could address whether the EC50 of METH is changed in chronic Se-deficient and Sepp1-KO mice. Moreover, since much of what is known about METH is derived from studies with AMPH, whether AMPH affects the phenotypes used in this study in the same way could be explored. In addition, it would be instructive to compare the impact of METH to cocaine or similar DAT-selective uptake inhibitor.

The nature of K_{ATP} channel reduction of the METH response should be further investigated by examining the downstream effects of K_{ATP} channel activity. Although Ca^{2+} influx appears to contribute to METH-induced DA release, the signaling pathways and role of Ca^{2+}stores involved need to be elucidated. Pharmacological effectors of intracellular Ca^{2+} stores and moderating proteins can be used in combination with extracellular Ca^{2+} manipulation to tease apart this relationship.

Involvement of endocannabinoids can be further characterized with different combinations of agonists and antagonists. Ultimately, mass spectrometry should be used to measure endocannabinoid levels as the present findings appear to be caused by a change in production or metabolism.

Genetic deletion of Sepp1 creates a striatal environment in which FSCV D2R dysfunction has unmasked an increase in vesicular DA release caused by METH. Kinetic analysis of ligand-D2R interactions should be performed to determine if there is a change in kinetic activity of striatal D2R. Disruption of a signaling pathway is another possibility, and thus AC and Kv1.2 voltage-gated K^+ channel involvement should be studied. Vesicular DA storage could also be investigated in Sepp1KO mice. This can be done by using the VMAT-2 inhibitor reserpine to deplete DA vesicles and observe time course of depletion. Different stimulation paradigms can also be used to interrogate specific vesicular pools.

The rescuing effect of Sepp1 protein provides a useful tool to investigate this phenotype. This study supports the prospect that Sepp1 can induce intracellular signaling via interaction with ApoER2. Further investigation should be aimed at identifying the secondary messengers involved and characterizing the potential functional association between ApoER2 and D2R receptors. Moreover, the specific role of Sepp1 in the dopaminergic system can be discerned by continuing to phenotype the Sepp1KO mouse model in parallel with chronic Se-deficient mice.

Technical limitations of this study can be alleviated by using alternative methods to measure DA concentrations. Fast-scan controlled-adsorption voltammetry (FSCAV) is a relatively new voltammetry technique that can provide absolute measurement of DA concentrations (Atcherley et al., 2015). This would provide a useful tool to help resolve current uncertainties in measuring METH-induced DA efflux in brain slices.

Since this study was based upon the neuroprotective ability of Se against METH, oxidative stress and cell death should be assayed under the same experimental conditions wherein Se-deficiency leads to a reduction in neuroprotection. This can help reveal the relationship between DA release and neurotoxicity. Moreover, it can shed light on the seemingly paradoxical ability of GPx to protect against METH toxicity while promoting METH-induced DA efflux. Connecting the physiological responses observed in brain slices to changes in neurotoxicity would help clarify the physiological relevance of our findings.

REFERENCES

Aizenman E, McCord MC, Saadi RA, Hartnett KA, He K (2010) Complex role of zinc in methamphetamine toxicity in vitro. Neuroscience 171:31-39.

Akbaraly NT, Arnaud J, Hininger-Favier I, Gourlet V, Roussel AM, Berr C (2005) Selenium and mortality in the elderly: results from the EVA study. Clin Chem 51:2117-2123.

Akesson B, Martensson B (1991) Chromatography of selenoproteins in human serum using matrix-bound heparin. Int J Vitam Nutr Res 61:72-76.

Alderson HL, Parkinson JA, Robbins TW, Everitt BJ (2001) The effects of excitotoxic lesions of the nucleus accumbens core or shell regions on intravenous heroin self-administration in rats. Psychopharmacology (Berl) 153:455-463.

Allmang C, Wurth L, Krol A (2009) The selenium to selenoprotein pathway in eukaryotes: more molecular partners than anticipated. Biochim Biophys Acta 1790:1415-1423.

Ammar EM, Couri D (1981) Acute toxicity of sodium selenite and selenomethionine in mice after ICV or IV administration. Neurotoxicology 2:383-386.

Andersen OM, Yeung CH, Vorum H, Wellner M, Andreassen TK, Erdmann B, Mueller EC, Herz J, Otto A, Cooper TG, Willnow TE (2003) Essential role of the apolipoprotein E receptor-2 in sperm development. J Biol Chem 278:23989-23995.

Andres MA, Cooke IM, Bellinger FP, Berry MJ, Zaporteza MM, Rueli RH, Barayuga SM, Chang L (2015) Methamphetamine acutely inhibits voltage-gated calcium channels but chronically up-regulates L-type channels. J Neurochem 134:56-65.

Anzalone A, Lizardi-Ortiz JE, Ramos M, De Mei C, Hopf FW, Iaccarino C, Halbout B, Jacobsen J, Kinoshita C, Welter M, Caron MG, Bonci A, Sulzer D, Borrelli E (2012) Dual control of dopamine synthesis and release by presynaptic and postsynaptic dopamine D2 receptors. J Neurosci 32:9023-9034.

Arteel GE, Franken S, Kappler J, Sies H (2000) Binding of selenoprotein P to heparin: characterization with surface plasmon resonance. Biol Chem 381:265-268.

Arteel GE, Mostert V, Oubrahim H, Briviba K, Abel J, Sies H (1998) Protection by selenoprotein P in human plasma against peroxynitrite-mediated oxidation and nitration. Biol Chem 379:1201-1205.

Atcherley CW, Wood KM, Parent KL, Hashemi P, Heien ML (2015) The coaction of tonic and phasic dopamine dynamics. Chem Commun (Camb) 51:2235-2238.

Aumann KD, Bedorf N, Brigelius-Flohe R, Schomburg D, Flohe L (1997) Glutathione peroxidase revisited--simulation of the catalytic cycle by computer-assisted molecular modelling. Biomed Environ Sci 10:136-155.

Avshalumov MV, Rice ME (2003) Activation of ATP-sensitive K+ (K(ATP)) channels by H2O2 underlies glutamate-dependent inhibition of striatal dopamine release. Proc Natl Acad Sci U S A 100:11729-11734.

Avshalumov MV, Chen BT, Koos T, Tepper JM, Rice ME (2005) Endogenous hydrogen peroxide regulates the excitability of midbrain dopamine neurons via ATP-sensitive potassium channels. J Neurosci 25:4222-4231.

Azad GK, Tomar RS (2014) Ebselen, a promising antioxidant drug: mechanisms of action and targets of biological pathways. Mol Biol Rep 41:4865-4879.

Azad GK, Singh V, Mandal P, Singh P, Golla U, Baranwal S, Chauhan S, Tomar RS (2014) Ebselen induces reactive oxygen species (ROS)-mediated cytotoxicity in Saccharomyces cerevisiae with inhibition of glutamate dehydrogenase being a target. FEBS Open Bio 4:77-89.

Ballester J, Valentine G, Sofuoglu M (2017) Pharmacological treatments for methamphetamine addiction: current status and future directions. Expert Rev Clin Pharmacol 10:305-314.

Barayuga SM, Pang X, Andres MA, Panee J, Bellinger FP (2013) Methamphetamine decreases levels of glutathione peroxidases 1 and 4 in SH-SY5Y neuronal cells: protective effects of selenium. Neurotoxicology 37:240-246.
Barger SW (2013) Apolipoprotein E acts at pre-synaptic sites...among others. J Neurochem 124:1-3.
Beaulieu JM, Gainetdinov RR (2011) The physiology, signaling, and pharmacology of dopamine receptors. Pharmacol Rev 63:182-217.
Beck MA, Levander OA, Handy J (2003) Selenium deficiency and viral infection. J Nutr 133:1463S-1467S.
Beffert U, Weeber EJ, Durudas A, Qiu S, Masiulis I, Sweatt JD, Li WP, Adelmann G, Frotscher M, Hammer RE, Herz J (2005) Modulation of synaptic plasticity and memory by Reelin involves differential splicing of the lipoprotein receptor Apoer2. Neuron 47:567-579.
Behne D, Hilmert H, Scheid S, Gessner H, Elger W (1988) Evidence for specific selenium target tissues and new biologically important selenoproteins. Biochim Biophys Acta 966:12-21.
Bellinger FP, Raman AV, Rueli RH, Bellinger MT, Dewing AS, Seale LA, Andres MA, Uyehara-Lock JH, White LR, Ross GW, Berry MJ (2012) Changes in selenoprotein P in substantia nigra and putamen in Parkinson's disease. J Parkinsons Dis 2:115-126.
Berendse HW, Groenewegen HJ (1990) Organization of the thalamostriatal projections in the rat, with special emphasis on the ventral striatum. J Comp Neurol 299:187-228.
Blake SM, Strasser V, Andrade N, Duit S, Hofbauer R, Schneider WJ, Nimpf J (2008) Thrombospondin-1 binds to ApoER2 and VLDL receptor and functions in postnatal neuronal migration. EMBO J 27:3069-3080.
Blaschko H, Richter D, Schlossmann H (1937) The inactivation of adrenaline. J Physiol 90:1-17.
Bogdanski DF, Brodie BB (1969) The effects of inorganic ions on the storage and uptake of H3-norepinephrine by rat heart slices. J Pharmacol Exp Ther 165:181-189.
Bossert JM, Poles GC, Wihbey KA, Koya E, Shaham Y (2007) Differential effects of blockade of dopamine D1-family receptors in nucleus accumbens core or shell on reinstatement of heroin seeking induced by contextual and discrete cues. J Neurosci 27:12655-12663.
Brenneisen P, Steinbrenner H, Sies H (2005) Selenium, oxidative stress, and health aspects. Mol Aspects Med 26:256-267.
Brigelius-Flohe R, Banning A (2006) Part of the series: from dietary antioxidants to regulators in cellular signaling and gene regulation. Sulforaphane and selenium, partners in adaptive response and prevention of cancer. Free Radic Res 40:775-787.
Brown JM, Hanson GR, Fleckenstein AE (2000) Methamphetamine rapidly decreases vesicular dopamine uptake. J Neurochem 74:2221-2223.
Brown JM, Riddle EL, Sandoval V, Weston RK, Hanson JE, Crosby MJ, Ugarte YV, Gibb JW, Hanson GR, Fleckenstein AE (2002) A single methamphetamine administration rapidly decreases vesicular dopamine uptake. J Pharmacol Exp Ther 302:497-501.
Bulteau AL, Chavatte L (2015) Update on selenoprotein biosynthesis. Antioxid Redox Signal 23:775-794.
Burk RF, Hill KE (1994) Selenoprotein P. A selenium-rich extracellular glycoprotein. J Nutr 124:1891-1897.
Burk RF, Hill KE (1999) Orphan selenoproteins. Bioessays 21:231-237.
Burk RF, Hill KE (2005) Selenoprotein P: an extracellular protein with unique physical characteristics and a role in selenium homeostasis. Annu Rev Nutr 25:215-235.
Burk RF, Hill KE (2009) Selenoprotein P-expression, functions, and roles in mammals. Biochim Biophys Acta 1790:1441-1447.
Burk RF, Hill KE, Olson GE, Weeber EJ, Motley AK, Winfrey VP, Austin LM (2007) Deletion of apolipoprotein E receptor-2 in mice lowers brain selenium and causes severe neurological dysfunction and death when a low-selenium diet is fed. J Neurosci 27:6207-6211.

Burk RF, Hill KE, Motley AK, Winfrey VP, Kurokawa S, Mitchell SL, Zhang W (2014) Selenoprotein P and apolipoprotein E receptor-2 interact at the blood-brain barrier and also within the brain to maintain an essential selenium pool that protects against neurodegeneration. FASEB J 28:3579-3588.

Byrns CN, Pitts MW, Gilman CA, Hashimoto AC, Berry MJ (2014) Mice lacking selenoprotein P and selenocysteine lyase exhibit severe neurological dysfunction, neurodegeneration, and audiogenic seizures. J Biol Chem 289:9662-9674.

Cadet JL, Ladenheim B, Hirata H (1998) Effects of toxic doses of methamphetamine (METH) on dopamine D1 receptors in the mouse brain. Brain Res 786:240-242.

Cadet JL, Jayanthi S, Deng X (2003) Speed kills: cellular and molecular bases of methamphetamine-induced nerve terminal degeneration and neuronal apoptosis. FASEB J 17:1775-1788.

Cagniard B, Beeler JA, Britt JP, McGehee DS, Marinelli M, Zhuang X (2006) Dopamine scales performance in the absence of new learning. Neuron 51:541-547.

Calipari ES, Ferris MJ (2013) Amphetamine mechanisms and actions at the dopamine terminal revisited. J Neurosci 33:8923-8925.

Cameron DL, Wessendorf MW, Williams JT (1997) A subset of ventral tegmental area neurons is inhibited by dopamine, 5-hydroxytryptamine and opioids. Neuroscience 77:155-166.

Cameron KN, Solis E, Jr., Ruchala I, De Felice LJ, Eltit JM (2015) Amphetamine activates calcium channels through dopamine transporter-mediated depolarization. Cell Calcium 58:457-466.

Cardinal RN, Howes NJ (2005) Effects of lesions of the nucleus accumbens core on choice between small certain rewards and large uncertain rewards in rats. BMC Neurosci 6:37.

Castano A, Cano J, Machado A (1993) Low selenium diet affects monoamine turnover differentially in substantia nigra and striatum. J Neurochem 61:1302-1307.

Castano A, Ayala A, Rodriguez-Gomez JA, Herrera AJ, Cano J, Machado A (1997) Low selenium diet increases the dopamine turnover in prefrontal cortex of the rat. Neurochem Int 30:549-555.

Castano A, Ayala A, Rodriguez-Gomez JA, de la Cruz CP, Revilla E, Cano J, Machado A (1995) Increase in dopamine turnover and tyrosine hydroxylase enzyme in hippocampus of rats fed on low selenium diet. J Neurosci Res 42:684-691.

Chang CH, Grace AA (2014) Amygdala-ventral pallidum pathway decreases dopamine activity after chronic mild stress in rats. Biol Psychiatry 76:223-230.

Chater TE, Goda Y (2014) The role of AMPA receptors in postsynaptic mechanisms of synaptic plasticity. Front Cell Neurosci 8:401.

Chebib M, Johnston GA (1999) The 'ABC' of GABA receptors: a brief review. Clin Exp Pharmacol Physiol 26:937-940.

Chen J, Berry MJ (2003) Selenium and selenoproteins in the brain and brain diseases. J Neurochem 86:1-12.

Chen X, Xing J, Jiang L, Qian W, Wang Y, Sun H, Wang Y, Xiao H, Wang J, Zhang J (2016) Involvement of calcium/calmodulin-dependent protein kinase II in methamphetamine-induced neural damage. J Appl Toxicol 36:1460-1467.

Cheng WH, Ho YS, Valentine BA, Ross DA, Combs GF, Jr., Lei XG (1998) Cellular glutathione peroxidase is the mediator of body selenium to protect against paraquat lethality in transgenic mice. J Nutr 128:1070-1076.

Chergui K, Charlety PJ, Akaoka H, Saunier CF, Brunet JL, Buda M, Svensson TH, Chouvet G (1993) Tonic activation of NMDA receptors causes spontaneous burst discharge of rat midbrain dopamine neurons in vivo. Eur J Neurosci 5:137-144.

Chinopoulos C, Adam-Vizi V (2001) Mitochondria deficient in complex I activity are depolarized by hydrogen peroxide in nerve terminals: relevance to Parkinson's disease. J Neurochem 76:302-306.

Chittum HS, Himeno S, Hill KE, Burk RF (1996) Multiple forms of selenoprotein P in rat plasma. Arch Biochem Biophys 325:124-128.
Cidon S, Nelson N (1983) A novel ATPase in the chromaffin granule membrane. J Biol Chem 258:2892-2898.
Cidon S, Ben-David H, Nelson N (1983) ATP-driven proton fluxes across membranes of secretory organelles. J Biol Chem 258:11684-11688.
Civil ID, McDonald MJ (1978) Acute selenium poisoning: case report. N Z Med J 87:354-356.
Clapper JR, Vacondio F, King AR, Duranti A, Tontini A, Silva C, Sanchini S, Tarzia G, Mor M, Piomelli D (2009) A second generation of carbamate-based fatty acid amide hydrolase inhibitors with improved activity in vivo. ChemMedChem 4:1505-1513.
Cohen JY, Haesler S, Vong L, Lowell BB, Uchida N (2012) Neuron-type-specific signals for reward and punishment in the ventral tegmental area. Nature 482:85-88.
Conrad M, Schneider M, Seiler A, Bornkamm GW (2007) Physiological role of phospholipid hydroperoxide glutathione peroxidase in mammals. Biol Chem 388:1019-1025.
Cotter R, Pei Y, Mus L, Harmeier A, Gainetdinov RR, Hoener MC, Canales JJ (2015) The trace amine-associated receptor 1 modulates methamphetamine's neurochemical and behavioral effects. Front Neurosci 9:39.
Covey DP, Juliano SA, Garris PA (2013) Amphetamine elicits opposing actions on readily releasable and reserve pools for dopamine. PLoS One 8:e60763.
Covey DP, Bunner KD, Schuweiler DR, Cheer JF, Garris PA (2016) Amphetamine elevates nucleus accumbens dopamine via an action potential-dependent mechanism that is modulated by endocannabinoids. Eur J Neurosci 43:1661-1673.
Cubells JF, Rayport S, Rajendran G, Sulzer D (1994) Methamphetamine neurotoxicity involves vacuolation of endocytic organelles and dopamine-dependent intracellular oxidative stress. J Neurosci 14:2260-2271.
Cuitino L, Matute R, Retamal C, Bu G, Inestrosa NC, Marzolo MP (2005) ApoER2 is endocytosed by a clathrin-mediated process involving the adaptor protein Dab2 independent of its Rafts' association. Traffic 6:820-838.
D'Arcangelo G (2005) Apoer2: a reelin receptor to remember. Neuron 47:471-473.
Daberkow DP, Brown HD, Bunner KD, Kraniotis SA, Doellman MA, Ragozzino ME, Garris PA, Roitman MF (2013) Amphetamine paradoxically augments exocytotic dopamine release and phasic dopamine signals. J Neurosci 33:452-463.
Daubner SC, Le T, Wang S (2011) Tyrosine hydroxylase and regulation of dopamine synthesis. Arch Biochem Biophys 508:1-12.
del Marmol V, Solano F, Sels A, Huez G, Libert A, Lejeune F, Ghanem G (1993) Glutathione depletion increases tyrosinase activity in human melanoma cells. J Invest Dermatol 101:871-874.
del Marmol V, Ito S, Bouchard B, Libert A, Wakamatsu K, Ghanem G, Solano F (1996) Cysteine deprivation promotes eumelanogenesis in human melanoma cells. J Invest Dermatol 107:698-702.
Demirci K, Naziroglu M, Ovey IS, Balaban H (2017) Selenium attenuates apoptosis, inflammation and oxidative stress in the blood and brain of aged rats with scopolamine-induced dementia. Metab Brain Dis 32:321-329.
Donovan J, Copeland PR (2010) Threading the needle: getting selenocysteine into proteins. Antioxid Redox Signal 12:881-892.
Dreyer JK, Herrik KF, Berg RW, Hounsgaard JD (2010) Influence of phasic and tonic dopamine release on receptor activation. J Neurosci 30:14273-14283.

Drukarch B, Jongenelen CA, Schepens E, Langeveld CH, Stoof JC (1996) Glutathione is involved in the granular storage of dopamine in rat PC 12 pheochromocytoma cells: implications for the pathogenesis of Parkinson's disease. J Neurosci 16:6038-6045.
Dumanis SB, Cha HJ, Song JM, Trotter JH, Spitzer M, Lee JY, Weeber EJ, Turner RS, Pak DT, Rebeck GW, Hoe HS (2011) ApoE receptor 2 regulates synapse and dendritic spine formation. PLoS One 6:e17203.
Elsworth JD, Roth RH (1997) Dopamine synthesis, uptake, metabolism, and receptors: relevance to gene therapy of Parkinson's disease. Exp Neurol 144:4-9.
Epp O, Ladenstein R, Wendel A (1983) The refined structure of the selenoenzyme glutathione peroxidase at 0.2-nm resolution. Eur J Biochem 133:51-69.
Ferris MJ, Calipari ES, Yorgason JT, Jones SR (2013) Examining the complex regulation and drug-induced plasticity of dopamine release and uptake using voltammetry in brain slices. ACS Chem Neurosci 4:693-703.
Flohe L (1988) Glutathione peroxidase. Basic Life Sci 49:663-668.
Floor E, Leventhal PS, Wang Y, Meng L, Chen W (1995) Dynamic storage of dopamine in rat brain synaptic vesicles in vitro. J Neurochem 64:689-699.
Floresco SB, Todd CL, Grace AA (2001) Glutamatergic afferents from the hippocampus to the nucleus accumbens regulate activity of ventral tegmental area dopamine neurons. J Neurosci 21:4915-4922.
Floresco SB, West AR, Ash B, Moore H, Grace AA (2003) Afferent modulation of dopamine neuron firing differentially regulates tonic and phasic dopamine transmission. Nat Neurosci 6:968-973.
Fog JU, Khoshbouei H, Holy M, Owens WA, Vaegter CB, Sen N, Nikandrova Y, Bowton E, McMahon DG, Colbran RJ, Daws LC, Sitte HH, Javitch JA, Galli A, Gether U (2006) Calmodulin kinase II interacts with the dopamine transporter C terminus to regulate amphetamine-induced reverse transport. Neuron 51:417-429.
Fomenko DE, Gladyshev VN (2003) Identity and functions of CxxC-derived motifs. Biochemistry 42:11214-11225.
Ford CP (2014) The role of D2-autoreceptors in regulating dopamine neuron activity and transmission. Neuroscience 282:13-22.
Freeman AS, Bunney BS (1987) Activity of A9 and A10 dopaminergic neurons in unrestrained rats: further characterization and effects of apomorphine and cholecystokinin. Brain Res 405:46-55.
French SJ, Hailstone JC, Totterdell S (2003) Basolateral amygdala efferents to the ventral subiculum preferentially innervate pyramidal cell dendritic spines. Brain Res 981:160-167.
Fuchigami T, Sato Y, Tomita Y, Takano T, Miyauchi SY, Tsuchiya Y, Saito T, Kubo K, Nakajima K, Fukuda M, Hattori M, Hisanaga S (2013) Dab1-mediated colocalization of multi-adaptor protein CIN85 with Reelin receptors, ApoER2 and VLDLR, in neurons. Genes Cells 18:410-424.
Garris PA, Christensen JR, Rebec GV, Wightman RM (1997) Real-time measurement of electrically evoked extracellular dopamine in the striatum of freely moving rats. J Neurochem 68:152-161.
German CL, Hanson GR, Fleckenstein AE (2012) Amphetamine and methamphetamine reduce striatal dopamine transporter function without concurrent dopamine transporter relocalization. J Neurochem 123:288-297.
Giambalvo CT (1992a) Protein kinase C and dopamine transport--2. Effects of amphetamine in vitro. Neuropharmacology 31:1211-1222.
Giambalvo CT (1992b) Protein kinase C and dopamine transport--1. Effects of amphetamine in vivo. Neuropharmacology 31:1201-1210.
Gonon FG (1988) Nonlinear relationship between impulse flow and dopamine released by rat midbrain dopaminergic neurons as studied by in vivo electrochemistry. Neuroscience 24:19-28.

Grace AA (1991) Phasic versus tonic dopamine release and the modulation of dopamine system responsivity: a hypothesis for the etiology of schizophrenia. Neuroscience 41:1-24.
Grace AA (1995) The tonic/phasic model of dopamine system regulation: its relevance for understanding how stimulant abuse can alter basal ganglia function. Drug Alcohol Depend 37:111-129.
Grace AA (2012) Dopamine system dysregulation by the hippocampus: implications for the pathophysiology and treatment of schizophrenia. Neuropharmacology 62:1342-1348.
Grace AA (2016) Dysregulation of the dopamine system in the pathophysiology of schizophrenia and depression. Nat Rev Neurosci 17:524-532.
Grace AA, Bunney BS (1983) Intracellular and extracellular electrophysiology of nigral dopaminergic neurons--1. Identification and characterization. Neuroscience 10:301-315.
Grace AA, Bunney BS (1984a) The control of firing pattern in nigral dopamine neurons: single spike firing. J Neurosci 4:2866-2876.
Grace AA, Bunney BS (1984b) The control of firing pattern in nigral dopamine neurons: burst firing. J Neurosci 4:2877-2890.
Grace AA, Bunney BS (1985) Opposing effects of striatonigral feedback pathways on midbrain dopamine cell activity. Brain Res 333:271-284.
Grace AA, Onn SP (1989) Morphology and electrophysiological properties of immunocytochemically identified rat dopamine neurons recorded in vitro. J Neurosci 9:3463-3481.
Graybiel AM, Aosaki T, Flaherty AW, Kimura M (1994) The basal ganglia and adaptive motor control. Science 265:1826-1831.
Haigh JR, Phillips JH (1993) Indirect coupling of calcium transport in chromaffin granule ghosts to the proton pump. Neuroreport 4:571-574.
Halpin LE, Collins SA, Yamamoto BK (2014) Neurotoxicity of methamphetamine and 3,4-methylenedioxymethamphetamine. Life Sci 97:37-44.
Hanslick JL, Lau K, Noguchi KK, Olney JW, Zorumski CF, Mennerick S, Farber NB (2009) Dimethyl sulfoxide (DMSO) produces widespread apoptosis in the developing central nervous system. Neurobiol Dis 34:1-10.
Harata NC, Aravanis AM, Tsien RW (2006) Kiss-and-run and full-collapse fusion as modes of exo-endocytosis in neurosecretion. J Neurochem 97:1546-1570.
Heimer L, Alheid GF, de Olmos JS, Groenewegen HJ, Haber SN, Harlan RE, Zahm DS (1997) The accumbens: beyond the core-shell dichotomy. J Neuropsychiatry Clin Neurosci 9:354-381.
Herrman JL (1977) The properties of a rat serum protein labelled by the injection of sodium selenite. Biochim Biophys Acta 500:61-70.
Hill KE, Lyons PR, Burk RF (1992) Differential regulation of rat liver selenoprotein mRNAs in selenium deficiency. Biochem Biophys Res Commun 185:260-263.
Hill KE, Zhou J, McMahan WJ, Motley AK, Atkins JF, Gesteland RF, Burk RF (2003) Deletion of selenoprotein P alters distribution of selenium in the mouse. J Biol Chem 278:13640-13646.
Ho YS, Magnenat JL, Bronson RT, Cao J, Gargano M, Sugawara M, Funk CD (1997) Mice deficient in cellular glutathione peroxidase develop normally and show no increased sensitivity to hyperoxia. J Biol Chem 272:16644-16651.
Hoe HS, Tran TS, Matsuoka Y, Howell BW, Rebeck GW (2006) DAB1 and Reelin effects on amyloid precursor protein and ApoE receptor 2 trafficking and processing. J Biol Chem 281:35176-35185.
Hoe HS, Wessner D, Beffert U, Becker AG, Matsuoka Y, Rebeck GW (2005) F-spondin interaction with the apolipoprotein E receptor ApoEr2 affects processing of amyloid precursor protein. Mol Cell Biol 25:9259-9268.
Hoffman AF, Spivak CE, Lupica CR (2016) Enhanced Dopamine Release by Dopamine Transport Inhibitors Described by a Restricted Diffusion Model and Fast-Scan Cyclic Voltammetry. ACS Chem Neurosci 7:700-709.

Hondal RJ, Ma S, Caprioli RM, Hill KE, Burk RF (2001) Heparin-binding histidine and lysine residues of rat selenoprotein P. J Biol Chem 276:15823-15831.
Howell BW, Hawkes R, Soriano P, Cooper JA (1997) Neuronal position in the developing brain is regulated by mouse disabled-1. Nature 389:733-737.
Howlett AC, Breivogel CS, Childers SR, Deadwyler SA, Hampson RE, Porrino LJ (2004) Cannabinoid physiology and pharmacology: 30 years of progress. Neuropharmacology 47 Suppl 1:345-358.
Huang CL, Huang NK, Shyue SK, Chern Y (2003) Hydrogen peroxide induces loss of dopamine transporter activity: a calcium-dependent oxidative mechanism. J Neurochem 86:1247-1259.
Hussain K, Cosgrove KE (2005) From congenital hyperinsulinism to diabetes mellitus: the role of pancreatic beta-cell KATP channels. Pediatr Diabetes 6:103-113.
Iacobucci GJ, Popescu GK (2017) NMDA receptors: linking physiological output to biophysical operation. Nat Rev Neurosci 18:236-249.
Ikemoto S (2007) Dopamine reward circuitry: two projection systems from the ventral midbrain to the nucleus accumbens-olfactory tubercle complex. Brain Res Rev 56:27-78.
Ikemoto S, Witkin BM (2003) Locomotor inhibition induced by procaine injections into the nucleus accumbens core, but not the medial ventral striatum: implication for cocaine-induced locomotion. Synapse 47:117-122.
Imai H, Matsuoka M, Kumagai T, Sakamoto T, Koumura T (2017) Lipid Peroxidation-Dependent Cell Death Regulated by GPx4 and Ferroptosis. Curr Top Microbiol Immunol 403:143-170.
Imam SZ, Newport GD, Islam F, Slikker W, Jr., Ali SF (1999) Selenium, an antioxidant, protects against methamphetamine-induced dopaminergic neurotoxicity. Brain Res 818:575-578.
Ingram SL, Prasad BM, Amara SG (2002) Dopamine transporter-mediated conductances increase excitability of midbrain dopamine neurons. Nat Neurosci 5:971-978.
Johnson KM, Jeng YJ (1991) Pharmacological evidence for N-methyl-D-aspartate receptors on nigrostriatal dopaminergic nerve terminals. Can J Physiol Pharmacol 69:1416-1421.
Jones SR, Gainetdinov RR, Wightman RM, Caron MG (1998) Mechanisms of amphetamine action revealed in mice lacking the dopamine transporter. J Neurosci 18:1979-1986.
Justice JB, Jr. (1993) Quantitative microdialysis of neurotransmitters. J Neurosci Methods 48:263-276.
Kahlig KM, Galli A (2003) Regulation of dopamine transporter function and plasma membrane expression by dopamine, amphetamine, and cocaine. Eur J Pharmacol 479:153-158.
Kahlig KM, Binda F, Khoshbouei H, Blakely RD, McMahon DG, Javitch JA, Galli A (2005) Amphetamine induces dopamine efflux through a dopamine transporter channel. Proc Natl Acad Sci U S A 102:3495-3500.
Kahya MC, Naziroglu M, Ovey IS (2017) Modulation of Diabetes-Induced Oxidative Stress, Apoptosis, and Ca2+ Entry Through TRPM2 and TRPV1 Channels in Dorsal Root Ganglion and Hippocampus of Diabetic Rats by Melatonin and Selenium. Mol Neurobiol 54:2345-2360.
Kantor L, Gnegy ME (1998) Protein kinase C inhibitors block amphetamine-mediated dopamine release in rat striatal slices. J Pharmacol Exp Ther 284:592-598.
Kantor L, Hewlett GH, Park YH, Richardson-Burns SM, Mellon MJ, Gnegy ME (2001) Protein kinase C and intracellular calcium are required for amphetamine-mediated dopamine release via the norepinephrine transporter in undifferentiated PC12 cells. J Pharmacol Exp Ther 297:1016-1024.
Kawano T, Zoga V, Gemes G, McCallum JB, Wu HE, Pravdic D, Liang MY, Kwok WM, Hogan Q, Sarantopoulos C (2009) Suppressed Ca2+/CaM/CaMKII-dependent K(ATP) channel activity in primary afferent neurons mediates hyperalgesia after axotomy. Proc Natl Acad Sci U S A 106:8725-8730.
Khoshbouei H, Sen N, Guptaroy B, Johnson L, Lund D, Gnegy ME, Galli A, Javitch JA (2004) N-terminal phosphorylation of the dopamine transporter is required for amphetamine-induced efflux. PLoS Biol 2:E78.

Kim HC, Jhoo WK, Choi DY, Im DH, Shin EJ, Suh JH, Floyd RA, Bing G (1999) Protection of methamphetamine nigrostriatal toxicity by dietary selenium. Brain Res 851:76-86.
Kofalvi A, Rodrigues RJ, Ledent C, Mackie K, Vizi ES, Cunha RA, Sperlagh B (2005) Involvement of cannabinoid receptors in the regulation of neurotransmitter release in the rodent striatum: a combined immunochemical and pharmacological analysis. J Neurosci 25:2874-2884.
Koob GF, Le Moal M (2001) Drug addiction, dysregulation of reward, and allostasis. Neuropsychopharmacology 24:97-129.
Krebs MO, Desce JM, Kemel ML, Gauchy C, Godeheu G, Cheramy A, Glowinski J (1991) Glutamatergic control of dopamine release in the rat striatum: evidence for presynaptic N-methyl-D-aspartate receptors on dopaminergic nerve terminals. J Neurochem 56:81-85.
Krueger BK (1990) Kinetics and block of dopamine uptake in synaptosomes from rat caudate nucleus. J Neurochem 55:260-267.
Kurokawa S, Bellinger FP, Hill KE, Burk RF, Berry MJ (2014) Isoform-specific binding of selenoprotein P to the beta-propeller domain of apolipoprotein E receptor 2 mediates selenium supply. J Biol Chem 289:9195-9207.
Lambert RC, Bessaih T, Crunelli V, Leresche N (2014) The many faces of T-type calcium channels. Pflugers Arch 466:415-423.
Larsen KE, Fon EA, Hastings TG, Edwards RH, Sulzer D (2002) Methamphetamine-induced degeneration of dopaminergic neurons involves autophagy and upregulation of dopamine synthesis. J Neurosci 22:8951-8960.
Latreche L, Jean-Jean O, Driscoll DM, Chavatte L (2009) Novel structural determinants in human SECIS elements modulate the translational recoding of UGA as selenocysteine. Nucleic Acids Res 37:5868-5880.
Laube B, Kuhse J, Betz H (1998) Evidence for a tetrameric structure of recombinant NMDA receptors. J Neurosci 18:2954-2961.
LaVoie MJ, Hastings TG (1999) Dopamine quinone formation and protein modification associated with the striatal neurotoxicity of methamphetamine: evidence against a role for extracellular dopamine. J Neurosci 19:1484-1491.
LeDoux JE (2000) Emotion circuits in the brain. Annu Rev Neurosci 23:155-184.
Lee GH, D'Arcangelo G (2016) New Insights into Reelin-Mediated Signaling Pathways. Front Cell Neurosci 10:122.
Leeb C, Eresheim C, Nimpf J (2014) Clusterin is a ligand for apolipoprotein E receptor 2 (ApoER2) and very low density lipoprotein receptor (VLDLR) and signals via the Reelin-signaling pathway. J Biol Chem 289:4161-4172.
Lei XG, Cheng WH, McClung JP (2007) Metabolic regulation and function of glutathione peroxidase-1. Annu Rev Nutr 27:41-61.
Liss B, Bruns R, Roeper J (1999) Alternative sulfonylurea receptor expression defines metabolic sensitivity of K-ATP channels in dopaminergic midbrain neurons. EMBO J 18:833-846.
Liu CC, Liu CC, Kanekiyo T, Xu H, Bu G (2013) Apolipoprotein E and Alzheimer disease: risk, mechanisms and therapy. Nat Rev Neurol 9:106-118.
Liu PS, Liaw CT, Lin MK, Shin SH, Kao LS, Lin LF (2003) Amphetamine enhances Ca2+ entry and catecholamine release via nicotinic receptor activation in bovine adrenal chromaffin cells. Eur J Pharmacol 460:9-17.
Lodge DJ, Grace AA (2006) The hippocampus modulates dopamine neuron responsivity by regulating the intensity of phasic neuron activation. Neuropsychopharmacology 31:1356-1361.
Maccarrone M (2017) Metabolism of the Endocannabinoid Anandamide: Open Questions after 25 Years. Front Mol Neurosci 10:166.

Maccarrone M, De Chiara V, Gasperi V, Viscomi MT, Rossi S, Oddi S, Molinari M, Musella A, Finazzi-Agro A, Centonze D (2009) Lipid rafts regulate 2-arachidonoylglycerol metabolism and physiological activity in the striatum. J Neurochem 109:371-381.
Mack F, Bonisch H (1979) Dissociation constants and lipophilicity of catecholamines and related compounds. Naunyn Schmiedebergs Arch Pharmacol 310:1-9.
Maldonado-Irizarry CS, Kelley AE (1995) Excitatory amino acid receptors within nucleus accumbens subregions differentially mediate spatial learning in the rat. Behav Pharmacol 6:527-539.
Mantle TJ, Tipton KF, Garrett NJ (1976) Inhibition of monoamine oxidase by amphetamine and related compounds. Biochem Pharmacol 25:2073-2077.
Mayer ML, Westbrook GL, Guthrie PB (1984) Voltage-dependent block by Mg2+ of NMDA responses in spinal cord neurones. Nature 309:261-263.
Mechoulam R, Parker LA (2013) The endocannabinoid system and the brain. Annu Rev Psychol 64:21-47.
Meiser J, Weindl D, Hiller K (2013) Complexity of dopamine metabolism. Cell Commun Signal 11:34.
Meldrum BS (2000) Glutamate as a neurotransmitter in the brain: review of physiology and pathology. J Nutr 130:1007S-1015S.
Melega WP, Williams AE, Schmitz DA, DiStefano EW, Cho AK (1995) Pharmacokinetic and pharmacodynamic analysis of the actions of D-amphetamine and D-methamphetamine on the dopamine terminal. J Pharmacol Exp Ther 274:90-96.
Mendelev N, Mehta SL, Idris H, Kumari S, Li PA (2012) Selenite stimulates mitochondrial biogenesis signaling and enhances mitochondrial functional performance in murine hippocampal neuronal cells. PLoS One 7:e47910.
Meredith GE, Blank B, Groenewegen HJ (1989) The distribution and compartmental organization of the cholinergic neurons in nucleus accumbens of the rat. Neuroscience 31:327-345.
Meredith GE, Agolia R, Arts MP, Groenewegen HJ, Zahm DS (1992) Morphological differences between projection neurons of the core and shell in the nucleus accumbens of the rat. Neuroscience 50:149-162.
Miyazaki I, Asanuma M (2008) Dopaminergic neuron-specific oxidative stress caused by dopamine itself. Acta Med Okayama 62:141-150.
Moghadaszadeh B, Beggs AH (2006) Selenoproteins and their impact on human health through diverse physiological pathways. Physiology (Bethesda) 21:307-315.
Mohammad-Zadeh LF, Moses L, Gwaltney-Brant SM (2008) Serotonin: a review. J Vet Pharmacol Ther 31:187-199.
Moquin KF, Michael AC (2009) Tonic autoinhibition contributes to the heterogeneity of evoked dopamine release in the rat striatum. J Neurochem 110:1491-1501.
Moretto MB, Thomazi AP, Godinho G, Roessler TM, Nogueira CW, Souza DO, Wofchuk S, Rocha JB (2007) Ebselen and diorganylchalcogenides decrease in vitro glutamate uptake by rat brain slices: prevention by DTT and GSH. Toxicol In Vitro 21:639-645.
Morimura T, Ogawa M (2009) Relative importance of the tyrosine phosphorylation sites of Disabled-1 to the transmission of Reelin signaling. Brain Res 1304:26-37.
Moron JA, Brockington A, Wise RA, Rocha BA, Hope BT (2002) Dopamine uptake through the norepinephrine transporter in brain regions with low levels of the dopamine transporter: evidence from knock-out mouse lines. J Neurosci 22:389-395.
Mundorf ML, Hochstetler SE, Wightman RM (1999) Amine weak bases disrupt vesicular storage and promote exocytosis in chromaffin cells. J Neurochem 73:2397-2405.
Murataeva N, Straiker A, Mackie K (2014) Parsing the players: 2-arachidonoylglycerol synthesis and degradation in the CNS. Br J Pharmacol 171:1379-1391.
Nader J, Rapino C, Gennequin B, Chavant F, Francheteau M, Makriyannis A, Duranti A, Maccarrone M, Solinas M, Thiriet N (2014) Prior stimulation of the endocannabinoid system prevents

methamphetamine-induced dopaminergic neurotoxicity in the striatum through activation of CB2 receptors. Neuropharmacology 87:214-221.
Nestler EJ, Carlezon WA, Jr. (2006) The mesolimbic dopamine reward circuit in depression. Biol Psychiatry 59:1151-1159.
Nimpf J, Schneider WJ (2000) From cholesterol transport to signal transduction: low density lipoprotein receptor, very low density lipoprotein receptor, and apolipoprotein E receptor-2. Biochim Biophys Acta 1529:287-298.
Niswender CM, Conn PJ (2010) Metabotropic glutamate receptors: physiology, pharmacology, and disease. Annu Rev Pharmacol Toxicol 50:295-322.
Olson GE, Winfrey VP, Nagdas SK, Hill KE, Burk RF (2005) Selenoprotein P is required for mouse sperm development. Biol Reprod 73:201-211.
Olson GE, Winfrey VP, Nagdas SK, Hill KE, Burk RF (2007) Apolipoprotein E receptor-2 (ApoER2) mediates selenium uptake from selenoprotein P by the mouse testis. J Biol Chem 282:12290-12297.
Parkinson JA, Willoughby PJ, Robbins TW, Everitt BJ (2000) Disconnection of the anterior cingulate cortex and nucleus accumbens core impairs Pavlovian approach behavior: further evidence for limbic cortical-ventral striatopallidal systems. Behav Neurosci 114:42-63.
Parkinson JA, Olmstead MC, Burns LH, Robbins TW, Everitt BJ (1999) Dissociation in effects of lesions of the nucleus accumbens core and shell on appetitive pavlovian approach behavior and the potentiation of conditioned reinforcement and locomotor activity by D-amphetamine. J Neurosci 19:2401-2411.
Pasinetti GM, Morgan DG, Johnson SA, Millar SL, Finch CE (1990) Tyrosine hydroxylase mRNA concentration in midbrain dopaminergic neurons is differentially regulated by reserpine. J Neurochem 55:1793-1799.
Paton DM (1973) Mechanism of efflux of noradrenaline from adrenergic nerves in rabbit atria. Br J Pharmacol 49:614-627.
Perez-Reyes E, Lee JH (2014) Ins and outs of T-channel structure function. Pflugers Arch 466:627-633.
Perez-Velazquez JL, Valiante TA, Carlen PL (1994) Modulation of gap junctional mechanisms during calcium-free induced field burst activity: a possible role for electrotonic coupling in epileptogenesis. J Neurosci 14:4308-4317.
Pertwee RG (2006) The pharmacology of cannabinoid receptors and their ligands: an overview. Int J Obes (Lond) 30 Suppl 1:S13-18.
Peter D, Jimenez J, Liu Y, Kim J, Edwards RH (1994) The chromaffin granule and synaptic vesicle amine transporters differ in substrate recognition and sensitivity to inhibitors. J Biol Chem 269:7231-7237.
Peters MM, Hill KE, Burk RF, Weeber EJ (2006) Altered hippocampus synaptic function in selenoprotein P deficient mice. Mol Neurodegener 1:12.
Picciotto MR, Higley MJ, Mineur YS (2012) Acetylcholine as a neuromodulator: cholinergic signaling shapes nervous system function and behavior. Neuron 76:116-129.
Pitts MW, Raman AV, Hashimoto AC, Todorovic C, Nichols RA, Berry MJ (2012) Deletion of selenoprotein P results in impaired function of parvalbumin interneurons and alterations in fear learning and sensorimotor gating. Neuroscience 208:58-68.
Pitts MW, Kremer PM, Hashimoto AC, Torres DJ, Byrns CN, Williams CS, Berry MJ (2015) Competition between the Brain and Testes under Selenium-Compromised Conditions: Insight into Sex Differences in Selenium Metabolism and Risk of Neurodevelopmental Disease. J Neurosci 35:15326-15338.
Porciuncula LO, Rocha JB, Ghisleni G, Tavares RG, Souza DO (2004) The effects of ebselen on [3H]glutamate uptake by synaptic vesicles from rat brain. Brain Res 1027:192-195.

Pothos EN, Larsen KE, Krantz DE, Liu Y, Haycock JW, Setlik W, Gershon MD, Edwards RH, Sulzer D (2000) Synaptic vesicle transporter expression regulates vesicle phenotype and quantal size. J Neurosci 20:7297-7306.
Powers WJ (2009) PET studies of cerebral metabolism in Parkinson disease. J Bioenerg Biomembr 41:505-508.
Premasekharan G, Nguyen K, Contreras J, Ramon V, Leppert VJ, Forman HJ (2011) Iron-mediated lipid peroxidation and lipid raft disruption in low-dose silica-induced macrophage cytokine production. Free Radic Biol Med 51:1184-1194.
Qiu S, Korwek KM, Pratt-Davis AR, Peters M, Bergman MY, Weeber EJ (2006) Cognitive disruption and altered hippocampus synaptic function in Reelin haploinsufficient mice. Neurobiol Learn Mem 85:228-242.
Rasekh HR, Davis MD, Cooke LW, Mazzio EA, Reams RR, Soliman KF (1997) The effect of selenium on the central dopaminergic system: a microdialysis study. Life Sci 61:1029-1035.
Rayman MP (2005) Selenium in cancer prevention: a review of the evidence and mechanism of action. Proc Nutr Soc 64:527-542.
Rayman MP (2012) Selenium and human health. Lancet 379:1256-1268.
Reddy SS, Connor TE, Weeber EJ, Rebeck W (2011) Similarities and differences in structure, expression, and functions of VLDLR and ApoER2. Mol Neurodegener 6:30.
Reeves MA, Hoffmann PR (2009) The human selenoproteome: recent insights into functions and regulation. Cell Mol Life Sci 66:2457-2478.
Rehni AK, Singh TG (2013) Selenium induced anticonvulsant effect: a potential role of prostaglandin E(1) receptor activation linked mechanism. J Trace Elem Med Biol 27:31-39.
Ren Q, Ma M, Yang C, Zhang JC, Yao W, Hashimoto K (2015) BDNF-TrkB signaling in the nucleus accumbens shell of mice has key role in methamphetamine withdrawal symptoms. Transl Psychiatry 5:e666.
Riaz MA, Stammler A, Borgers M, Konrad L (2017) Clusterin signals via ApoER2/VLDLR and induces meiosis of male germ cells. Am J Transl Res 9:1266-1276.
Ricaurte GA, Schuster CR, Seiden LS (1980) Long-term effects of repeated methylamphetamine administration on dopamine and serotonin neurons in the rat brain: a regional study. Brain Res 193:153-163.
Rice ME, Patel JC, Cragg SJ (2011) Dopamine release in the basal ganglia. Neuroscience 198:112-137.
Ritz MC, Kuhar MJ (1989) Relationship between self-administration of amphetamine and monoamine receptors in brain: comparison with cocaine. J Pharmacol Exp Ther 248:1010-1017.
Rizzoli SO, Betz WJ (2005) Synaptic vesicle pools. Nat Rev Neurosci 6:57-69.
Romero-Ramos M, Venero JL, Cano J, Machado A (2000) Low selenium diet induces tyrosine hydroxylase enzyme in nigrostriatal system of the rat. Brain Res Mol Brain Res 84:7-16.
Roper J, Ashcroft FM (1995) Metabolic inhibition and low internal ATP activate K-ATP channels in rat dopaminergic substantia nigra neurones. Pflugers Arch 430:44-54.
Rotruck JT, Pope AL, Ganther HE, Swanson AB, Hafeman DG, Hoekstra WG (1973) Selenium: biochemical role as a component of glutathione peroxidase. Science 179:588-590.
Rubaiy HN (2016) The therapeutic agents that target ATP-sensitive potassium channels. Acta Pharm 66:23-34.
Saddoris MP, Wang X, Sugam JA, Carelli RM (2016) Cocaine Self-Administration Experience Induces Pathological Phasic Accumbens Dopamine Signals and Abnormal Incentive Behaviors in Drug-Abstinent Rats. J Neurosci 36:235-250.
Saito Y, Takahashi K (2002) Characterization of selenoprotein P as a selenium supply protein. Eur J Biochem 269:5746-5751.

Saito Y, Sato N, Hirashima M, Takebe G, Nagasawa S, Takahashi K (2004) Domain structure of bi-functional selenoprotein P. Biochem J 381:841-846.
Saito Y, Hayashi T, Tanaka A, Watanabe Y, Suzuki M, Saito E, Takahashi K (1999) Selenoprotein P in human plasma as an extracellular phospholipid hydroperoxide glutathione peroxidase. Isolation and enzymatic characterization of human selenoprotein p. J Biol Chem 274:2866-2871.
Salgado S, Kaplitt MG (2015) The Nucleus Accumbens: A Comprehensive Review. Stereotact Funct Neurosurg 93:75-93.
Samuvel DJ, Jayanthi LD, Manohar S, Kaliyaperumal K, See RE, Ramamoorthy S (2008) Dysregulation of dopamine transporter trafficking and function after abstinence from cocaine self-administration in rats: evidence for differential regulation in caudate putamen and nucleus accumbens. J Pharmacol Exp Ther 325:293-301.
Santamaria A, Vazquez-Roman B, La Cruz VP, Gonzalez-Cortes C, Trejo-Solis MC, Galvan-Arzate S, Jara-Prado A, Guevara-Fonseca J, Ali SF (2005) Selenium reduces the proapoptotic signaling associated to NF-kappaB pathway and stimulates glutathione peroxidase activity during excitotoxic damage produced by quinolinate in rat corpus striatum. Synapse 58:258-266.
Sasakura C, Suzuki KT (1998) Biological interaction between transition metals (Ag, Cd and Hg), selenide/sulfide and selenoprotein P. J Inorg Biochem 71:159-162.
Saunders C, Ferrer JV, Shi L, Chen J, Merrill G, Lamb ME, Leeb-Lundberg LM, Carvelli L, Javitch JA, Galli A (2000) Amphetamine-induced loss of human dopamine transporter activity: an internalization-dependent and cocaine-sensitive mechanism. Proc Natl Acad Sci U S A 97:6850-6855.
Savaskan NE, Ufer C, Kuhn H, Borchert A (2007) Molecular biology of glutathione peroxidase 4: from genomic structure to developmental expression and neural function. Biol Chem 388:1007-1017.
Savaskan NE, Brauer AU, Kuhbacher M, Eyupoglu IY, Kyriakopoulos A, Ninnemann O, Behne D, Nitsch R (2003) Selenium deficiency increases susceptibility to glutamate-induced excitotoxicity. FASEB J 17:112-114.
Sazdanovic M, Sazdanovic P, Zivanovic-Macuzic I, Jakovljevic V, Jeremic D, Peljto A, Tosevski J (2011) Neurons of human nucleus accumbens. Vojnosanit Pregl 68:655-660.
Schmitz Y, Lee CJ, Schmauss C, Gonon F, Sulzer D (2001) Amphetamine distorts stimulation-dependent dopamine overflow: effects on D2 autoreceptors, transporters, and synaptic vesicle stores. J Neurosci 21:5916-5924.
Schomburg L (2011) Selenium, selenoproteins and the thyroid gland: interactions in health and disease. Nat Rev Endocrinol 8:160-171.
Schultz W (2016) Reward functions of the basal ganglia. J Neural Transm (Vienna) 123:679-693.
Seeher S, Carlson BA, Miniard AC, Wirth EK, Mahdi Y, Hatfield DL, Driscoll DM, Schweizer U (2014) Impaired selenoprotein expression in brain triggers striatal neuronal loss leading to co-ordination defects in mice. Biochem J 462:67-75.
Seiden LS, Sabol KE, Ricaurte GA (1993) Amphetamine: effects on catecholamine systems and behavior. Annu Rev Pharmacol Toxicol 33:639-677.
Sellings LH, Clarke PB (2003) Segregation of amphetamine reward and locomotor stimulation between nucleus accumbens medial shell and core. J Neurosci 23:6295-6303.
Seyedali A, Berry MJ (2014) Nonsense-mediated decay factors are involved in the regulation of selenoprotein mRNA levels during selenium deficiency. RNA 20:1248-1256.
Sharaf A, Rahhal B, Spittau B, Roussa E (2015) Localization of reelin signaling pathway components in murine midbrain and striatum. Cell Tissue Res 359:393-407.
Sharaf A, Bock HH, Spittau B, Bouche E, Krieglstein K (2013) ApoER2 and VLDLr are required for mediating reelin signalling pathway for normal migration and positioning of mesencephalic dopaminergic neurons. PLoS One 8:e71091.

Shi WX, Pun CL, Zhang XX, Jones MD, Bunney BS (2000) Dual effects of D-amphetamine on dopamine neurons mediated by dopamine and nondopamine receptors. J Neurosci 20:3504-3511.
Siciliano CA, Calipari ES, Ferris MJ, Jones SR (2014) Biphasic mechanisms of amphetamine action at the dopamine terminal. J Neurosci 34:5575-5582.
Sidenius U, Farver O, Jons O, Gammelgaard B (1999) Comparison of different transition metal ions for immobilized metal affinity chromatography of selenoprotein P from human plasma. J Chromatogr B Biomed Sci Appl 735:85-91.
Sidlo Z, Reggio PH, Rice ME (2008) Inhibition of striatal dopamine release by CB1 receptor activation requires nonsynaptic communication involving GABA, H2O2, and KATP channels. Neurochem Int 52:80-88.
Siegmund SV, Seki E, Osawa Y, Uchinami H, Cravatt BF, Schwabe RF (2006) Fatty acid amide hydrolase determines anandamide-induced cell death in the liver. J Biol Chem 281:10431-10438.
Solovyev ND (2015) Importance of selenium and selenoprotein for brain function: From antioxidant protection to neuronal signalling. J Inorg Biochem 153:1-12.
Sonders MS, Zhu SJ, Zahniser NR, Kavanaugh MP, Amara SG (1997) Multiple ionic conductances of the human dopamine transporter: the actions of dopamine and psychostimulants. J Neurosci 17:960-974.
Spallholz JE (1990) Selenium and glutathione peroxidase: essential nutrient and antioxidant component of the immune system. Adv Exp Med Biol 262:145-158.
Spanos M, Gras-Najjar J, Letchworth JM, Sanford AL, Toups JV, Sombers LA (2013) Quantitation of hydrogen peroxide fluctuations and their modulation of dopamine dynamics in the rat dorsal striatum using fast-scan cyclic voltammetry. ACS Chem Neurosci 4:782-789.
Spina MB, Cohen G (1989) Dopamine turnover and glutathione oxidation: implications for Parkinson disease. Proc Natl Acad Sci U S A 86:1398-1400.
Steinberg EE, Boivin JR, Saunders BT, Witten IB, Deisseroth K, Janak PH (2014) Positive reinforcement mediated by midbrain dopamine neurons requires D1 and D2 receptor activation in the nucleus accumbens. PLoS One 9:e94771.
Steinbrenner H, Sies H (2013) Selenium homeostasis and antioxidant selenoproteins in brain: implications for disorders in the central nervous system. Arch Biochem Biophys 536:152-157.
Stuber GD, Roitman MF, Phillips PE, Carelli RM, Wightman RM (2005) Rapid dopamine signaling in the nucleus accumbens during contingent and noncontingent cocaine administration. Neuropsychopharmacology 30:853-863.
Sulzer D (2011) How addictive drugs disrupt presynaptic dopamine neurotransmission. Neuron 69:628-649.
Sulzer D, Sonders MS, Poulsen NW, Galli A (2005) Mechanisms of neurotransmitter release by amphetamines: a review. Prog Neurobiol 75:406-433.
Sulzer D, Pothos E, Sung HM, Maidment NT, Hoebel BG, Rayport S (1992) Weak base model of amphetamine action. Ann N Y Acad Sci 654:525-528.
Sunde RA, Raines AM (2011) Selenium regulation of the selenoprotein and nonselenoprotein transcriptomes in rodents. Adv Nutr 2:138-150.
Sunde RA, Thompson KM, Evenson JK, Thompson BM (2009) Blood glutathione peroxidase-1 mRNA levels can be used as molecular biomarkers to determine dietary selenium requirements in rats. Exp Biol Med (Maywood) 234:1271-1279.
Sutherland M, Shankaranarayanan P, Schewe T, Nigam S (2001) Evidence for the presence of phospholipid hydroperoxide glutathione peroxidase in human platelets: implications for its involvement in the regulatory network of the 12-lipoxygenase pathway of arachidonic acid metabolism. Biochem J 353:91-100.

Takebe G, Yarimizu J, Saito Y, Hayashi T, Nakamura H, Yodoi J, Nagasawa S, Takahashi K (2002) A comparative study on the hydroperoxide and thiol specificity of the glutathione peroxidase family and selenoprotein P. J Biol Chem 277:41254-41258.
Toppo S, Flohe L, Ursini F, Vanin S, Maiorino M (2009) Catalytic mechanisms and specificities of glutathione peroxidases: variations of a basic scheme. Biochim Biophys Acta 1790:1486-1500.
Torres GE, Gainetdinov RR, Caron MG (2003) Plasma membrane monoamine transporters: structure, regulation and function. Nat Rev Neurosci 4:13-25.
Trouillon R, Ewing AG (2014) Actin controls the vesicular fraction of dopamine released during extended kiss and run exocytosis. ACS Chem Biol 9:812-820.
Ufer C, Wang CC, Fahling M, Schiebel H, Thiele BJ, Billett EE, Kuhn H, Borchert A (2008) Translational regulation of glutathione peroxidase 4 expression through guanine-rich sequence-binding factor 1 is essential for embryonic brain development. Genes Dev 22:1838-1850.
Ursini F, Maiorino M, Roveri A (1997) Phospholipid hydroperoxide glutathione peroxidase (PHGPx): more than an antioxidant enzyme? Biomed Environ Sci 10:327-332.
Ursini F, Maiorino M, Brigelius-Flohe R, Aumann KD, Roveri A, Schomburg D, Flohe L (1995) Diversity of glutathione peroxidases. Methods Enzymol 252:38-53.
Van Bockstaele EJ, Pickel VM (1995) GABA-containing neurons in the ventral tegmental area project to the nucleus accumbens in rat brain. Brain Res 682:215-221.
van der Plasse G, Schrama R, van Seters SP, Vanderschuren LJ, Westenberg HG (2012) Deep brain stimulation reveals a dissociation of consummatory and motivated behaviour in the medial and lateral nucleus accumbens shell of the rat. PLoS One 7:e33455.
Wagner GC, Ricaurte GA, Seiden LS, Schuster CR, Miller RJ, Westley J (1980) Long-lasting depletions of striatal dopamine and loss of dopamine uptake sites following repeated administration of methamphetamine. Brain Res 181:151-160.
Wang JK (1991) Presynaptic glutamate receptors modulate dopamine release from striatal synaptosomes. J Neurochem 57:819-822.
Watanabe C, Kasanuma Y, Satoh H (1997) Deficiency of selenium enhances the K+-induced release of dopamine in the striatum of mice. Neurosci Lett 236:49-52.
Weeber EJ, Beffert U, Jones C, Christian JM, Forster E, Sweatt JD, Herz J (2002) Reelin and ApoE receptors cooperate to enhance hippocampal synaptic plasticity and learning. J Biol Chem 277:39944-39952.
Weisgraber KH, Roses AD, Strittmatter WJ (1994) The role of apolipoprotein E in the nervous system. Curr Opin Lipidol 5:110-116.
Wenger T, Moldrich G, Furst S (2003) Neuromorphological background of cannabis addiction. Brain Res Bull 61:125-128.
Wess J (2003) Novel insights into muscarinic acetylcholine receptor function using gene targeting technology. Trends Pharmacol Sci 24:414-420.
Wheeler DS, Underhill SM, Stolz DB, Murdoch GH, Thiels E, Romero G, Amara SG (2015) Amphetamine activates Rho GTPase signaling to mediate dopamine transporter internalization and acute behavioral effects of amphetamine. Proc Natl Acad Sci U S A 112:E7138-7147.
Wightman RM, Haynes CL (2004) Synaptic vesicles really do kiss and run. Nat Neurosci 7:321-322.
Wilson TM, Scholz RW, Drake TR (1983) Selenium toxicity and porcine focal symmetrical poliomyelomalacia: description of a field outbreak and experimental reproduction. Can J Comp Med 47:412-421.
Wilson TM, Hammerstedt RH, Palmer IS, deLahunta A (1988) Porcine focal symmetrical poliomyelomalacia: experimental reproduction with oral doses of encapsulated sodium selenite. Can J Vet Res 52:83-88.

Wimalasena K (2011) Vesicular monoamine transporters: structure-function, pharmacology, and medicinal chemistry. Med Res Rev 31:483-519.
Wirth EK, Conrad M, Winterer J, Wozny C, Carlson BA, Roth S, Schmitz D, Bornkamm GW, Coppola V, Tessarollo L, Schomburg L, Kohrle J, Hatfield DL, Schweizer U (2010) Neuronal selenoprotein expression is required for interneuron development and prevents seizures and neurodegeneration. FASEB J 24:844-852.
Wise RA (1998) Drug-activation of brain reward pathways. Drug Alcohol Depend 51:13-22.
Wise RA (2004) Dopamine, learning and motivation. Nat Rev Neurosci 5:483-494.
Wong DF, Brasic JR, Singer HS, Schretlen DJ, Kuwabara H, Zhou Y, Nandi A, Maris MA, Alexander M, Ye W, Rousset O, Kumar A, Szabo Z, Gjedde A, Grace AA (2008) Mechanisms of dopaminergic and serotonergic neurotransmission in Tourette syndrome: clues from an in vivo neurochemistry study with PET. Neuropsychopharmacology 33:1239-1251.
Wu Q, Reith ME, Wightman RM, Kawagoe KT, Garris PA (2001) Determination of release and uptake parameters from electrically evoked dopamine dynamics measured by real-time voltammetry. J Neurosci Methods 112:119-133.
Xing B, Li YC, Gao WJ (2016) Norepinephrine versus dopamine and their interaction in modulating synaptic function in the prefrontal cortex. Brain Res 1641:217-233.
Xu CM, Wang J, Wu P, Xue YX, Zhu WL, Li QQ, Zhai HF, Shi J, Lu L (2011) Glycogen synthase kinase 3beta in the nucleus accumbens core is critical for methamphetamine-induced behavioral sensitization. J Neurochem 118:126-139.
Yamaguchi T, Sheen W, Morales M (2007) Glutamatergic neurons are present in the rat ventral tegmental area. Eur J Neurosci 25:106-118.
Yang DH, Smith ER, Roland IH, Sheng Z, He J, Martin WD, Hamilton TC, Lambeth JD, Xu XX (2002) Disabled-2 is essential for endodermal cell positioning and structure formation during mouse embryogenesis. Dev Biol 251:27-44.
Yang WS, SriRamaratnam R, Welsch ME, Shimada K, Skouta R, Viswanathan VS, Cheah JH, Clemons PA, Shamji AF, Clish CB, Brown LM, Girotti AW, Cornish VW, Schreiber SL, Stockwell BR (2014) Regulation of ferroptotic cancer cell death by GPX4. Cell 156:317-331.
Yant LJ, Ran Q, Rao L, Van Remmen H, Shibatani T, Belter JG, Motta L, Richardson A, Prolla TA (2003) The selenoprotein GPX4 is essential for mouse development and protects from radiation and oxidative damage insults. Free Radic Biol Med 34:496-502.
Yokoyama H, Tsuchihashi N, Kasai N, Matsue T, Uchida I, Mori N, Ohya-Nishiguchi H, Kamada H (1997) Hydrogen peroxide augmentation in a rat striatum after methamphetamine injection as monitored in vivo by a Pt-disk microelectrode. Biosens Bioelectron 12:1037-1041.
Yoneda S, Suzuki KT (1997) Equimolar Hg-Se complex binds to selenoprotein P. Biochem Biophys Res Commun 231:7-11.
Yoo MH, Gu X, Xu XM, Kim JY, Carlson BA, Patterson AD, Cai H, Gladyshev VN, Hatfield DL (2010) Delineating the role of glutathione peroxidase 4 in protecting cells against lipid hydroperoxide damage and in Alzheimer's disease. Antioxid Redox Signal 12:819-827.
Yoo SE, Chen L, Na R, Liu Y, Rios C, Van Remmen H, Richardson A, Ran Q (2012) Gpx4 ablation in adult mice results in a lethal phenotype accompanied by neuronal loss in brain. Free Radic Biol Med 52:1820-1827.
Yorgason JT, Espana RA, Jones SR (2011) Demon voltammetry and analysis software: analysis of cocaine-induced alterations in dopamine signaling using multiple kinetic measures. J Neurosci Methods 202:158-164.
Youn HS, Lim HJ, Choi YJ, Lee JY, Lee MY, Ryu JH (2008) Selenium suppresses the activation of transcription factor NF-kappa B and IRF3 induced by TLR3 or TLR4 agonists. Int Immunopharmacol 8:495-501.

Yu S, Zhu L, Shen Q, Bai X, Di X (2015) Recent advances in methamphetamine neurotoxicity mechanisms and its molecular pathophysiology. Behav Neurol 2015:103969.
Yuan C, Gao J, Guo J, Bai L, Marshall C, Cai Z, Wang L, Xiao M (2014) Dimethyl sulfoxide damages mitochondrial integrity and membrane potential in cultured astrocytes. PLoS One 9:e107447.
Zamponi GW (2016) Targeting voltage-gated calcium channels in neurological and psychiatric diseases. Nat Rev Drug Discov 15:19-34.
Zhang X, Min KW, Wimalasena J, Baek SJ (2012) Cyclin D1 degradation and p21 induction contribute to growth inhibition of colorectal cancer cells induced by epigallocatechin-3-gallate. J Cancer Res Clin Oncol 138:2051-2060.
Zhang Y, Zhou Y, Schweizer U, Savaskan NE, Hua D, Kipnis J, Hatfield DL, Gladyshev VN (2008) Comparative analysis of selenocysteine machinery and selenoproteome gene expression in mouse brain identifies neurons as key functional sites of selenium in mammals. J Biol Chem 283:2427-2438.
Zhou J, Scholes J, Hsieh JT (2003) Characterization of a novel negative regulator (DOC-2/DAB2) of c-Src in normal prostatic epithelium and cancer. J Biol Chem 278:6936-6941.
Zia S, Islam F (2000) Selenium altered the levels of lipids, lipid peroxidation, and sulfhydryl groups in straitum and thalamus of rat. Biol Trace Elem Res 77:251-259.